NTNU – Trondheim
Norwegian University of
Science and Technology

Separating photosinthetic hydrogen production from photosynthetic oxygen production

Ewelina Grad

Biotechnology
Submission date: July 2015
Supervisor: Martin Frank Hohmann-Marriott, IBT

Norwegian University of Science and Technology
Department of Biotechnology

Separating photosynthetic hydrogen production from photosynthetic oxygen production

Norwegian University of Science and Technology, Institute of Biotechnology

Ewelina Grad

7/15/2015

Masters in Biotechnology (2 years)

Supervisor: Martin Frank Hohmann-Marriott, IBT

Abstract

The goal of this thesis is to develop concepts to separate photosynthetic hydrogen production from oxygen production. For this the strains will be generate and with deficient in the photosystems (PSI and PSII) that mediate oxygen production and hydrogen production, respectively. The potential to interfacing these two strains via artificial and natural electron transport systems will be evaluated. The growth experiment will be estimated for mutants on different iron and manganese sources, with light or dark condition.

Cyanobacteria are large and diverse group of prokaryote. It is composed of two main membrane, cell wall and cytoplasmic membrane. Within the membrane the photosynthetic apparatus is incorporated where photosynthesis take place. Photosynthesis is the most important process on Earth, by which the oxygen gas is produced and released. The photosynthesis began with light been absorbed by the pigment on the surface of the photosystem II. Energy from the absorbed electron then is used for water oxidation. The electron from water molecule together with electron from the light are transferred to cytochrome b6f complex. Cytochrome b6f complex catalyzes the transfer of electrons from plastoquinol to plastocyanin. It mediates the electrons from photosystem II complex to photosystem I complex. The electron is re-energies and then used to drive synthesis ATP.

The *Synechocystis* sp. PCC6803 was used to create mutants with deficient photosystems (PSI and PSII). The mutant with deficient in PSI was created by deletion *slr1834-1835* gene, that is responsible for production P700 apoprotein subunit Ia and Ib. The PSII deficient were create by deletion *slr0906* gene, which produce core light harvesting protein. The growth experiments were performed with different iron and manganese sources and exposed to the dark condition and light condition. The results showed that all mutants possess ability to growth on all the media that was made for this experiment. However, there are small differences in growth rate on different media. The Δslr1834-1835 showed increased growth on media that were supplemented with manganese sources exposed to dark condition, compared to the Δslr0906 mutant. The Δslr0906 showed increased growth rate on media supplemented with

iron and manganese sources exposed to dark condition. The strains grown on media exposed to light condition showed increased growth rate compared to the growth under the darkness. The strains that were grown under the light condition showed the most increased growth rate over the time. The interfacing two strains via artificial and natural electron transport systems will not be evaluated. This is due to lack of time.

Sammendrag

Målet med denne oppgaven er å utvikle konsepter for å kunne skille fotosyntesehydrogenproduksjonfra oksygen produksjon. For å kunne utføre dette, cyanobakteriastammersom er mangelfulle i fotosystemer (PSI og PSII) som formidler hendholdsvis oksygenproduksjon og hydrogenproduksjon skal genereres. Potensialet til tilkoplingen av disse to stammene via kunstige og naturlige elektrontransportsystemene vil bli evaluert. Vekstforsøket vil bli estimert for mutanter i forskjellige jern- og mangankilder, med lys eller mørk tilstand.

Cyanobakterier er stor og mangfoldig gruppe av prokaryote. De er sammensatt av to hovedmembraner, cellevegg og cytoplasmisk membran. Innenfor membranen inngår fotosyntese anordningen der fotosyntesen foregår. Fotosyntese er den viktigste prosessen på jorden , ved hjelp av hvilken oksygengass produseres og frigjøres . Fotosyntesen begynte ved at lys ble absorbert av pigmentene på overflaten av fotosystem II .Energien fra den absorberte elektronen deretter brukes for vannoksidasjon . Elektronen fra vannmolekylet overføres sammen med elektronen fra lyset til cytokrom b6f kompleks. Cytokrom b6f kompleks katalyserer overføring av elektroner fra plastoquinol til plastocyanin. Den formidler elektronene fra fotosystem II kompleks til fotosystem I kompleks. Elektronet blir gjennladet og deretter brukt til å drive syntese ATP.

Synechocystis sp. PCC6803 ble brukt til å lage mutanter med mangler fotosystem(PSI og PSII) . Mutanten med mangler i PSI ble opprettet ved sletting av slr1834-1835 genet , som er ansvarlig for produksjonen av P700 apoprotein underenhet Ia og Ib . PSII mangelen var opprettet ved sletting av slr0906 genen , som produserer kjernelys høste protein.

Vekstеksperimenter ble utført med forskjellige jern og mangan kilder og utsatt for både mørk og lys tilstand . Resultatene viste at alle mutanter vokser på alle forskjellige jern- og mangankilder . Men det er små forskjeller i vekstrate på ulike medier. Δslr1834-1835 viste økt vekst på medium som ble supplert med mangan kilder utsatt for mørke forhold , sammenlignet med Δslr0906 mutanten. Slr0906 viste økt veksttakt på medium supplert med jern og mangan kilder utsatt for mørk tilstandstammene dyrket på media som ble utsatt for lys

viste økt vekst sammenlignet med vekst i mørk tilstand. Stammene som ble dyrket under lys tilstand viste den mest økte veksthastighet over tid.

På grunn av tidsmangel vill grensesnittet av stammene Δslr1834-1835 og Δslr0906 via kunstige og naturlige elektrontransportsystemenevil ikke bli vurdert.

Acknowledgements

First, I would like to thank my brother Marcel for his tremendous help both financial and spiritually, and that he was always been for me. I would like to thank my family for their support and encourage me in tough times. It's been hard year for me; I lost a lot that is dear to me. I lost my house where I grew up and friend, family member, beloved dog Kruszi. In addition to that my dad got a cancer. This very much affected my life and my work. However, despite all bed things that happened to me in the end there was the one good news; my dad survive and he will be fine. This gives me motivation to keep moving forward and to complete my work on my thesis. I would like to thank Bruno for his constant positive attitude, motivation and his faith in my own strength.

I want to thank Associate Professor Martin Hohmann-Marriott for guiding me and his optimistic support, and PhD student Jacob Lamb for help and support in the laboratory. I would like to express my gratitude to them for all their support. I want to thank other lab fellows from department of Biotechnology by providing me friendly help in the lab.

I want to thank my dear friend Azra for her friendship and irreplaceable support during this year.

Niniejszą pracę dedykuję moim wspaniałym

Rodzicom,

którzy zawsze we mnie wierzyli i wspierali.

To ich mądrości i miłości zawdzięczam to, kim jestem.

Table of Contents

1 Introduction

Introduction

Cyanobacteria are one of the largest and diverse groups of prokaryotes. In the past the cyanobacteria were described as blue-green algae, however this name is misleading because the cyanobacteria are not true algae, which belong to group of eukaryote. The cyanobacteria mechanism of photosynthesis shows similarities to the photosystem found in eukaryotes. Cyanobacteria are resilient organisms that are highly flexible and can adjust to number types of environment. Therefore, cyanobacteria are found in almost any environment, starting from distilled water, freshwater, marine environment to extreme ones like hot springs, benthos, hot desert, tropical rain forest and Antarctic cold desert. All existing cyanobacteria are photoautotrophs; however there are some species that can growth photoheterotrophically (Srivastava, Rai, & Neilan, 2013),(Blankenship, 2002).

Cyanobacteria are one of the largest groups of organisms that produced 20 %-30% oxygen productivity on global scale. In addition cyanobacteria show ability to fix atmospheric N_2 to form biologically accessible compound. In order to fix N2 cyanobacteria contain enzyme nitrogenase, which is sensitive to O2. The oxygen molecule produced by the photosystem II in cyanobacteria is incompatible during nitrogen fixation. Therefore, cyanobacteria possess remarkably adaptation abilities, in which can solve this problem in many different ways. One of them is to change the characteristic of the cell to heterocyst in which create filamentous form of cell that growth as a string. In this type of cell the photosystem is absent, and the cell dos not diffuse oxygen molecule inside the cell. The other way to adapt is to perform N2 fixation during dark condition when the cell do not produce oxygen molecule. In some of the group of cyanobacteria there are species that have ability to switch H_2O to H_2S in order to produce electron, in that case the elemental sulfur is produced. However in absent of H_2S organisms is capable to produce O2 in the same manner as other cyanobacteria (Blankenship, 2002)

The cyanobacteria cell is compost of two main membranes, first is cell wall and the second is cytoplasmic membrane. The cell wall is compost of murein and cytoplasmic membrane separates cytoplasm from the periplasm. Most cyanobacteria contain large internal system of

thylakoid membrane. Within the membrane the photosynthetic apparatus are incorporated (Blankenship, 2002). Therefore, oxygenic photosynthesis takes place in thylakoid membrane. The structure of cyanobacteria cell membrane is simply described in Figure 1.

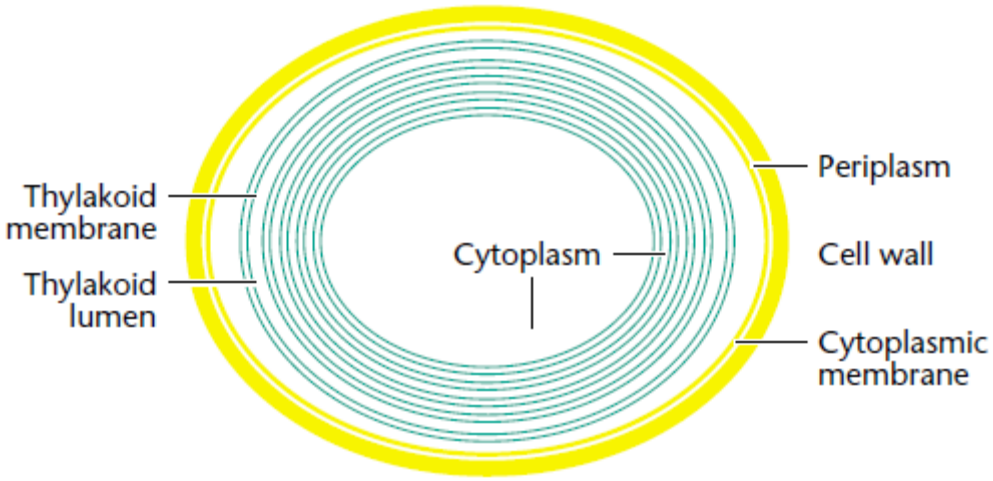

Figure 1 Schematic structure represents intercellular membranes and compartments located in the cyanobacteria cell. Thylakoid membranes is consist of chlorophyll *a*, is involved in photosynthetic and respiratory electron transfer. Cytoplasmic membrane system contains carotenoids and performs only respiratory electron transfer. The thylakoid lumen is a space between a pair of thylakoid membrane. The thylakoid membrane is the place where the protons produced during the photosynthetic and respiratory electron transfer are collected (Srivastava et al., 2013)(Wimp FJ Vergas, 2001).

The cyanobacteria mechanism of oxygenic photosynthesis is high comparable to that one in oxygenic eukaryotes. Therefore, cyanobacteria can be use as a model organism to study how the system is regulated and different aspects of oxygenic photosynthesis (Srivastava et al., 2013).

Iron metabolism

Iron is a trace element that's plays important role in photosynthetic apparatus. It may be associated with biosynthesis of chlorophyll and phycobilin pigments, with many components within the photosystem II and photosystem I, nitrate assimilation and as well with electron transport (Wei Xing, Wen-min Huang, Dun-hai Li, & Yong-ding Liu, 2006). The iron acquisition showed great importance in variety of metabolism processes within almost all organisms living on Earth. However, in order to imbibed the iron from the environments microorganisms have to create various uptake systems (Briat et al., 1995). Cyanobacteria are

the one of the organisms that requires large number of iron for supplying the Fe-rich photosynthetic apparatus. In the highly variable environment, in order to maintain homeostasis cyanobacteria species acquire large numbers of genomes that code for transporters. The genes encoding iron transporters include iron-responsive elements, iron storage complexes and iron transporters. In order to bind iron metals from the environment microorganisms produce siderophore. The siderophore has small molecular weight and are responsible for scavenging irons Fe(III) from the environment (Chauvat & Cassier-Chauvat, 2013, p. 57). Ones the iron is bound create the ferric-siderophore complexes, therefore the iron can be transported inside the cell. This transport can occur by the siderophore transport system. The release of iron from the siderophore usually take place in the cytoplasm (Lis, Kranzler, Keren, & Shaked, 2015a).

Manganese metabolism

The manganese is the essential trace mineral element for the electron transfer apparatus in all microorganisms. Therefore, plants and cyanobacteria create special uptake and accumulation system in order to store metals irons (Bartsevich & Pakrasi, 1996). In photosynthetic apparatus the Mn atoms are located within the photosystem II in thylakoid membranes, where carried out the process of water oxidation (Ogawa, 2002). Therefore, Mn can be specific only for photosystem II complex. Although under restricted number of quantity of manganese the high-affinity MntABC transport system is triggered in cyanobacteria. Therefore, inactivation of this transporting system leads to reduction of activity of photosystem II (Shcolnick & Keren, 2006).

Oxygenic photosynthesis

Oxygenic photosynthesis is the one of the most essential biological process on the earth. All higher organisms depend on oxygen in the atmosphere, which is produced by oxygenic organisms. Within oxygenic organisms the light energy is converting into chemical energy, which can be stored. During this process oxygen gas is secreted and released as a byproduct. This is followed by the reduction of carbon, using the energy obtained from light. Thereby, energy equivalents and carbonbased molecules can be used by the oxygenic organism to drive all the necessary cellular processes (Srivastava et al., 2013)(Blankenship, 2002)(Wim FJ Vermaas, 2001).

Photosynthesis begins with energy being absorbed; this energy comes from the sunlight. Before light reaches the surface of the earth, it is attenuated by scattering and molecules that exist in the atmosphere. The fraction of solar light left after being absorbed by the atmosphere can then be utilized on the surface of the earth. The visible light range together with wavelengths from 700 to 1000 nanometers (nm), are significant in carrying out the process of photosynthesis. Oxygenic photosynthetic organisms contain pigments that absorb light in the visible light range. Furthermore, many algae and plants appear green, as they reflect yellow and green wavelengths of light. Red and blue wavelengths of light are absorbed by these pigments and provide the energy that is used for photosynthetic carbon fixation. On Earth the production of oxygen is important for all of the higher organisms. The organisms that can drive this process are called photoautotrophs. The photoautotrophic group includes plants, algae, cyanobacteria and photosynthetic bacteria (Blankenship, 2002).

Within algae, oxygenic photosynthesis starts in the thylakoid membrane where antenna system (PBSs) containing pigment molecules absorb light. This excitation energy is then transferred to the reaction center (RC) complex. The manganese oxide cluster (Mn_40_xCa) then oxidizes water molecules into 4 protons, 4 electrons and oxygen molecule. These electrons are then transferred by the redox active tyrosine molecule (Tyr) to RC of photosystem II (PSII). Within the RC excitation energy will pass the electrons to a series of proteins located in thylakoid membrane. Plastoquinone A (QA) is electron acceptor of PSII which accepts one electron and transfer one by one to the plastoquinone B (QB). Next plastoquinone B molecule accepts and transfers two of those electrons simultaneously and collects two protons from stroma and transfers them to the thylakoid space. This protons transfer increases the hydrogen ion gradient over the thylakoid membrane. The hydrogen ion gradient allows ATP synthase to phosphorylate ADT to ATP. The low energy electrons leaving the PSII are then transported to photosystem I (PSI). Within PSI the electrons are reenergized and transport via an electron transport pathway to ferredoxin-$NADP^+$ reductase (FNR). FNR is an enzyme that reduces NADP+ to form NADHP ("Z-Scheme Figure Legend," n.d.).

Photosynthesis and respiration in cyanobacteria

Cyanobacteria are found to be oldest photosynthetic organisms on Earth, is have been estimated to be 3.5 bilin years old, respectively. The reason why cyanobacteria are the evolutionary oldest organisms lies in their ability to perform effective metabolic pathway. This organism is in one of the few groups that can perform oxygenic photosynthesis and respiration spontaneously and as well they are located in the same compartments within the cell. Therefore, they are resilient and highly flexible to various types of environment. The combinations of photosynthesis along with respiration require electron transport that is catalyzed by the protein complexes located within the membrane. The thylakoid membrane contains both electron transport chains for photosynthesis and respiration. Within oxygenic photosynthesis conversion water molecule and CO_2 to sugar take place, however the respiration converts sugar to water and CO_2. Therefore the cytoplasmic membrane contains respiratory electron pathway, in which there is no photosynthetic components associated with. The thylakoid membrane contain photosynthetic electron transport, however in many cyanobacteria the respiratory electron transfer take place alike in thylakoid and cytoplasmic membrane. The photosynthesis and respiration electron transport chains are simply described in Figure 2. The cyanobacteria thylakoid membranes containing the photosynthesis and respiration electron transfer utilize many redox-active components. Utilizing the redox-active components includes the plastoquinone (PQ) pool, cytochrome *b6f* complex and electron carriers plastocyanin or cytochrome c_{553} (cytochrome *c6*) (Wim FJ Vermaas, 2001).

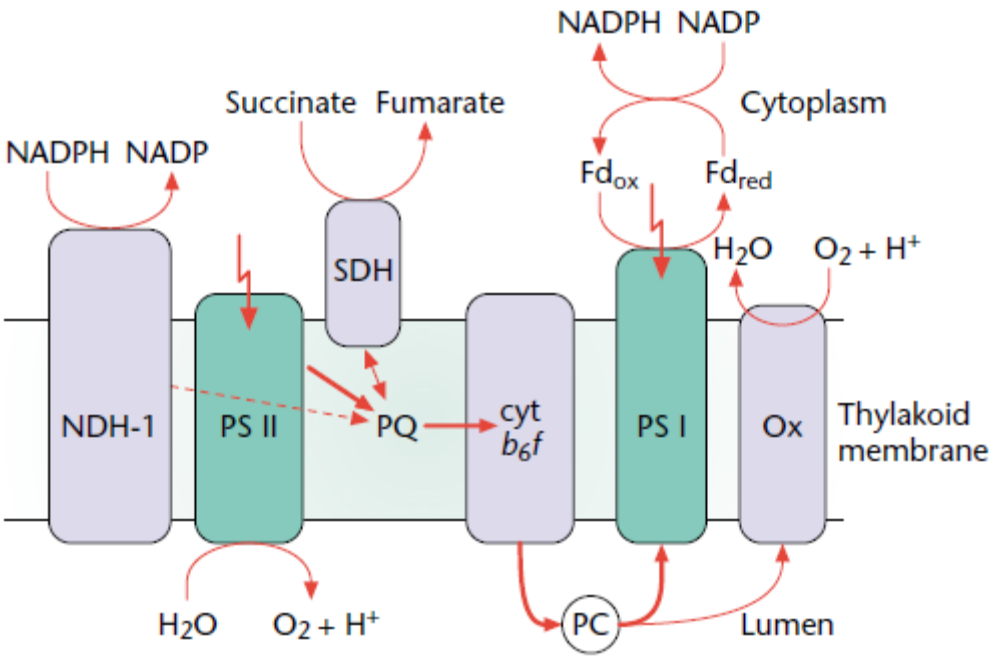

Figure 2 Schematic structure represent photosynthetic and respiration electron pathway in thylakoid membrane of the cyanobacterium *Synechocystis* sp. PCC 6803. The arrow signifies electron transfer pathways, the thunderbolts indicate light that is in the motion within the redox reaction in both photosystem. The thick arrows indicate the rate of the corresponding reactions. Electron transport complexes are PSII and PSI, and for respiration are designated as NDH-1, SDH together with terminal oxidase. PQ, cyt *b6f* and PC are sheering this same electron transport pathway. The arrow drowns in both way indicated SDH electron flow. Abbreviations: cyt b6f, the cytochrome b6f complex; Fdox and Fdred, ferredoxin in oxidized and reduced forms, respectively; NADP(H), nicotinamide – adenine dinucleotide phosphate (reduced form); NDH-1, type 1 NADPH dehydrogenase; Ox, terminal oxidase; PC, plastocyanin; PQ, plastoquinone; PS I, photosystem I; PS II, photosystem II; SDH, succinate dehydrogenase (Wim FJ Vermaas, 2001).

Electron pathway

Photosynthesis began from the light being absorbed by the pigments located on the surface of membrane in the photosynthetic organism. The absorption of lights the first phase in the electron pathway. Photosynthesis can be divided in four phases: first phase is light absorption where the energy transport is performed by antenna system; second phase is primary electron transfer in photosynthetic RC; third phase is energy stabilization carried out by secondary processes; the last phase is synthesis and transport of the final product. In those four phases there is only one phase that depends on the light and it is photon absorption. The other three phases do not hinge on light (Blankenship, 2002).

Energy transfer in antennas

The antenna complex contains various numbers of pigments associated with PSI and PSII. Mostly pigments are connected with proteins using highly specific bonds. The antenna complex may consist of a variety of pigments. The most common pigments are carotenoids and open chain tetrapyrrole found in phycobilisome antenna complex. The main function of the pigments is collecting light and transporting energy to the RC. The antenna systems do not function based on chemistry; they function based on a quantum physical process where excited energy migrates from one pigment to another (Blankenship, 2002; Freer et al., 1996).

Inside the antenna complex the absorbed light energy jumps from one short-wavelength- to other longer-wavelength-absorbing pigments. The short wavelength pigments are located peripherally while the longer wavelength pigments are placed close to the RC. The short wavelength pigments are higher energy pigments and the longer wavelength pigment are lower energy pigments. Therefore the energy transfers accurse from higher to lower pigments. The energy transport creates a unidirectional energy transfer downstream to the spectral gradient (Blankenship, 2002).

The entire surface that is created by the antenna complex increases the amount of absorbed energy compared to a single pigment. In situations of relatively diluted sunlight, an increased absorption surface area enhances the photon absorption. The sunlight hits the surface of the pigments, and the energy is transferred from the pigments to the RC (Blankenship, 2002; Freer et al., 1996).

In order to store the light energy the photon needs to be absorbed by one of the pigments located in photosynthetic complex (Blankenship, 2002)(Freer et al., 1996). The absorbed photon generates an excited state, in which results in charge separation within RC, liberating electrons from H_2O.

Electron transfer in reaction centres

The structure of PSI and PSII contain the RC, where the transformations of pure energy to chemical energy take place. The RC is located in the centers of the two photosystems and is composed of a multi-subunit protein complex-pigment. It integrates chlorophylls and electron transfer cofactors, for example quinines, iron sulfur centers and highly hydrophobic peptides. The RC is consisting of pigment dimer that is the primary electron donor. The dimer pigments are chemically identical to the pigments located in the antenna complex, however

there emplacement gives those dimer pigments distinct characteristics. The final stage of the transport of electron in the antenna complex is the transfer of energy to the dimer pigments. The energy transferred excites the dimer to excited state. The transfer of electrons in the RC is simply described in Figure 3. The excitation of the pigment (P) occurs by direct absorption of a photon which occurs rarely or more likely by transfer energy from the antenna complex. The excited pigment (P*) quickly loses an electron and this is transferred to the closest electron acceptor molecule (A). The transfer generates the ion pair (P^+A^-), known as primary reaction of photosynthesis. Within the primary reaction the electronic excitation has been converted to chemical redox energy. At this point the system is in position to lose the stored energy. In the primary reaction there is a possibility of losing the stored energy because the electron can be transferred back to P^+ from A^-, leading to the conversion of energy into heat and further transport of electrons cannot occur. However the system prevents this reverse electron transport by a series of quick secondary reactions. The secondary reaction performs separation of positive and negative charges. The secondary reaction is placed on the one side of the P+A-where acceptor is located. The result of oxidized and reduced pigments leads to the separation in the distance of the biological membrane. The quantum yield of the product carried out by the absorbed photon is 1.0 in which gives the system perfect efficiency (Blankenship, 2002).

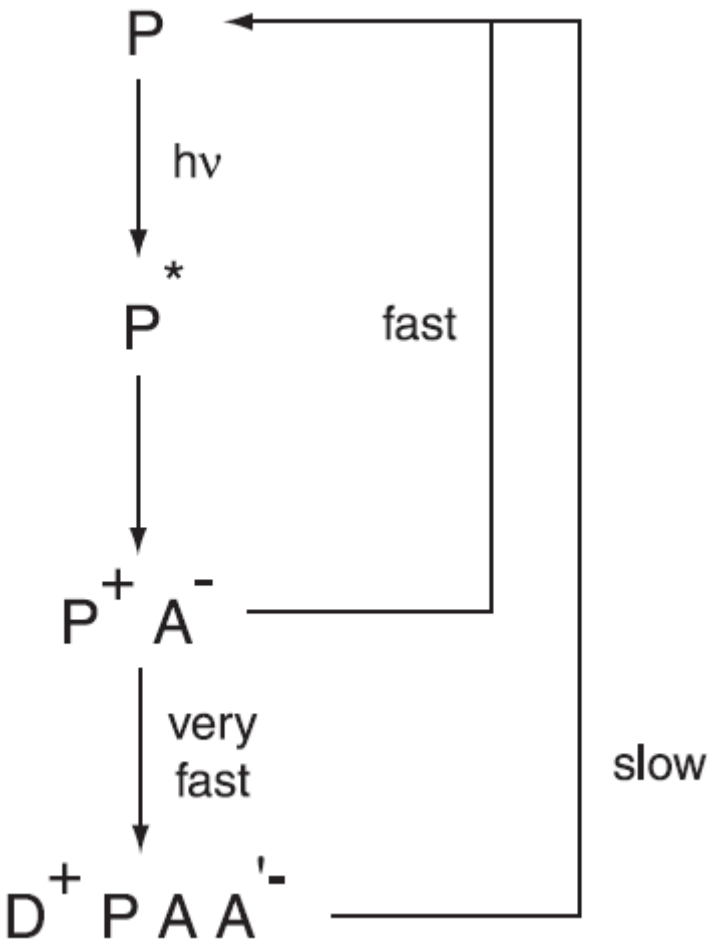

Figure 3 Schematic structure of electron transfer in reaction centers within the photosystems. Light energy excite pigment (P) to an excited state (P*). Excited pigment losses an electron to molecule (A), to form iron-pair state $P^{+}A^{-}$. Secondary reaction separates the charges by electron transfer from the electron donor (D) and from initial acceptor to secondary acceptor (A') (Blankenship, 2002).

Stabilization by secondary reaction

Photosynthesis starts with energy transfer from the excited chlorophyll pigments in the antenna complex to the RC where the acceptor pigment is located. After the excitation energy has been transferred, the rapid series of secondary chemical reaction occur where the separation of positive and negative charge takes place. All the photosynthetic RCs operate based on this reaction principle. However, depending on the photosynthetic organisms in which it is located this may contain a distinct pattern of electron transfer (Blankenship, 2002).

Within some organisms where the one light drives electron transfer and stabilization, the entire cyclic electron transfer chain occurs. Figure 4 shows energy input in the system caused by the photon absorption (vertical arrow) and further more spontaneous electron transfer,

wherein optionally the electron returns to the primary electron donor. In order to obtain a productive cyclic electron transfer process, part of the absorbed energy must be stored. The membrane proton movement and electron transfer results in pH differences or electrochemical gradient on both sides of the membrane. The pH differences and electrochemical gradient is then used in carrying out the synthesis of ATP (Blankenship, 2002).

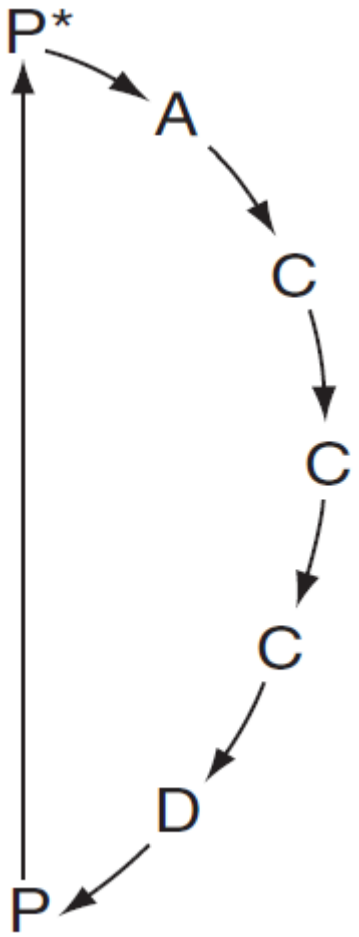

Figure 4 Schematic structure of cyclic electron transfer chain, found in anoxygenic photosynthetic bacteria. The vertical arrows describe photon absorption. P is primary electron donor, D, A and C is secondary donor, acceptor and carriers (Blankenship, 2002).

The oxygenic photosynthetic organisms contain two RC complexes that work simultaneously in noncyclic electron transport chain. The schematic structure of noncyclic electron transport chain is shown in Figure 5. The RCs are located in PSI and PSII. In PSII, oxidation of water molecules takes place and oxygen is released as a byproduct. The extracted electron from the

water molecule is then transferred to PSI. In a matter of few seconds the light driven electron transfer takes place and eventually the intermediate electron acceptor $NADP^+$ is reduced. During the process, protons are transported across the thylakoid membrane creating a pH gradient. The energy is then used to drive the synthesis of ATP (Blankenship, 2002).

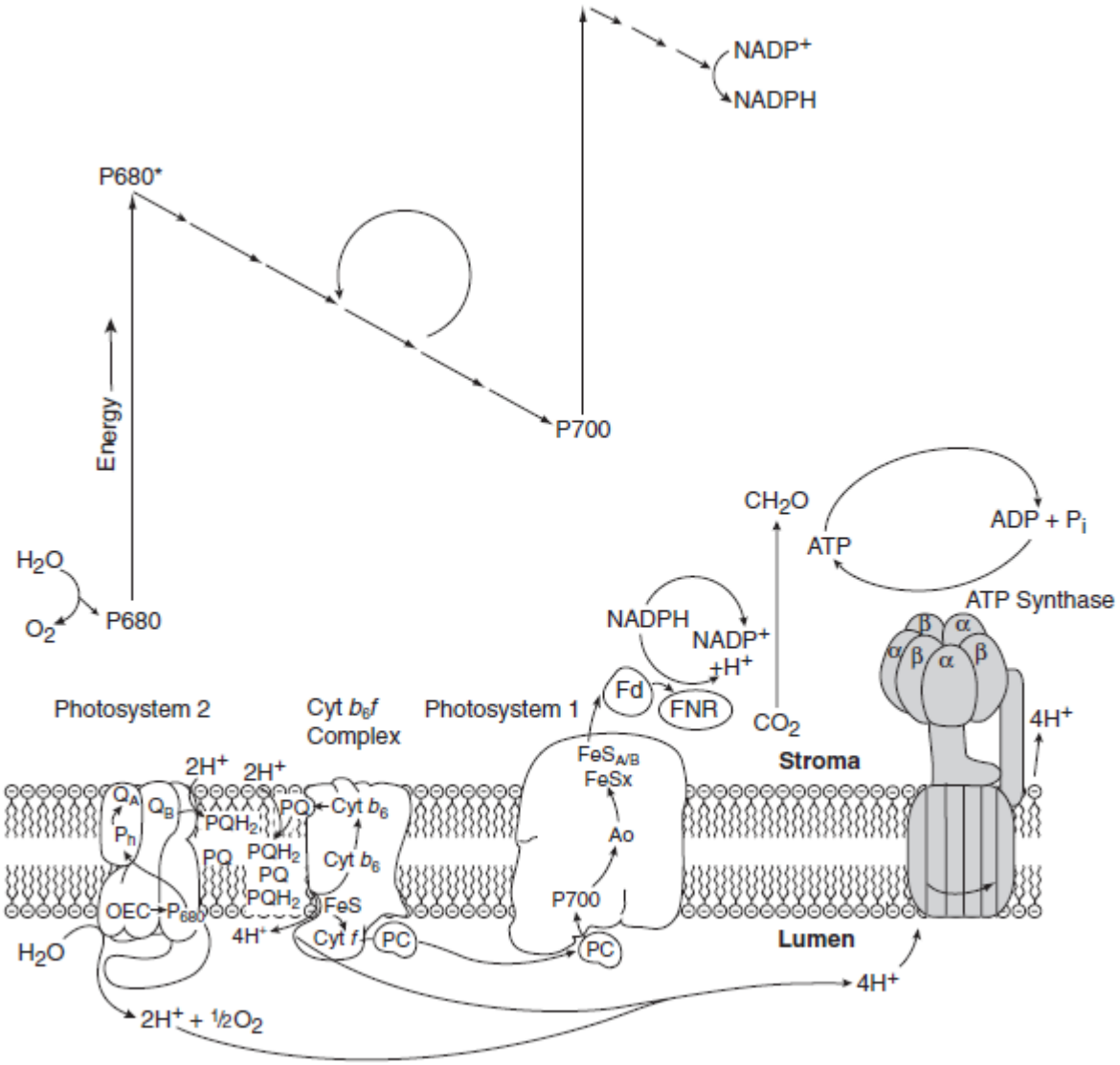

Figure 5 Schematic structure represents noncyclic electron transfer chain, found in oxygenic photosynthetic organisms. (a) General electron transfer pathway. (b) Schematic diagram of protein complexes incorporated in photosynthetic membrane (Blankenship, 2002).

Synthesis and transport of the final product

Synthesis and transport of photosynthetic products is the last phase. The stable product is produced and released to drive all necessary intercellular processes. This phase includes the use of intermediate reduced compound NADPH, which is provided by FNR associated with PSI. Synthesis of the final product requires phosphate bond energy from ATP which is responsible for carbon fixation [Figure 6]. Therefore, sugar and carbon can be assimilated by the photosynthetic organism (Blankenship, 2002).

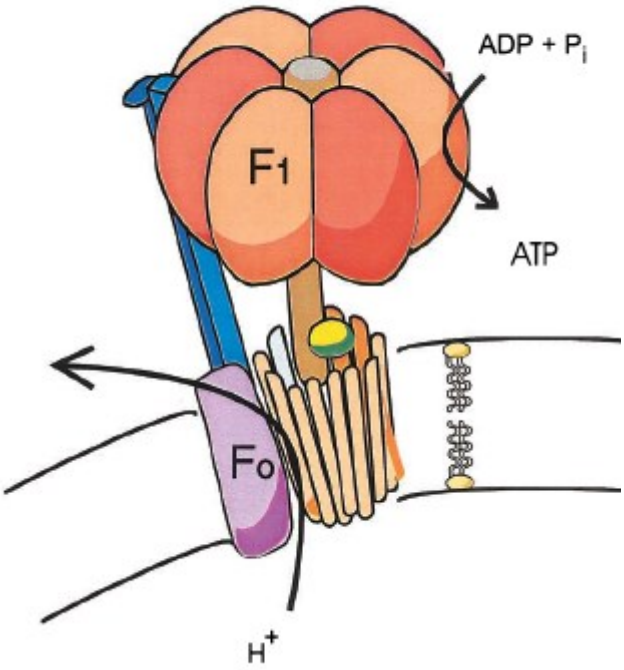

Figure 6 Structure of the ATP synthase enzyme (Blankenship, 2002).

Components

Within the photosynthetic membrane two complexes convert the light energy into chemical energy for the photosynthetic organism. The two compounds are called PSI and PSII.

PSII

Photosystem II is one of the most important complexes for all living organisms that inhabit the Earth. It carries out the process of water oxidation, where the water molecule is split into hydrogen and oxygen gas. The reaction scheme is shown in Eq.1.

$$2H_2O + 2PQ \rightarrow O_2 + 2PQH_2 \quad (1)$$

where PQ indicates oxidized plastoquinone and PQH is reduced plastoquinone(Blankenship, 2002). Evolved oxygen is released into the atmosphere and the energy that is obtained from this process is used for further chemical reactions by PSI. The water oxidation is carried out by oxygen-evolving complex (OEC). The OEC is composed of tetranuclear Mn cluster, where four oxidizing equivalents are captured from photochemical reaction within the photoactive pigments (Blankenship, 2002).

The structure of the PSII protein complex is shown in Figure 7. Within the complex proteins D1 and D2 can be distinguished as main core subunits. PSII also contains many other associate proteins, in which the function role for most is not clear yet. Therefore, the experiments were performed where many proteins have been deleted from the photosystem complex, even though these mutants showed the same growth as the wild-type organisms. Those mutants show tremendous ability to grow, and insignificance of the subunits within the photosystem.

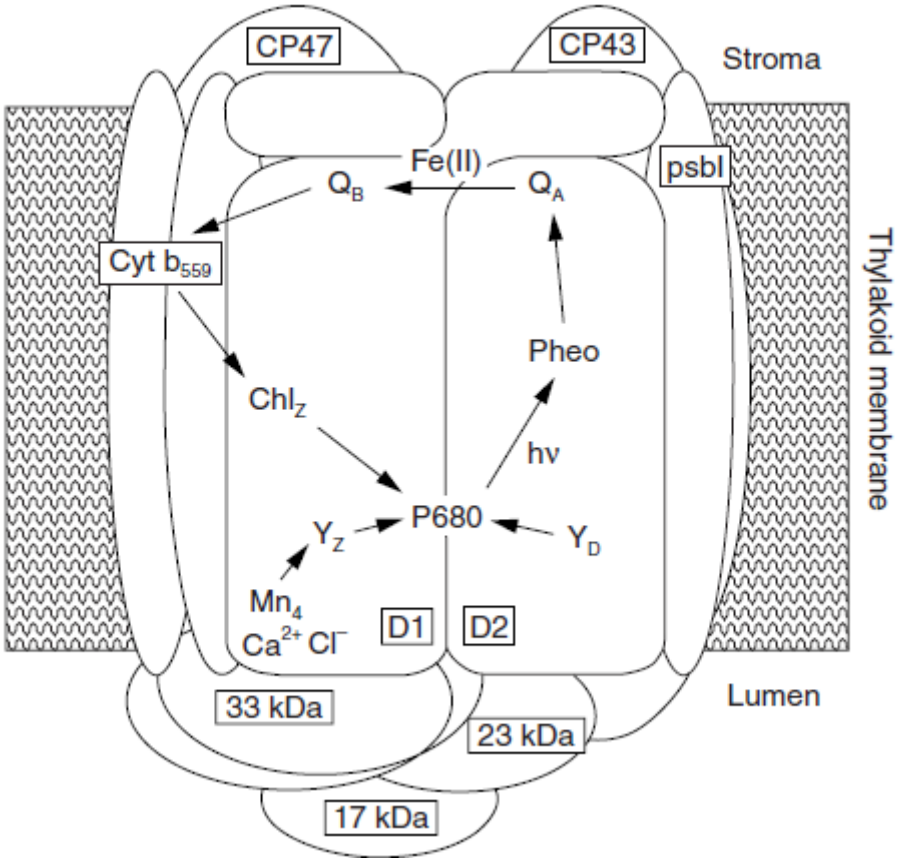

Figure 7 Schematic structure of photosystem II, the protein subunits are indicated by name or by molecular masses. More characteristic of protein are given in text (Blankenship, 2002).

The PSII RC consists of proteins D1 and D2, cytochrome b_6f and small peptide PsbO gene product. The peptide PsbO is the one of the units that has been studied for a long time compared with cytochrome b_{559} in which the function role is not yet known. The PSII RC also includes β-carotene, six chlorophyll *a* molecules, two pheophytin *a* molecules, and the two core antenna complexes CP43 and CP47 (Blankenship, 2002).

In a large number of photosynthetic organisms the antenna complex shows a wide variation. Therefore, it is used to define the groups of photosynthetic organisms. The large number of antenna complex shows different variation of the structure and as well types of the pigments. The antenna complex mostly contains pigment-bound proteins, where the pigments and proteins are bound in the specific structure complex. The antenna complex can be divided into two groups: integral antenna complex and peripheral antenna complex. The integral antenna complexes consist of the proteins that pass through the lipid bilayer. The peripheral antenna complexes contain the proteins that do not pass through the membrane, but these complexes are attached to the thylakoid membrane. This type of the antenna complex can be

found in cyanobacteria and red algae. Phycobilisomes are an example of such peripheral antenna complexes (Freer et al., 1996).

A various numbers of the phycobilisome are found in photosynthetic organisms. The hemidiscoidal phycobilisome is one of the types of the phycobilisomes which it is well studied. The structure of the phycobilisome is shown in Figure 8. The structure of the phycobilisome includes biliproteins and linkers. The biliproteins are two or three pigment-proteins while the linker consists of a group of proteins associated with antenna complexes. The biliproteins have three different types: allophycocyanin and phycocyanin (van Thor, Gruters, Matthijs, & Hellingwerf, 1999). Allophycocyanin form the center of the antenna complex, where the phycocyanin is connected to the core and where the phycoerythrin is attached to the phycocyanin. All together forms the rods of the phycobilisome (van Thor et al., 1999)(Blankenship, 2002) (Srivastava et al., 2013).

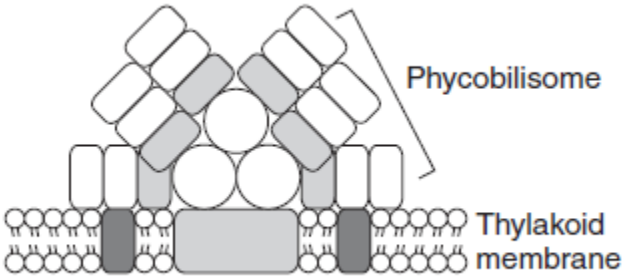

Figure 8 Schematic structure of Phycobilisome (Blankenship, 2002)

PSI

Photosystem I is integral protein complex of the membrane, where the light is being absorbed and used for electron transfer from plastocyanin to ferredoxin. The high resolution structure of PSI is known from X-ray crystallographic studies. The crystallographic studies where performed at 2.5 Å resolutions. The PSI complex found in cyanobacteria it consist of ninety six chlorophyll a molecules, twenty two β-carotenes, twelve protein subunits, four lipid molecules, three [4Fe-4S] clusters and two phylloquinone (Xu et al., 2011)(Blankenship, 2002)

Within the PSI RC electron transfer occurs between primary electron donor P-700 and acceptors: A0 (chlorophyll), A1 (a phylloquinone) and Fx, Fa and Fb (4Fe-4S iron-sulphur centres). P700 is a dimmer of chlorophyll a molecules and Spa and Past are the two main subunits of the PSI. These subunits form the core of PSI where bind to the P700 and electron acceptors A0, A1 and Fix. In order to stabilized the entire complex the core binds to other additional cofactors. The Pac is peripheral protein bind Far and Fib. When the electrons reach the PSI it generates excited state of P700 in which leads to charge separation. Electron is then transferred to A0, A1 and furthermore to series of three clusters where ultimate reaches a ferredoxin molecule. On the lumen side of thylakoid membrane the PSI complex recessive electron that was donated from the plastocyanin. In cyanobacteria and algae the plastocyanin can be replace by cytochrome c6 under specific condition. In order to maintain the structure of RC proteins environment around P700 plays important role. Furthermore, P700 plays major function in granting special properties of the P700 chlorophyll pair, and in electron transfer from the cytochrome c6 to P700 (Xu et al., 2011).

Aim of the project

The aim of this project is to develop concepts to separate photosynthetic hydrogen production from oxygen production. For this the student will generate and strains deficient in the photosystems (PSI and PSII) that mediate oxygen production and hydrogen production, respectively. The growth will be conducted to evaluate the effect of different metals on the growth of each of the mutants. The potential to interfacing these two strains via artificial and natural electron transport systems will be evaluated.

2 Material and Methods

Material and Methods

The *Synechocystis* sp. PCC 6803 cells were cultured on BG11 agar plates contained 5 mM glucose **(**Table 2), 20 am atrazine (for selected strains)(Table 3), and appropriate antibiotic were added if necessary. BG-11 liquid cultures containing 5 mM glucose and appropriate antibiotic were added if necessary (Table 1). The liquid cell cultures were aerated by an aquarium pump (Figure 9). The air was filtrated through distilled water which maintained hydration of the cultures. Both liquid and agar plates with cell cultures were grown under continuous illumination 30 $\mu E.m^{-2}.s^{-1}$ at 30°C.

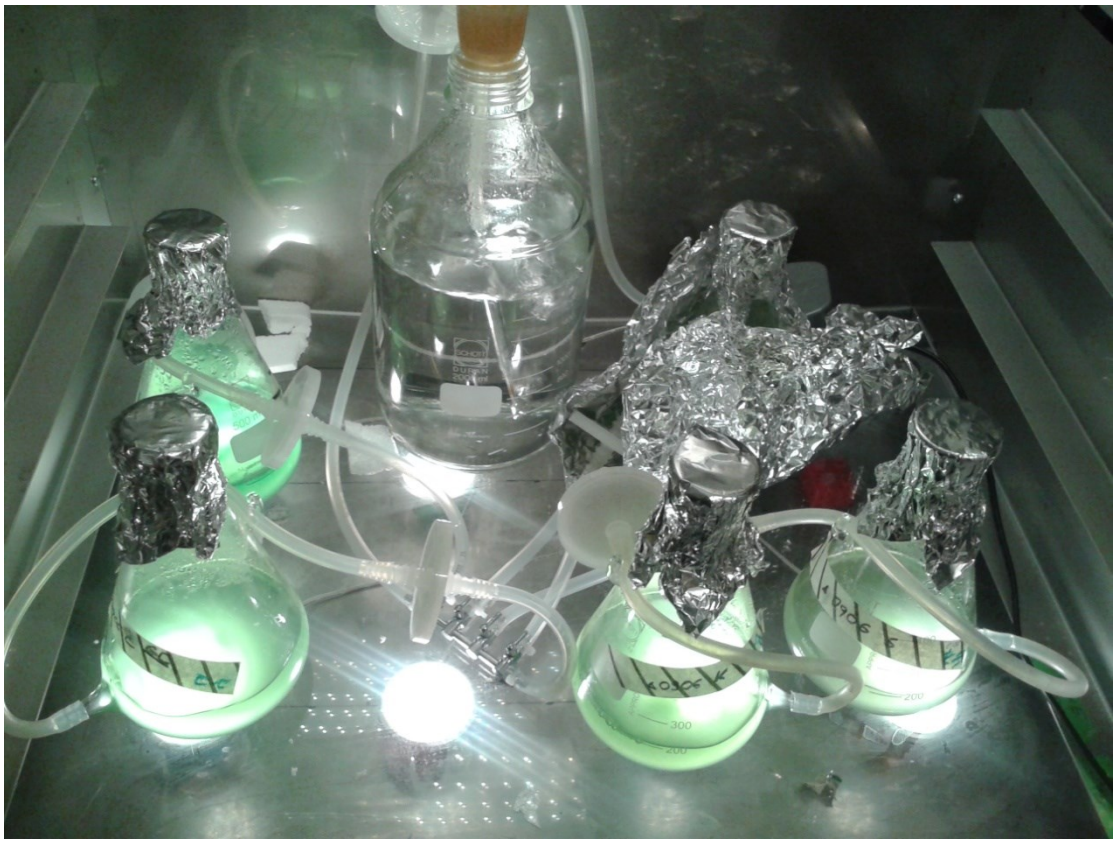

Figure 9 BG11 liquid cell cultures incubated under continuous illumination (30 $\mu E.m^{-2}.s^{-1}$) at 30°C.

Medium constituents:

BG-11 agar plates: BG-11 liquid media supplemented with 10 mM TES-Noah (pH 8.2); 0.3 % sodium thiosulfate; 1.5 % bacteriological agar.

100x BG-11**:** 1.76 M $NaNO_3$; 30.4 mM $MgSO_4.7H_2O$; 24.5 mM $CaCl_2{\cdot}2H_2O$; 2.86 mM $C_6H_8O_7$ (citric acid); 0.25 mM Neeta, (pH 8.0); 10 % (v/v) trace minerals, deionized water.

Trace Minerals**:** 42.26 mM H_3BO_3; 8.9 mM $MnCl_2.4H_2O$; 0.77 mM $ZnSO_4.7H_2O$; $Na_2Mo0_4{\cdot}H_20$; 0.32 mM $CuSO_4{\cdot}5H_2O$; 0.17 mM $Co(NO_3)_2{\cdot}6H_2O$.

BG-11 liquid media: 1x BG-11; 6 μg mL^{-1} ferric ammonium citrate (~16 mM final concentration); 20 μg mL^{-1} Na2CO2; 30.5 μg mL^{-1} K_2HPO_4.

Table 1 Antibiotics required for the Selection of *Synechocystis* sp. PCC 6803 Strains.

Antibiotic	Stock concentration	Final concentration	dilution factor
Kanamycin	50 mg / mL (water)	25 ug / mL	2000
Spectinomycin	50 mg / mL (water)	25 ug / mL	2000
Chloramphenicol	30 mg / mL (ethanol)	15 ug / mL	2000

Table 2 The carbon source for the selection of Synechocystis sp. PCC 6803 Strains.

Carbon source	Stock concentration	Final concentration	dilution factor
Glucose	1M (water)	5mM	200

Table 3 Herbicide for selection of strains *Synechocystis* sp. PCC 6803.

Herbicide	Stock concentration	Final concentration	dilution factor
Atrazin	20 mM (methanol)	20 uM	1000

Plasmid Construction

The primes were design for each deletion gene *slr1834-1835* and *slr0906* together with overlapping sequences containing (Figure 10-11). Plasmid contained left flanking region, antibiotic resistance cassette, right flank region and Litmus backbone.

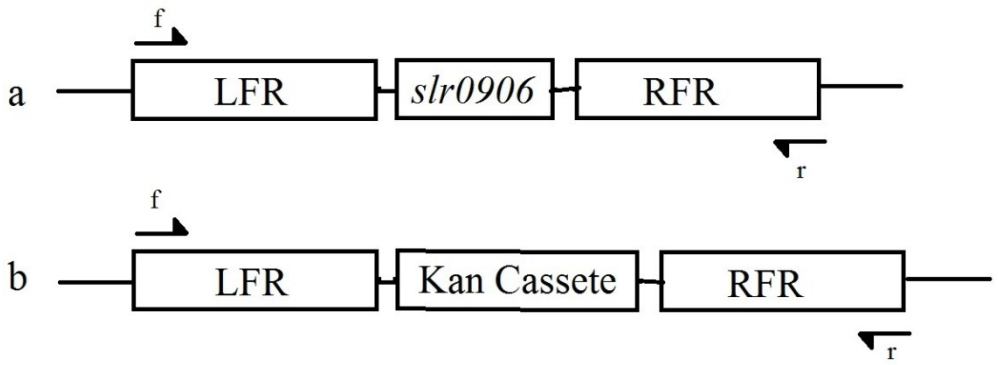

Figure 10 *slr0906* Genomic Deletion. (A) The wild-type genomic DNA map of the *slr0906* gene relative to the left flanking region (*LFR*) and the right flanking region (*RFR*) used for homologous integration of the kanamycin resistance cassette. (B) The genomic DNA map after homologous recombination of the kanamycin-resistance cassette. The relative position of both pLitmus-slr0906-Kan left fragment forward (f) and right fragment reverse (r) primers used for genotyping have been shown (Author self resource).

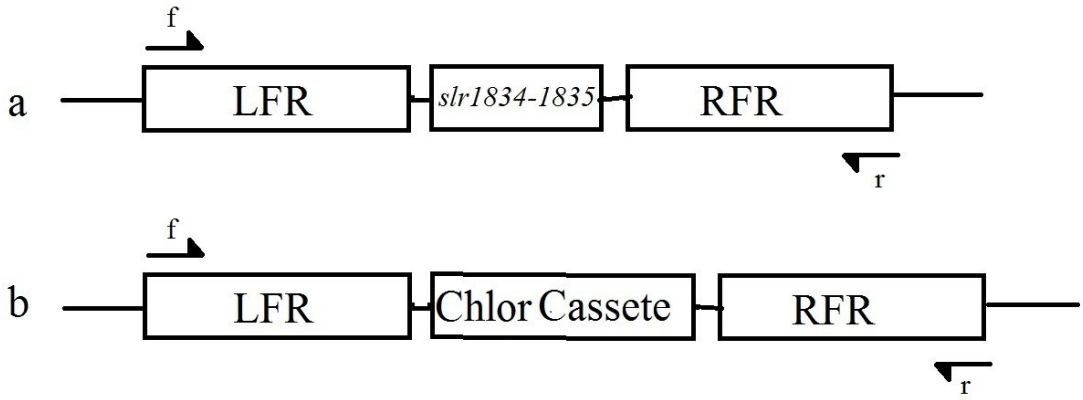

Figure 11 *slr1834-1835* Genomic Deletion. (a) The wild-type genomic DNA map of the *slr1834-1835* gene relative to the left flanking region (*LFR*) and the right flanking region (*RFR*) used for homologous integration of the chloramphenicol resistance cassette. (b) The genomic DNA map after homologous recombination of the chloramphenicol -resistance cassette. The relative position of both pLitmus-slr1834-1835-Chlor left fragment forward (f) and right fragment reverse (r) primers used for genotyping have been shown (Author self resource).

.

*slr*0906-Deletion

slr0906 left flank forward	cccagtcacgacGGAATGCCACAAGAACATCAAG
slr0906 left flank reverse	acaacgtggcggccgcAACCGAACAAGACAGACAGAG
Kanamycin-resistance cassette forward	gttcggttgcggccgcCACGTTGTGTCTCAAAATCTC
Kanamycin-resistance cassette reverse	atgctggggcggccgcTACAACCAATTAACCAATTCTG
slr0906 right flank forward	tggttgtagcggccgcCCCAGCATCGGGAGATTTAG
slr0906 right flank reverse	gctatgaccatgCCAGTTCCTGTTGTAGGTTGTA
Litmus forward	aacaggaactggCATGGTCATAGCTGTTTCC
Litmus reverse	ttgtggcattccGTCGTGACTGGGAAAACC

*slr*1834 + slr1835 Deletion

s*lr1834 + slr1835* left flank forward	cccagtcacgacTCCCAAGTTGCCCTACCTATAC
slr1834 + slr1835 left flank reverse	acaacgtggcggccgcGGCAAGACCTGCGTAACAATAA
Kanamycin-resistance cassette forward	gtcttgccgcggccgcCACGTTGTGTCTCAAAATCTC
Kanamycin-resistance cassette reverse	aatcgaacgcggccgcTACAACCAATTAACCAATTCTG
s*lr1834 + slr1835* right flank forward	tggttgtagcggccgcGTTCGATTAGGGCAGGGATATG
s*lr1834 + slr1835* right flank reverse	gctatgaccatgGGTCAACCTGCGACAGAATTA
Litmus forward	cgcaggttgaccCATGGTCATAGCTGTTTCC
Litmus reverse	ggcaacttgggaGTCGTGACTGGGAAAACC

Colony PCR

Synechocystis sp. PCC6803 cells were used as a template for amplification by colony PCR. The reactions were performed together with fallowing compounds: Phusion High-Fidelity DNA polymerase, dNTP, polymerase buffer and primers. PCR conditions were: (1) initial denaturing step at 98°C for 10 min (length of time is to ensure rupture of cells and denaturation of intracellular proteins); (2) 14 cycles of 98°C for 30 s, annealing at 62°C (-1°C per cycle) for 30 s, extension at 72°C for 30 s/kb; (3) 16 cycles of 98°C for 30 s, annealing at 62°C for 30 s, extension at 72°C for 30 s/kb; then (4) final extension at 72°C for 5 min. PCR products were separated by gel electrophoresis using gel green and visualized under UV light illumination.

Separation of DNA Samples by Gel Electrophoresis

Samples of DNA were separated by electrophoresis using 0.8% agarose gels in the presence of 20 µl GelGreen per 300 ml of gel. The conditions were: 95 V for 60 min. Prior to loading, samples were mixed with 10×loading buffer (0.25% bromophenol blue, 0.25% xylene cyanol FF and 30% glycerol).The DNA was visualized by exposure to a UV light. Gel images were captured using a GelDoc (BioRad, Molecular Imager, and ChemiDoc XRS+) with Image lab 4.1 software.

Cleaning the sample by PCR purification kit

The DNA samples were cleaned using QIA quick PCR purification kit. To one volume of PCR reaction, 5 volumes of the buffer PB were added and mixed. To bind DNA, samples were transferred into 2 ml collection tubes and centrifuged at full speed for 1 min. The supernatant was removed and XX µL of the buffer PE was added. Samples were centrifuge for 1 min, the supernatant was removed and the samples were centrifuge once again for 1 min. To elute DNA, buffer EB was added and incubated on the bench for at least1 min. The samples were then centrifuged and pure DNA samples were stored at -20 °C.

Nano-drop measurement

Two-to-three microliters of deionized water was applied onto the lower measurement pedestal to clean the sensor. Then using the nucleic acid application on the computer, a 1.5 µL aliquot of the blanking buffer was loaded onto the lower measurement pedestal. The sampling arm was lowered and the spectra measurement was initiated using software on the PC. The samples were then pipette with the volume of 1.5 µL directly onto the measurement pedestal and the spectra measurement where initiated. The software automatically calculated the nucleic acid concentration and purity ratios.

DNA ligation by Gibson assembly

All DNA fragments where ligated using Gibson assembly. The total concentration of DNA fragments that were assembled was 0.2 pmoles. To calculate the number of pmols of each fragment for optimal assembly the following formula was used:

pmols = (weight in ng) x 1,000 / (base pairs x 650 daltons)

50 ng of 5000 bp dsDNA is about 0.015 pmols.

50 ng of 500 bp dsDNA is about 0.15 pmols.

The concentration (ng per µL) of each fragment can be measured using the NanoDrop instrument. The sample was then incubated in a thermocycler at 50°C for 60 min.

Escherichia coli transformation

The competent cells of *E.coli* were prepared for transformation. The vector DNA was added to the culture and incubated. The cultures were transferred onto the solid LB media and growth incubated overnight at 37°C. The samples were verified by enzymatic digestion and visualized on agarose gel.

Making *E.coli* Competent Cells

A DH5α culture was inoculated with 20 mL SOC Media at 37°C.The overnight DH5α culture was transferred into 300mL of pre-warmed ΨB media and allowed to grow to OD_{600} between 0.3 – 0.4. Cells were then incubated on ice for 5 min, transferred to two pre-chilled 50 mL falcon tubes and centrifuged for 10 min at 4000 rpm at 4°C. In each tube, the supernatant was discarded and cells were resuspended with15 mL chilled TfBI buffer on ice and centrifuged immediately for 10 min at 4000 rpm, 4°C. Cell pellets were gently resuspended with 1 mL of chilled TfBII. Competent cells were snap frozen using liquid nitrogen in aliquots of 100 µL and stored in a -80°C freezer.

TfBI *buffer:* (30 mM potassium salt, 50 mM $MnCl_2$, 100 mMRbCl, 1mM $CaCl_2$, 14% glycerol, pH 5.8)

TfBII *buffer*: (10 mM MOPS, 75 mM $CaCl_2$, 1mM RbCl, 15% glycerol, pH 7.0)

Heat-shock transformation of *E.coli*

Frozen competent cells were thawed on ice for 5-10 min. Vector DNA was added, and cells were incubated on ice for a 30 min. Cells were then transferred to 37°C incubator for 2 min followed by a further 3 min incubation on ice. Cells at this point were then transferred into 2 mL LB media and left at 37°C with ~220 rpm shaking for 90min on an orbital culture shaker. The cell culture was plated directly onto an agar plate with appropriate antibiotics. Plates were inverted and incubated overnight at 37°C. The samples were verified by digestion with Not1 and visualized on 0.8% agarose gel.

DNA extraction

Transformed *E.coli* cells were used as a template for amplification in PCR. The reaction conditions are identical for those one used in colony PCR for *Synechocystis* sp. PCC 6803.

Transformation of Synechocystis sp. PCC 6803

A started culture was set up with an OD_{730} of 0.25 and grown overnight at 30°C, irradiation 30 $\mu E.m^{-2}.s^{-1}$. The OD_{730} of the culture was measured the following morning to be between 0.4 – 0.6. The cells were transferred to sterile 50 mL tube and spun down in the centrifuge set to 2500 g at room temperature. The OD_{730} was measured, the supernatant was discarded, and the cells were concentrated to an OD_{730} of 5.0. Five hundred microliters of culture was placed into sterile test tubes. The transformation DNA was added to each test tube and mixed gently. The tubes were transferred to a growth chamber at 30°C for six hours, with gentle mixing at 3 hours. Sterile filters (NucleporeTrak-Etch Membrane SN: 145318) were placed onto BG-11 + Glucose plates. The entire contents in test tubes were distributed onto the sterile filter that had been placed onto a BG-11 + Glucose plate. The samples were left to dry in the sterile hood for ~30 minutes and incubated overnight at 30 °C with 30 $\mu E.m^{-2}.s^{-1}$The filters were transferred to BG11 medium containing appropriate antibiotics, glucose and atrazine. After three or four weeks single colonies were picked and streaked-out weekly for three weeks to ensure complete segregation. Colony PCR was used to verify complete segregation.

Colony PCR and Sequencing

The colony PCR was used to isolate the sequence fragment. The 30 µl of fragment containing deletion mutation along with 5 µl of 5 pmol of primer were send for sequencing to GATC.

Growth experiment

The media for growth experiment were made with different iron and manganese source under the light and dark condition (Figure 12). The wild–type and strains were cultured and spotted on plates with OD 1 and 0.1. The plates with variation of iron and manganese sources were subjected to everyday shooting by camera. The parameter of growth rate was measured using custom program.

Figure 12 Starting from the left plates incubated under dark condition, covered with aluminum foil. From the right plates incubated under the light condition.

Media for growth experiment

The agar plates were prepared with 10 different conditions, six different iron source and four different manganese source exposed to the darkness. Four plates were prepared in combination of different iron and manganese sources and exposed to the light. The iron solutions were made containing six different irons at 18 mM of iron (Table 6). The manganese solutions were made containing four different manganese sources, 14 mM of manganese (Table 7). The calculated amount of ingredients was added and supplemented with dH_2O up to a volume of 100 mL. The agar plates were made together with ingredients used in BG11 media, with slight modification. Some modifications of fallowed media were preformed. The trace minerals were prepared with $MnCl_2$ substituted by NaCl (Table 4). The trace mineral were used to make special 100X BG11, without $MnCl_2$ (Table 5). The order of added media has been maintained: liquid media were added first, iron solution second and then solid media.

Table 4 Trace minerals. The elements were added and supplemented to volume of 1liter.

Element	Mass in milligrams
H_3BO_3	2.86
$ZnSO_4$	0.22
Na_2MoO_4	0.39
$CuSO_4$	0.079
$Co(NO_3)_2$	0,049
NaCl	1.07

Table 5 100X BG11. The mixture was supplemented to volume of 100 mL.

Element	Mass in milligrams	Mass in milliliters
$NaNO_3$	14.95	x
$MgSO_4$	0.75	x
$CaCl_2$	0.36	x
Citric acid	0.06	x
NaEDTA	x	0.11
Trace minerals (no $MnCl_2$)	x	10

Table 6 Iron sources. The mixture was supplemented to volume of 100 mL.

Iron solution	Mass in milligrams
1000X ammonium iron (II) citrate	600
1000X geothite	159
1000X ion (II) oxide	129
1000X ion (II, III) oxide	143
1000X potassium hexacyanoferrate (III)	99
1000X iron (III) chloride hexahydrate	486

Table 7 Manganese sources. The mixture was supplemented to volume of 100 mL

Iron solution	Mass in milligrams
1000X MnCl2	181
1000X Mn (III) oxide	111
1000X Mn (IV) oxide	122
1000X Mn (II, III) oxide	107

Growth experiment exposed to darkness

Media for agar plates with different iron sources and manganese are showed in Table 8.

Table 8 Media compositions for dark growth experiment. Symbol x – refers added ingredient, blank space – no added ingredient. Plates were numerated from one to ten (Author self resource).

Media	Ingredients	Amount of added ingredients	Plate number	1	2	3	4	5	6	7	8	9	10
			Name of metal sources	Mn (II, III) oxide	$MnCl_2$	Mn (III) oxide	Mn (IV) oxide	Iron (III) chloride hexahydrate	Potassium hexacyanoferrate (III)	Iron (II, III) oxide	Iron (II) oxide	Geothite	Ammonium iron (III) citrate
Liquid media	100X BG11 (w/o Mn, Fe, Phosphate or Carbonate)	100 µl		x	x	x	x	x	x	x	x	x	x
	1000X $NaCO_3$	100 µl		x	x	x	x	x	x	x	x	x	x
	1000X K_2HPO_4	100 µl		x	x	x	x	x	x	x	x	x	x
	1000X $MnCl_2$	100 µl		x	x	x	x	x	x				
	1M TES/NaOH buffer pH 8.2	1mL		x	x	x	x	x	x	x	x	x	x

	Glucose	500 µl		x	x	x	x	x	x	x	x	x	x
	1000X ammonium iron (III) citrate	100 µl								x	x	x	x
Solid media	Na-thiosulfate	0.3 g		x	x	x	x	x	x	x	x	x	x
	Agar	2 g		x	x	x	x	x	x	x	x	x	x
Iron solutions	1000X ammonium iron (III) citrate	100 µl											x
	1000X geothite	100 µl										x	
	1000X iron (II) oxide	100 µl									x		
	1000X iron (II, III) oxide	100 µl								x			
	1000X potassium hexacyanoferrate (III)	100 µl							x				
	1000X iron (III) chloride hexahydrate	100 µl						x					
Manganese solution	1000X MnCl2	100 µl			x								
	1000X Mn (III) oxide	100 µl				x							
	1000X Mn (IV) oxide	100 µl					x						
	1000X Mn (II, III) oxide	100 µl		x									

Growth experiment exposed to light

The combinations of iron and manganese sources are showed in Table 9.

Table 9 Media compositions for light growth experiment. Symbol x - refers added ingredient, blank space – no added ingredient (Author self resource).

Media	Ingredients	Amount of added ingredients	Plate numbers	1	2	3	4	5	6	7	8	9	10
			Name of metal sources	Mn (II, III) oxide	MnCl2	Mn (III) oxide	Mn (IV) oxide	Iron (III) chloride hexahydrate	Potassium hexacyanoferrate (III)	Iron (II, III) oxide	Iron (II) oxide	Geothite	Ammonium iron (III) citrate
Liquid media	100X BG11 (w/o Mn, Fe, Phosphate or Carbonate)	100 µl		x	x	x	x	x	x	x	x	x	x
	1000X $NaCO_3$	100 µl		x	x	x	x	x	x	x	x	x	x
	1000X K_2HPO_4	100 µl		x	x	x	x	x	x	x	x	x	x
	1M TES/NaOH buffer pH 8.2	1mL		x	x	x	x	x	x	x	x	x	x
	Glucose	500 µl		x	x	x	x	x	x	x	x	x	x
Solid media	Na-thiosulfate	0.3 g		x	x	x	x	x	x	x	x	x	x
	Agar	2 g		x	x	x	x	x	x	x	x	x	x
Iron and Manganese solutions mix	1000X ammonium iron (III) citrate + 1000X $MnCl_2$	100 µl											x
		100 µl			x								
	1000X ammonium iron (III) citrate + 1000X Mn (IV) oxide	100 µl											x
		100 µl					x						

	1000X iron (II) oxide + 1000X $MnCl_2$	100 µl									x		
		100 µl			x								
	1000X iron (II) oxide + 1000X Mn (IV) oxide	100 µl									x		
		100 µl					x						

Llabelling Petri dish with media for different variants

To maintain the order of performed pictures in a further step of growth experiment the plates with different variants [Table 8] were numbered from one to ten. The dotted line were made to separate two different concentration of the cells that was spotted. The arrow was positioned perpendicular to the dotted line to visualize the started point of spotted dots on the plate (Figure 13).

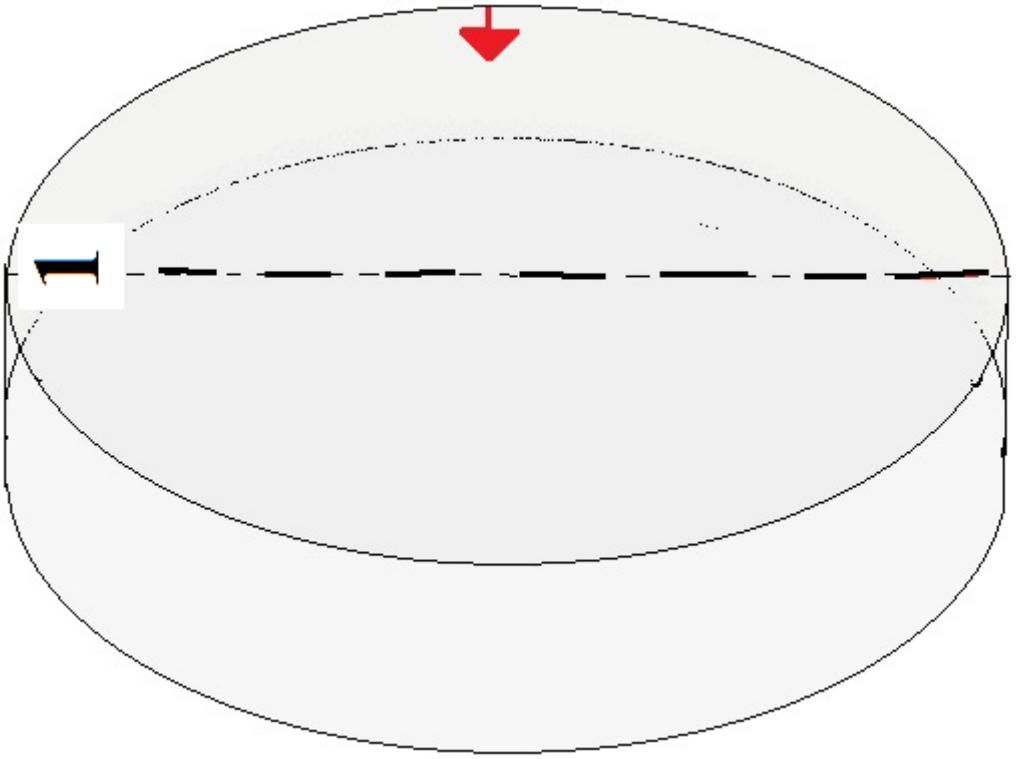

Figure 13 The petri plate with technical markings. The dotted line separates the sample application of the various dilutions, arrow represents startup dilution OD 1 (Author self resource).

.

Spotting

The mutant's Δslr1834-1835, Δslr0906 and wild-type were cultured to an OD 2.0. The 1 ml of each culture was transferred to eppendorf tube, and spin at 3000 g-force for 5 minutes. The supernatant were discarded and samples were resuspended with 1 ml of liquid BG11 medium. Each sample was measured using a spectrophotometer at 730nm. The cultures were diluted to an OD of 1 and 0.1. The samples were spotted in three replicates for each type at volume of 3 µl on the plate (Figure 14). The plates were leaved to dry completely in sterile hood. The plates were placed in 30°C incubator at constant illumination (30 $\mu E.m^{-2}.s^{-1}$).

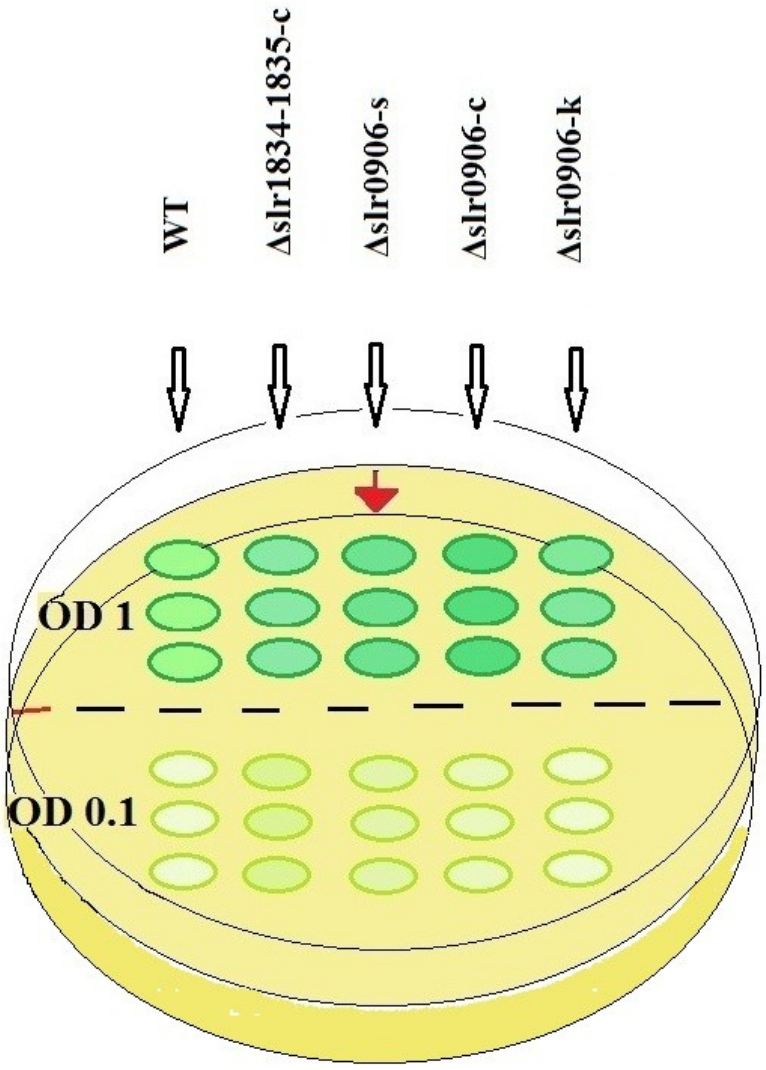

Figure 14 Petri dish with graphic representation of wild-type and mutants dots at OD 1 and 0.1 (Author self resource).

Plates image

The wild-type and mutants grown on media were placed on the custom-build stage and subjected to light source from beneath. Digital cameras were placed above the stage, targeted the plates (Figure 15).

Figure 15 Custom-build stage. Plate with one of the iron or manganese sources placed on stage, where the digital camera is positioned vertically from the top.

Growth measurement

The captured images were stored on memory card as JPEG and CRW formats. The custom program was used to generate a growth curve.

3 Results

Results

The wild-type *Synechocystis* sp. PCC6803 was used to generate deletion mutants of Δslr0906 (Figure 16, 18). The Δslr1834-1835 strain was ordered from the University of Otago, New Zealand (Figure 17).

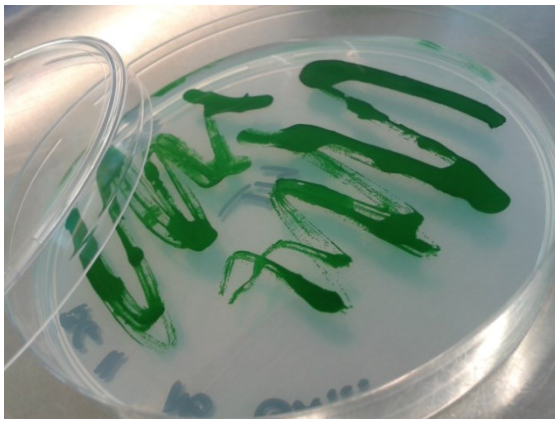

Figure 16 Wild-type *Synechocystis* sp. PCC6803 growth on BG11 solid media.

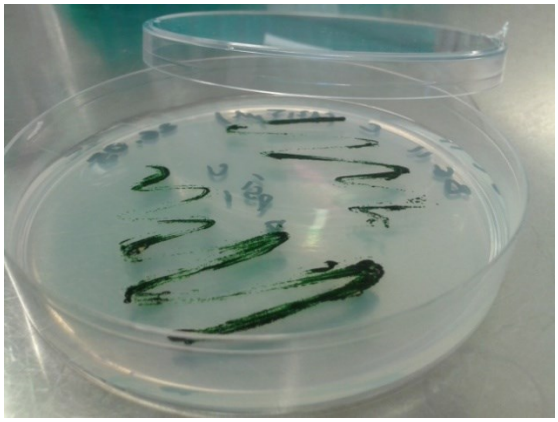

Figure 17 Δslr1834-1835 mutant grown on BG11 solid media supplemented with appropriate antibiotic, atrazine and glucose.

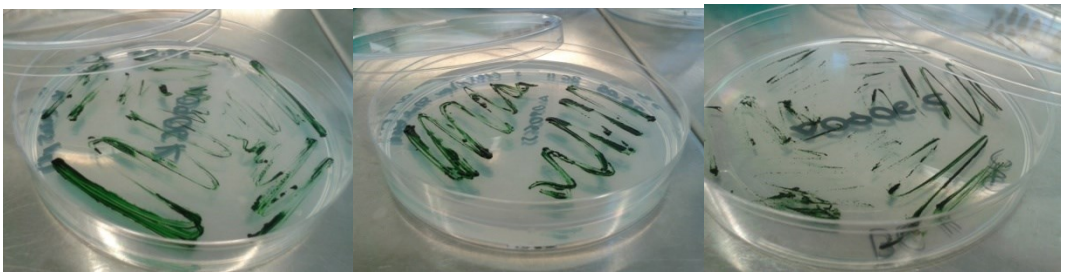

Figure 18 Δslr0906 grown on BG11 solid media supplemented with appropriate antibiotic and glucose. From the left: Δslr0906-k (Kanamycin), Δslr0906-s (Spectinomycin) and Δslr0906-c (Chloramphenicol).

Plasmid construction

The PCC6803 colony PCR with adequate primers was conducted. The electrophoresis gel image conformed product of knockout gene *slr0906*. The construct samples contains fragment of left flanking regions and right flanking region. The Litmus plasmid was used to generate kanamycin resistance cassette. The QIA quick PCR purification kit was used to purify DNA samples. The nano-drop measurement was used to measure concentration of the DNA fragments. The Gibson assembly was used to ligate DNA fragments, each samples has 0.2 pmoles. The plasmid containing DNA fragments with deleted mutation of *slr*0906 gene was constructed.

E.coli transformation

The deletion construct was transferred into *E. coli* DH5α by heat–shock transformation. The transformed cells were grown on the LB media; total 2 colonies appeared after 24 hours incubation at 37°C. The two colonies was transfer on the LB media, large number of colonies appeared after 24 hours incubation at 37°C. The digestion with restriction enzyme Not 1 conformed transformation (Figure 19). The restriction enzyme Not 1 cut the sequence in two places, on each end of the Litmus fragment, therefore the samples will have two bands one with ~3700 bp and second approximately 1000 bp. The colony PCR was used to extract DNA fragment containing *slr0906* gene deletion from transformed *E.coli* cells.

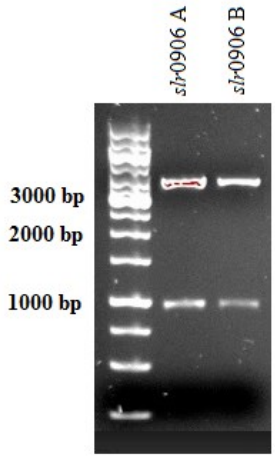

Figure 19 Gel electrophoresis image representing *E.coli*+*slr*0906 gene samples after *E. coli* minipreps, digested by Not1. The *slr*0906 A and B are the samples duplicated.

Synechocystis sp. PCC6803 transformation

The wild-type *Synechocystis* sp. PCC6803 was used, to grown starter cultures to OD 5. The transformation DNA was added on the sterile filters that were placed onto BG11 plates with glucose. The cells showed grown on the filters after 24 hours incubation at 30°C (Figure 20). These sterile filters were used to transfer onto new BG11 media with the corresponding antibiotic; couple colonies appeared after four weeks of incubation at 30°C (Figure 21). The colony PCR were used to verify complete segregation and transformation of PCC6803, the gel electrophoresis image were generation to confirm deletion of mutant Δslr0906 (Figure X). The Sequencing GATC was used and conformed sequence of inserter plasmid. The mutants were transferred on new BG11 media with appropriate antibiotic and leave to growth in order to maintain cell culture.

Figure 20 PCC6803 strains distributed throughout the whole filter, grown on BG11 media. The green surface is visible conforming cell growth.

Figure 21 Gene transformed into PCC6803. Green colonies are visible, which confirmed the complete transformation.

Synechocystis sp. PCC6803 mutants

The Δslr0906 mutant has deletion of *slr0906* gene, which is responsible in production of core light harvesting protein in photosystem II (Figure 23). In order to function properly the light reaction required iron as an essential component. Likewise, iron plays important function in photosynthetic electron transfer in cyanobacteria. The Δslr1834-1835 mutant has deletion of *slr1834-1835* gene, which is responsible for production P700 apoprotein subunit Ia and Ib in photosystem I. The main function of the protein is metal ion binding (Figure 22) (Briat et al., 1995).

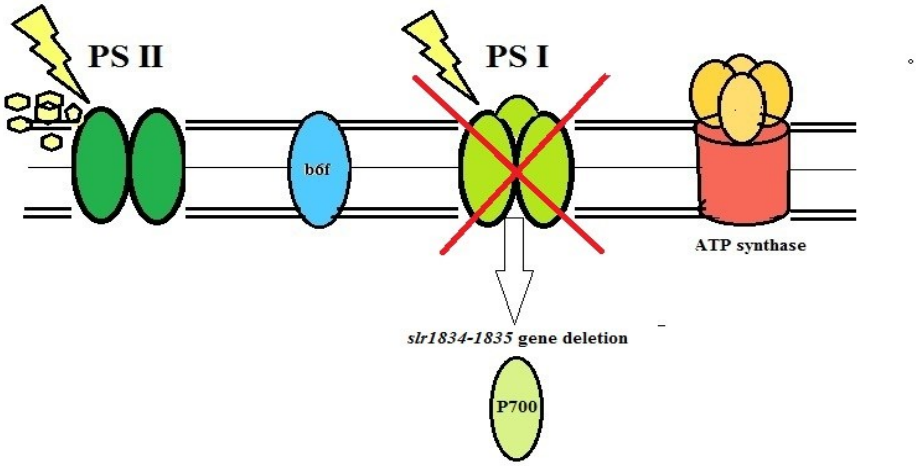

Figure 22 Photosystems simple graph describing active PSII complex and inactivated PSI complex in cyanobacteria. The deletion of *slr1834-1835* gene, encode P700 apoprotein in photosystem I. The red-cross indicated inactive photosystem (Author self resource).

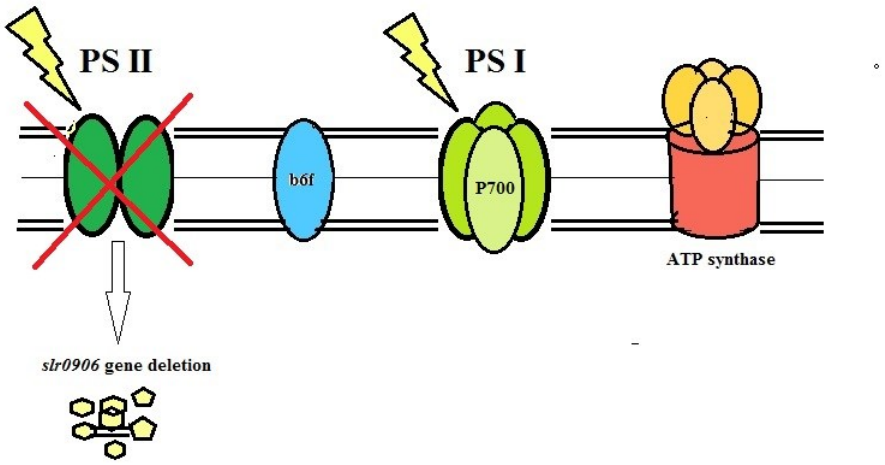

Figure 23 Photosystems simple graph describing active PSI complex and inactivated PSII complex in cyanobacteria. The deletion of *slr0906* gene, encodes core light harvesting protein in photosystem II. The red-cross indicated inactive photosystem (Author self resource).

Growth experiment under different iron and manganese sources

The conducted research showed a significant impact on the growth of the cyanobacterium in both iron and the manganese sources. The growth of the *Synechocystis* sp. PCC6803 strains were studied under one of the fallowed ingredients: iron sources (ammonium iron (III) citrate, goethite, iron (II) oxide, iron (II, III) oxide, potassium hexacyanoferrate (III), iron (III) chloride hexahydrate) and manganese sources (MnCl2, Mn (III) oxide, Mn (IV) oxide, Mn (II, III) oxide. Experiments were performed from the cultures grown on liquid BG11 medium and were dilute to an OD 1 and 0.1. The agar plate was used to spot-on the three microliters of samples in three replicates. In each experiment, growths of all the strains were obtained. Agar plates were imaged using digital camera once per day. The results were plotted into the graphs using commercial program. The generated graphs are showing below, error bars denote standard deviation (SD). The antibiotic resistance cassettes were inserted as needed in strains, shortcut description of antibiotics is presents as follows: c – Chloramphenicol, s – Spectinomycin and k – Kanamycin. All detailed data (values of cell density) are shown in appendix.

Dark condition

The *Synechocystis* sp. PCC6803 wild-type, and the mutant's Δslr1834-1835-c and Δslr0906-c, -s, -k was grown and exposed to the dark condition over a period of eight days (Figure 24). The plates were cover using aluminum foil (Figure 12). Analysis of wild-type and mutants showed an increase in concentrations of cells density along with the time axis in incubator at 30°C.

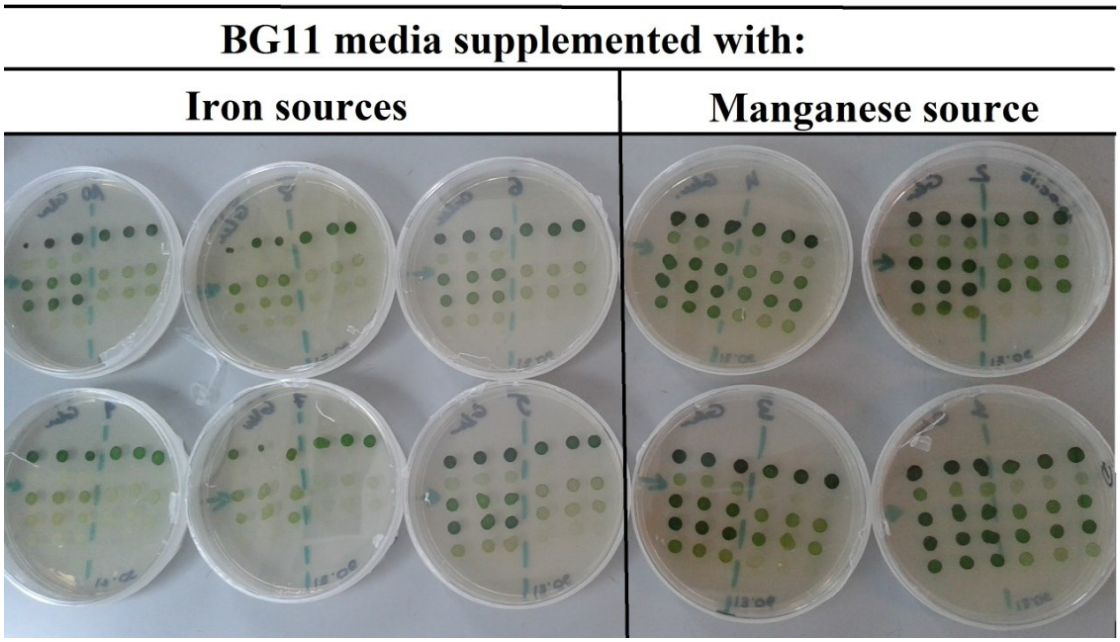

Figure 24 Growth experiment carried out under the dark condition. Order of spotted strains is shown in Figure 14.

Manganese (II, III) oxide

The strains growth curves were observed on the plates with the solid medium supplemented with manganese (II, III). The samples were diluted to an OD 1, the growth curves are showed in Figure 25. Initially in the first three days the wild-type and Δslr0906-c showed the negative volume of cell density, -98 and -39.7. The third day (71.1 h) to the second day (118.5h) of incubation showing significant increase of cell density in almost all of the strains. The Δslr0906-s in particular showing decreased growth (309.7 - cell density) on this media along with the time axis.

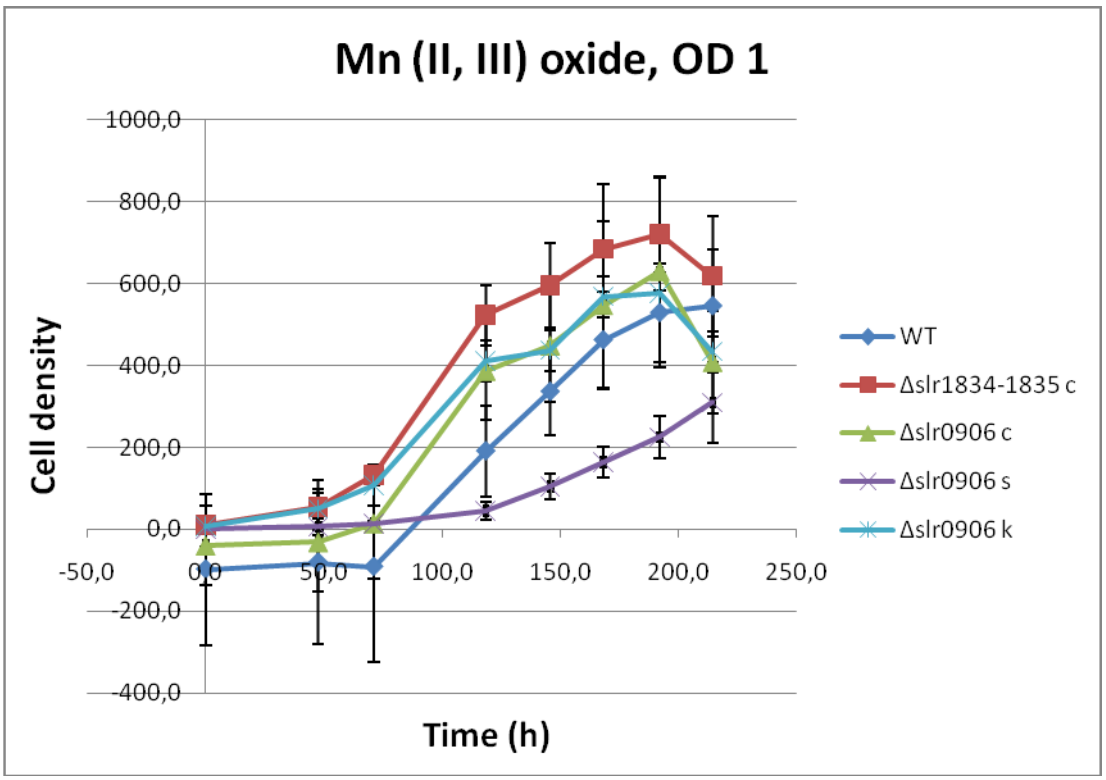

Figure 25 Growth curves of strains grown on manganese (II, III) oxide source in dark condition at 30°C. The optical density spotted strains is one. In the chart are shown error bars, marked as black lines. The error bars represent the lowest and highest values of cell density in each of the time points.

The strains growth curves were observed on the plates with the solid medium supplemented with manganese (II, III) oxide. The samples were diluted to an OD 0.1, the growth curves are showed in Figure 26. The wild-type demonstrate minuses growth along the time axis. It is noticeable that the Δslr1834-1835-c spotted on this medium with this dilution factor showed the most increased cell density up to 600. Other strains showed increase growth curve.

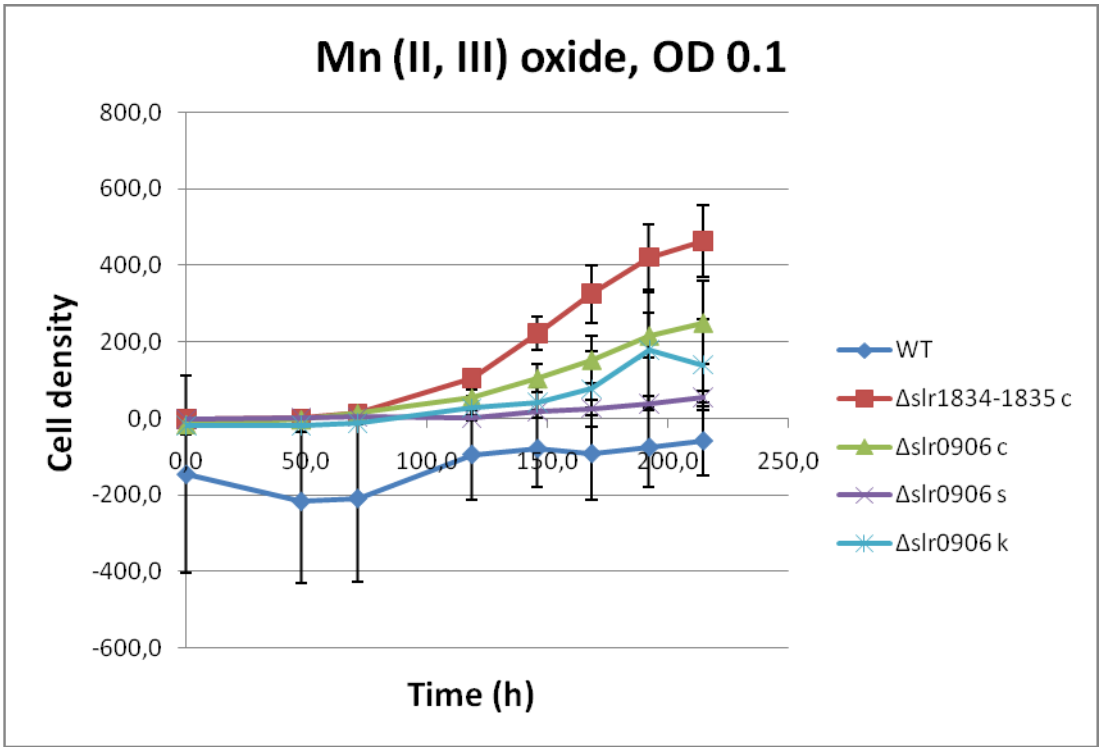

Figure 26 Growth curves of strains grown on manganese (II, III) oxide source in dark condition at 30°C. The optical density spotted strains is 0.1. In the chart are shown error bars, marked as black lines. The error bars represent the lowest and highest values of cell density in each of the time points.

Manganese (II) chloride

The strains growth curves were observed on the plates with the solid medium supplemented with manganese (II) chloride. The samples were diluted to an OD 1, the growth curves are showed in Figure 27. The Δslr1834-1835-c and Δslr0906-c,-k showed equal high growth curve up to 800 of cell density. The strains wild-type showed stable growth, however Δslr0906-s growth curve is minimal comparing to the others.

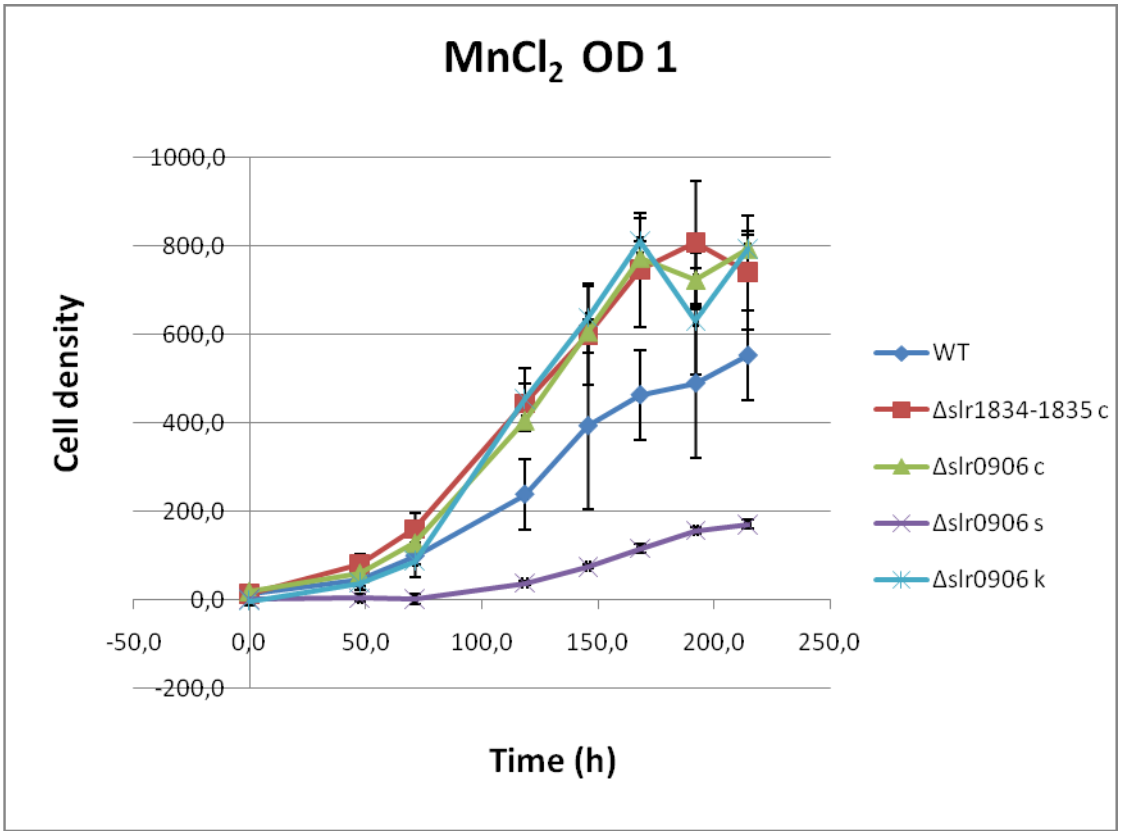

Figure 27 Growth curves of strains grown on manganese (II) chloride source in dark condition at 30°C. The optical density spotted strains is one. In the chart are shown error bars, marked as black lines. The error bars represent the lowest and highest values of cell density in each of the time points.

The strains growth curves were observed on the plates with the solid medium supplemented with manganese (II) chloride. The samples were diluted to an OD 0.1, the growth curves are showed in Figure 28. The Δslr0906-k showed decreasing growth curve in till 71.1 hours, however the growth curve between 192.1 h and 214.5 hours of incubation showing steady increased growth. The other strains showed stable growth curve along the time axis wherein the Δslr1834-1835-c increasing cell density.

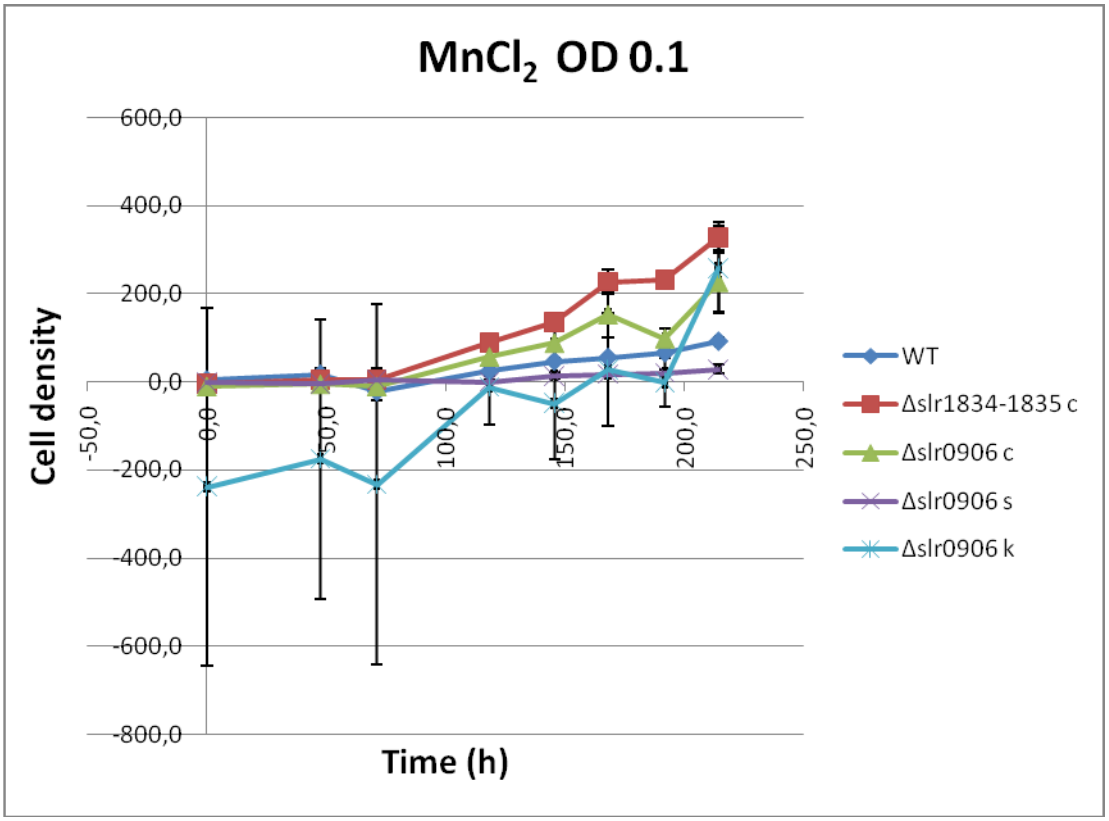

Figure 28 Growth curves of strains grown on manganese (II) chloride source in dark condition at 30°C. The optical density spotted strains is 0.1. In the chart are shown error bars, marked as black lines. The error bars represent the lowest and highest values of cell density in each of the time points.

Manngeses (III) oxide

The strains growth curves were observed on the plates with the solid medium supplemented with manganese (III) oxide. The samples were diluted to an OD 1, the growth curves are showed in Figure 29. The Δslr1834-1835-c and Δslr0906-c,-k showed equal high growth curves up to 800 cell density. The wild-type showed decreased growth up to 400 of cell density. The Δslr0906-s showed decreasing but significant growth at 100 of cell density along the time axis.

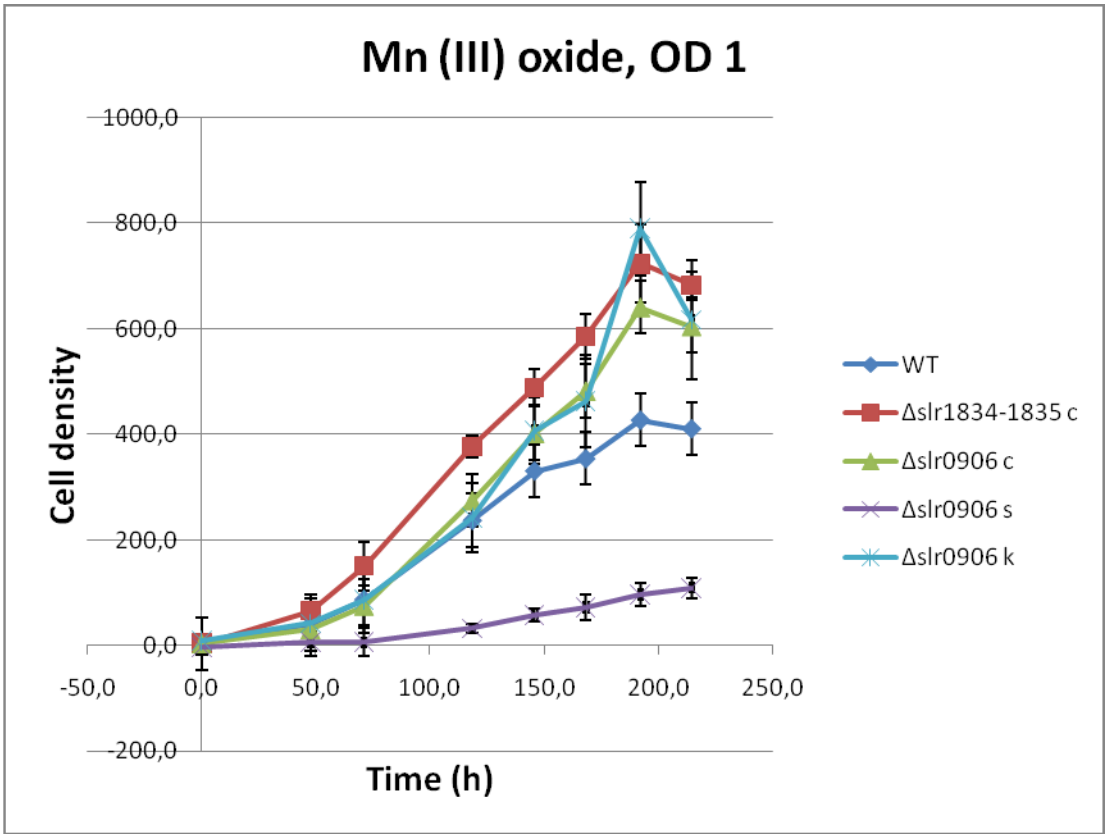

Figure 29 Growth curves of strains grown on manganese (III) oxide source in dark condition at 30°C. The optical density spotted strains is one. In the chart are shown error bars, marked as black lines. The error bars represent the lowest and highest values of cell density in each of the time points.

The strains growth curves were observed on the plates with the solid medium supplemented with manganese (III) oxide. The samples were diluted to an OD 0.1, the growth curves are showed in Figure 30. The Δslr1834-1835-c and Δslr0906-k showed the growth at 200 of cell density. The Δslr0906-c showed the growth at 114 cell density. The wild-type and Δslr0906-s showed growth approximately at 20 of cell density.

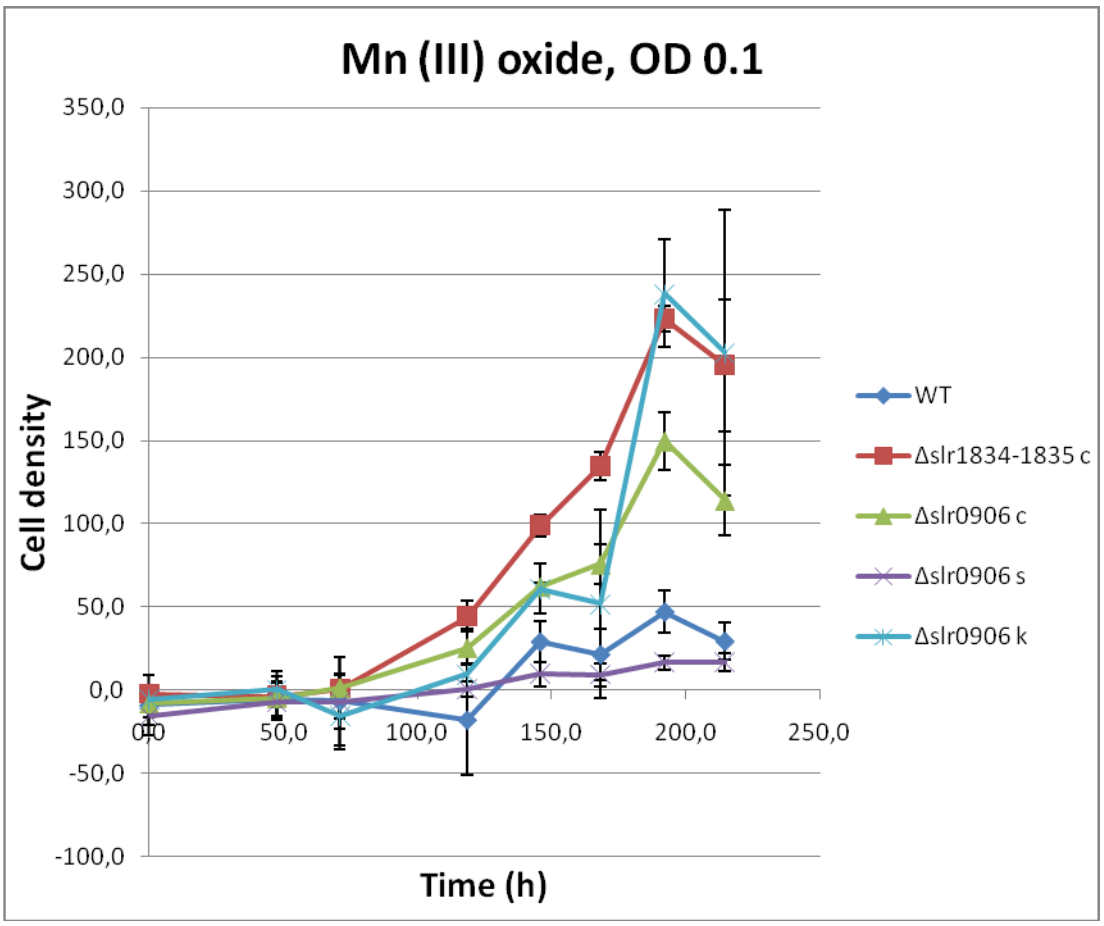

Figure 30 Growth curves of strains grown on manganese (III) oxide source in dark condition at 30°C. The optical density spotted strains is 0.1. In the chart are shown error bars, marked as black lines. The error bars represent the lowest and highest values of cell density in each of the time points.

Manganese (IV) oxide

The strains growth curves were observed on the plates with the solid medium supplemented with manganese (IV) oxide. The samples were diluted to an OD 1, the growth curves are showed in Figure 31. The wild-type, Δslr1834-1835-c and Δslr0906 c showed increased growth, however after 144.5 hours the growth curve is decreasing. The Δslr0906-k showed increased growth till 120.6 hours of incubation subsequently decreasing. The Δslr0906-k showed stable growth along the time axis.

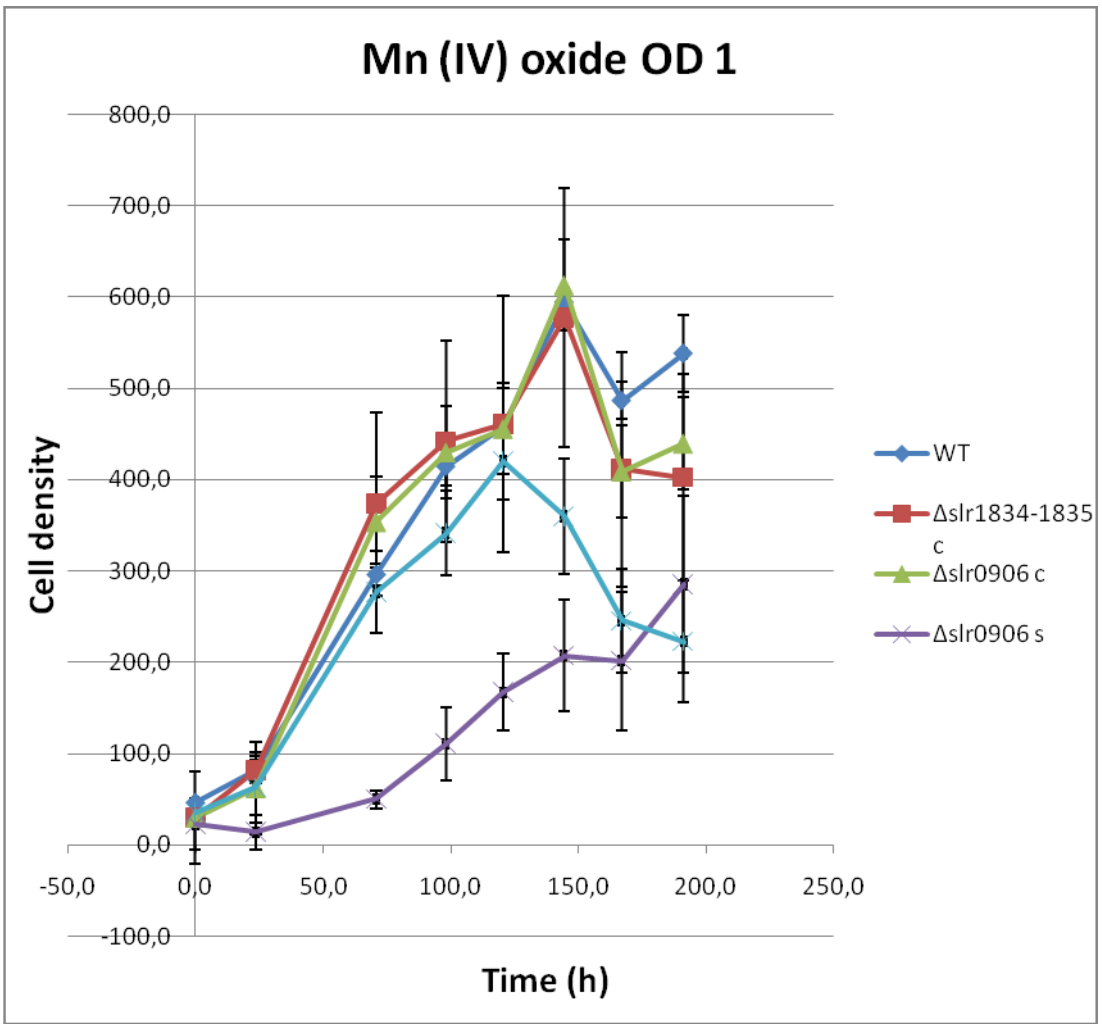

Figure 31 Growth curves of strains grown on manganese (IV) oxide source in dark condition at 30°C. The optical density spotted strains is one. In the chart are shown error bars, marked as black lines. The error bars represent the lowest and highest values of cell density in each of the time points.

The strains growth curves were observed on the plates with the solid medium supplemented with manngeses (IV) oxide. The samples were diluted to an OD 0.1 the growth curves are showed in Figure 32. The wild-type, Δslr0906-c,-k and Δslr1834-1835-c showed increasing growth after 145.7 hours of incubation, however the growth stabilized and decrease. The Δslr0906s growth curve showed minimal of cell density along the time axis.

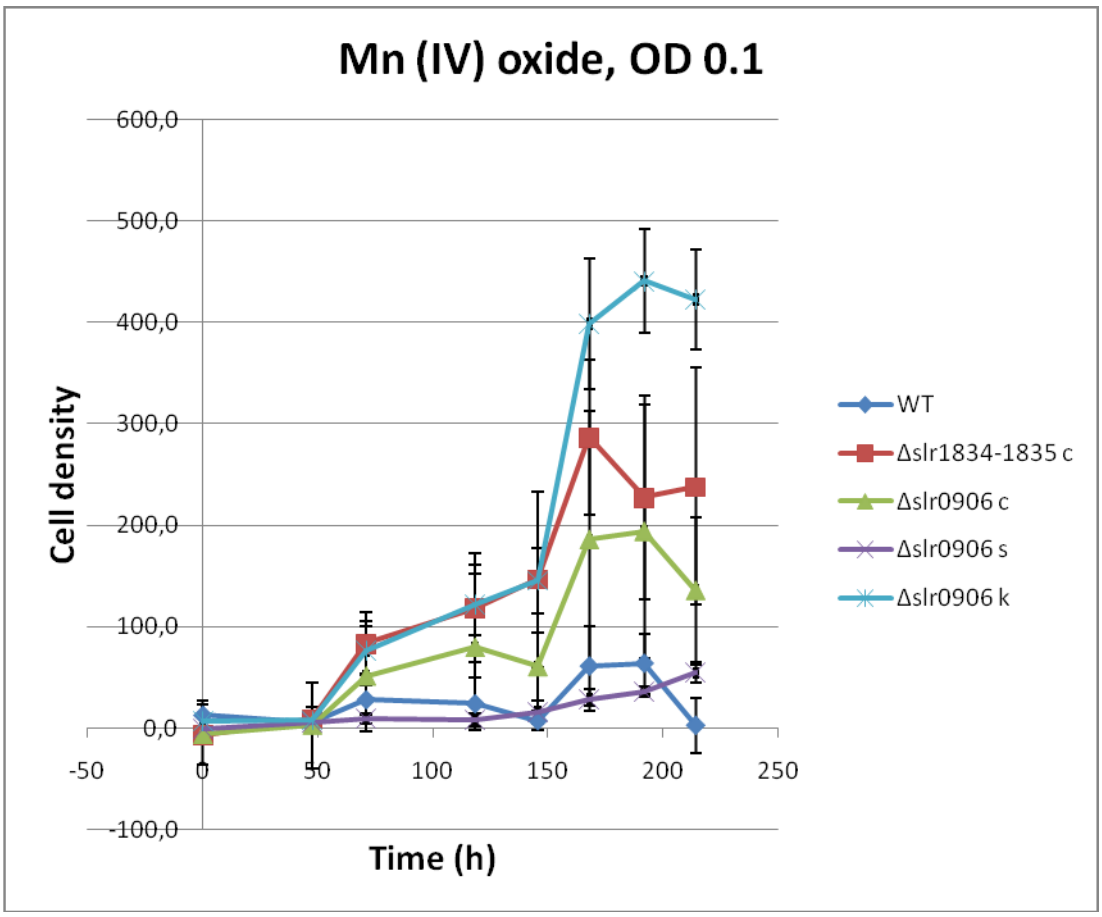

Figure 32 Growth curves of strains grown on manganese (IV) oxide source in dark condition at 30°C. The optical density spotted strains is 0.1. In the chart are shown error bars, marked as black lines. The error bars represent the lowest and highest values of cell density in each of the time points.

Iron (III) chloride hexahydrate

The strains growth curves were observed on the plates with the solid medium supplemented with iron (III) chloride hexahydrate. The samples were diluted to an OD 1 the growth curves are showed in Figure 33. The Δslr0906-s showed the decreasing growth along with the time axis. The wild-type, Δslr0906-c,-k and Δslr1834-1835-c showed increasing growth, however the Δslr0909k showed efficient growth up to 600 of cell density.

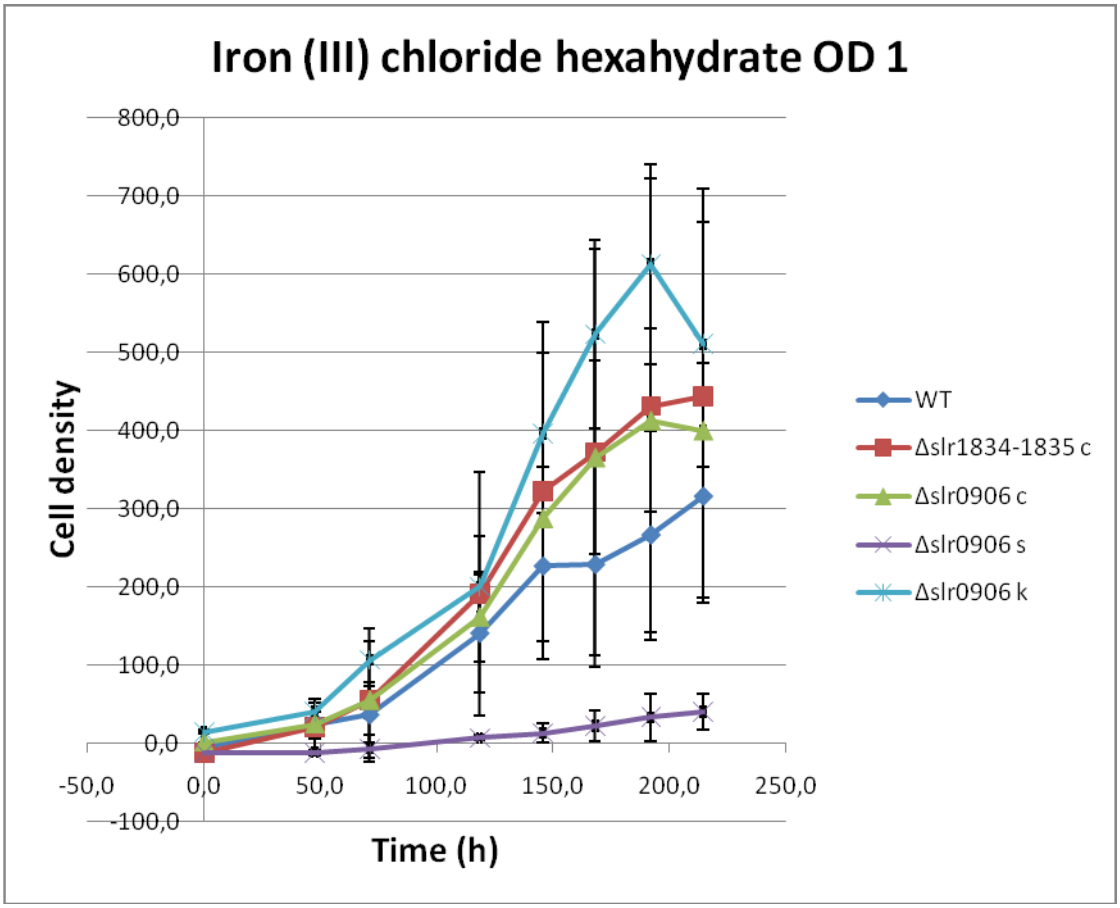

Figure 33 Growth curves of strains grown on iron (III) chloride hexahydrate source in dark condition at 30°C. The optical density spotted strains is one. In the chart are shown error bars, marked as black lines. The error bars represent the lowest and highest values of cell density in each of the time points.

The strains growth curve was observed on the plates with the solid medium supplemented with iron (III) chloride hexahydrate. The samples were diluted to an OD 0.1 the growth curves are showed in Figure 34. The wild-type and Δslr0906-c,-s showed decreasing growth along the time axis. The Δslr0906-k showed the decreased growth till 118.5 hours of incubation, however after this time growth stabilized and increased, also in the same time this strain showed the higher growth rate. The Δslr1834-1835-c showed increased growth along the time axis.

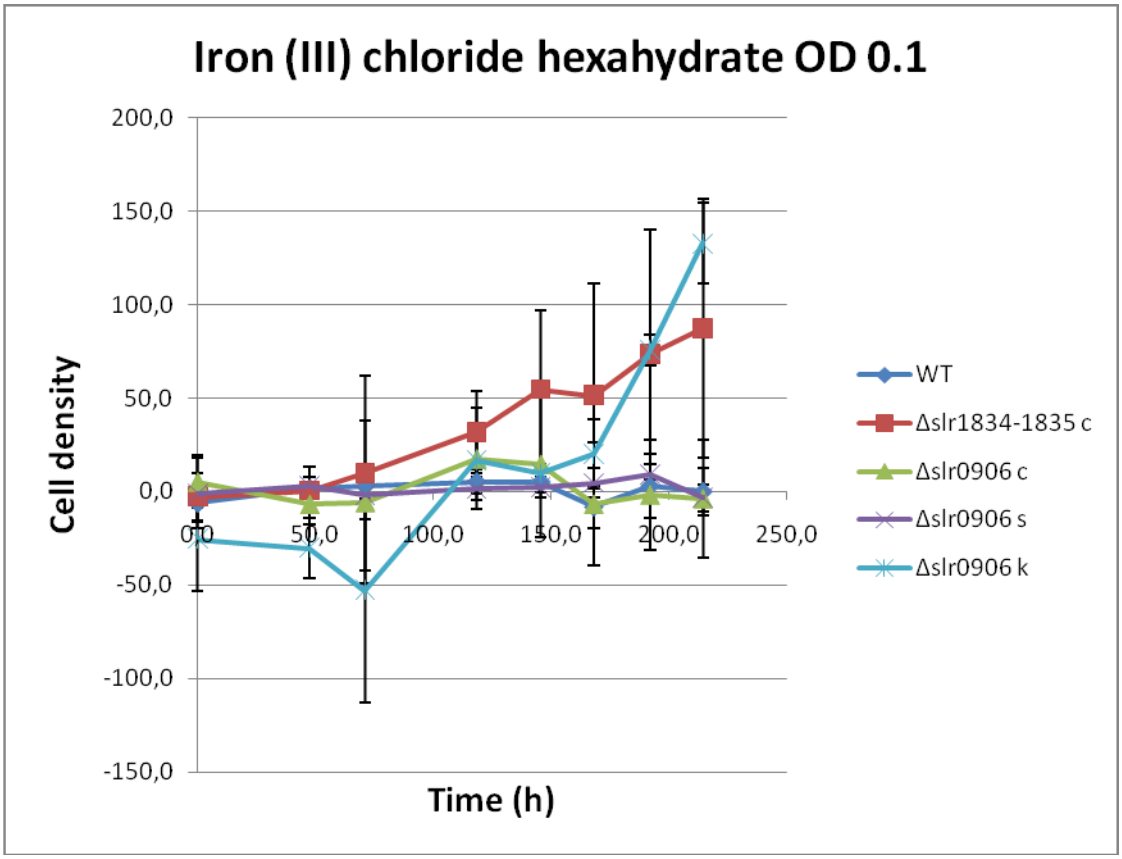

Figure 34 Growth curves of strains grown on iron (III) chloride hexahydrate source in dark condition at 30°C. The optical density spotted strains is 0.1. In the chart are shown error bars, marked as black lines. The error bars represent the lowest and highest values of cell density in each of the time points.

Potassium hexacyanoferrate (III)

The strains growth curve was observed on the plates with the solid medium supplemented with potassium hexacyanoferrate (III). The samples were diluted to an OD 1 the growth curves are showed in Figure 35. The Δslr0906-s the lowest growth curve, 84 of cell density and, the Δslr0906-k showed increasing growth curve up to 905.7 of cell density.

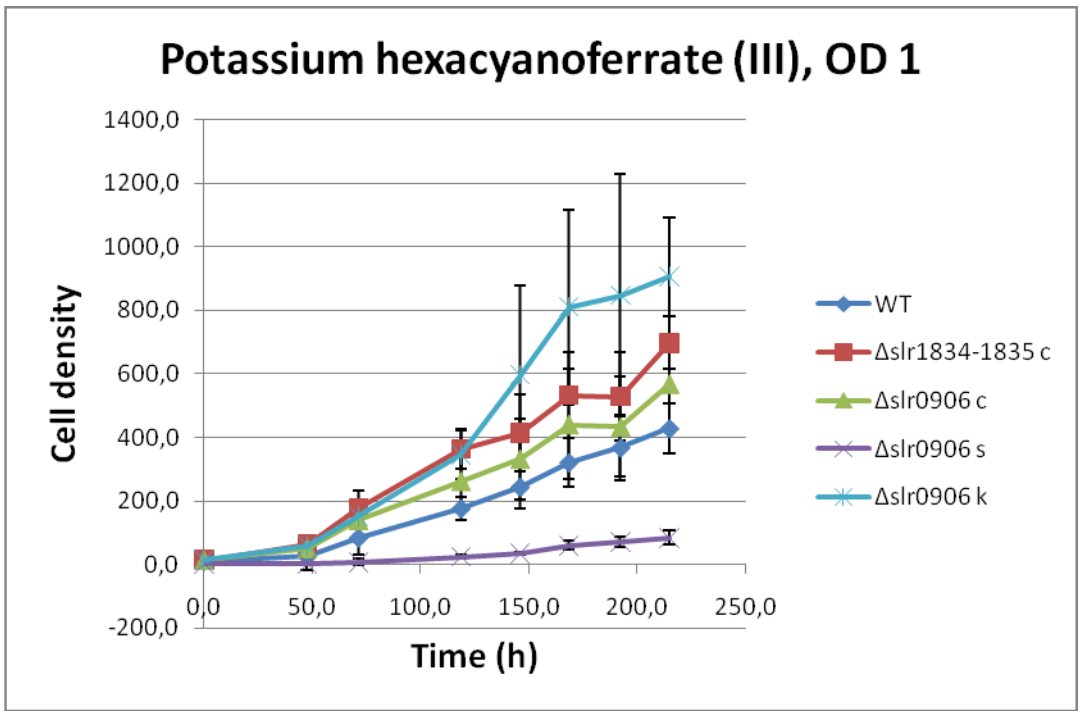

Figure 35 Growth curves of strains grown on potassium hexacyanoferrate (III) source in dark condition at 30°C. The optical density spotted strains is one. In the chart are shown error bars, marked as black lines. The error bars represent the lowest and highest values of cell density in each of the time points.

The strains growth curve was observed on the plates with the solid medium supplemented with potassium hexacyanoferrate (III). The samples were diluted to an OD 0.1 the growth curves are showed in Figure 36. The all the strains showed decreased growth; however the Δslr0906-c,-k and Δslr1834-1835-c showed increased growth from 192.1 hours of incubation. The wild-type and Δslr0906s showed minimal growth curve. The Δslr0906-k showed negative growth at 71.2 hours of incubation showed increased growth.

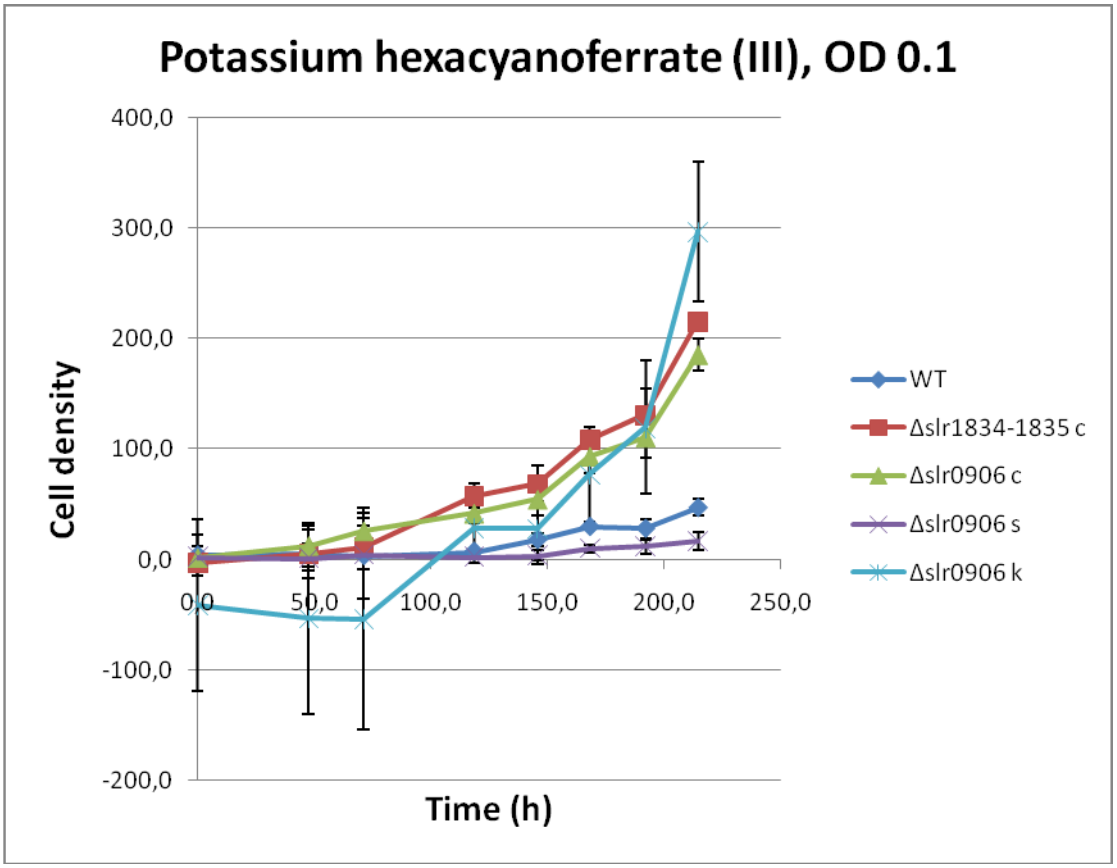

Figure 36 Growth curves of strains grown on potassium hexacyanoferrate (III) source in dark condition at 30°C. The optical density spotted strains is 0.1. In the chart are shown error bars, marked as black lines. The error bars represent the lowest and highest values of cell density in each of the time points.

Iron (II, III) oxide

The strains growth curves were observed on the plates with the solid medium supplemented with Iron (II, III) chloride. The samples were diluted to an OD 1, the growth curves are showed in Figure 37. The Δslr0906-k showed high growth curve on this medium compared to other strains. The wild-type, Δslr0906-c and Δslr1834-1835-c showed minimal and stable growth. The Δslr0906-s showed negative growth along the time axis.

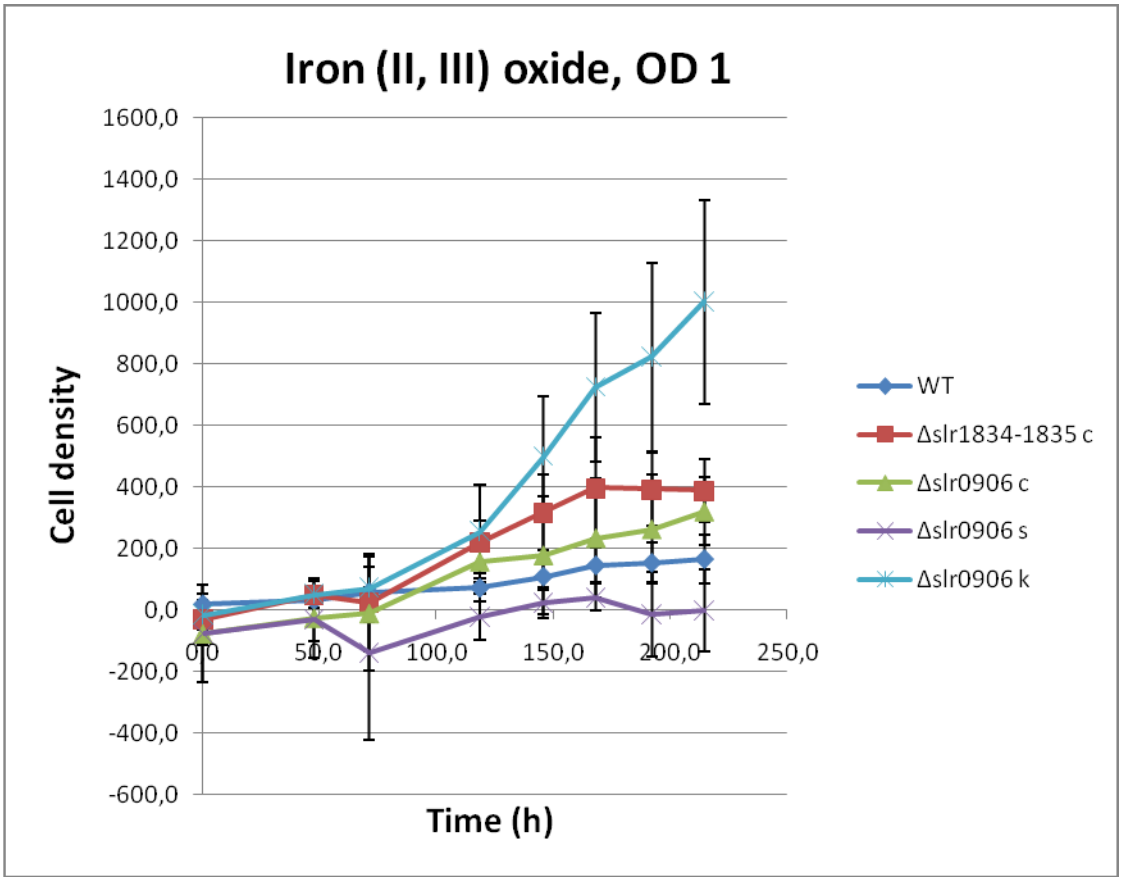

Figure 37 Growth curves of strains grown on iron (II, III) oxide source in dark condition at 30°C. The optical density spotted strains is one. In the chart are shown error bars, marked as black lines. The error bars represent the lowest and highest values of cell density in each of the time points.

The strains growth curves were observed on the plates with the solid medium supplemented with iron (II, III) chloride. The samples were diluted to an OD 0.1, the growth curves are showed in Figure 38. The wild-type and the strains showed the decreased growth curve, wherein the wild-type showed the negative growth along the time axis in till 145.7 hours of incubation from that time strain showed minimal but stable growth.

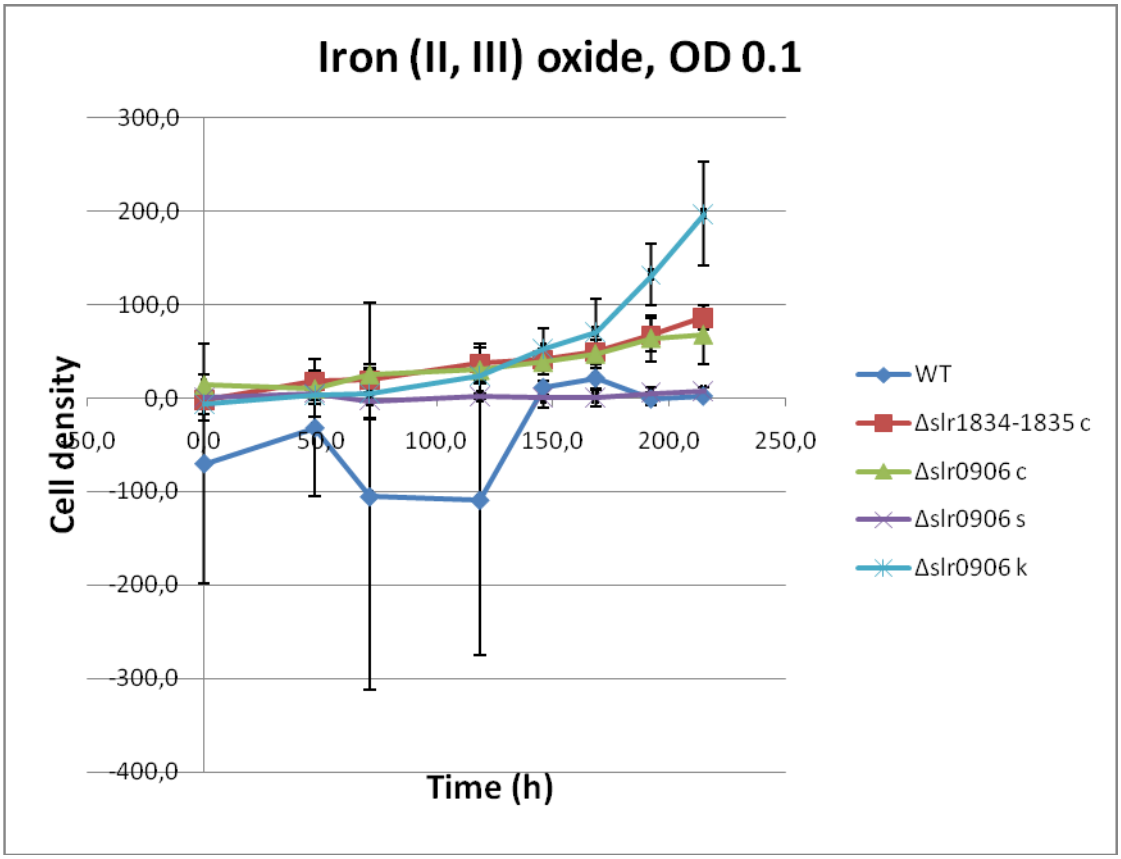

Figure 38 Growth curves of strains grown on iron (II, III) oxide source in dark condition at 30°C. The optical density spotted strains is 0.1. In the chart are shown error bars, marked as black lines. The error bars represent the lowest and highest values of cell density in each of the time points.

Iron (II) oxide

The strains growth curves were observed on the plates with the solid medium supplemented with iron (II) oxide. The samples were diluted to an OD 1, the growth curves are showed in Figure 39. The Δslr0906-k showed very large growth curve up to 1300 of cell density. The wild-type, Δslr0906-c, and Δslr1834-1835-c showed increased growth. The Δslr0906-s showed decreased growth curve.

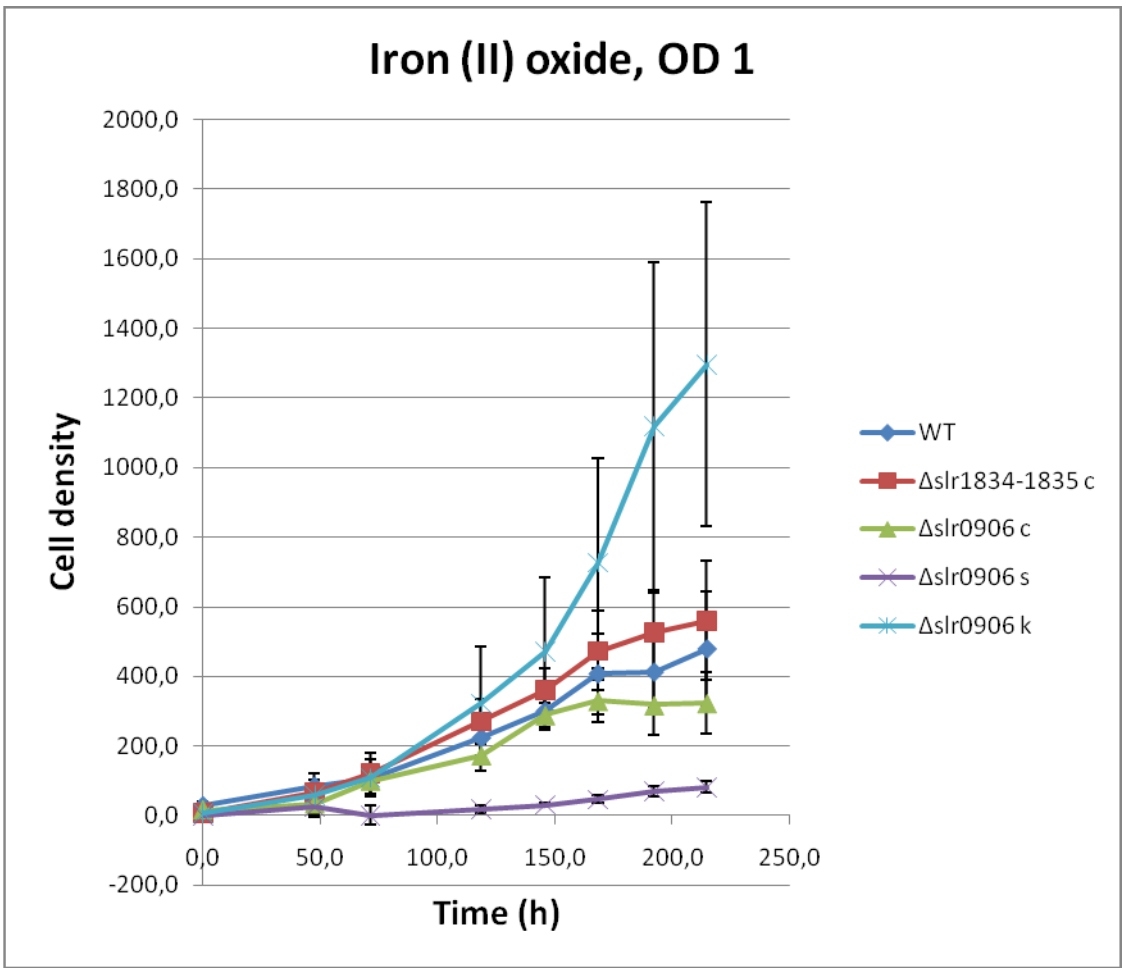

Figure 39 Growth curves of strains grown on iron (II) oxide source in dark condition at 30°C. The optical density spotted strains is one. In the chart are shown error bars, marked as black lines. The error bars represent the lowest and highest values of cell density in each of the time points.

The strains growth curves were observed on the plates with the solid medium supplemented with iron (II) chloride. The samples were diluted to an OD 0.1, the growth curves are showed in Figure 40. The Δslr0906-k showed increased growth compared to the others strains. The wild-type, Δslr0906-c, and Δslr1834-1835-c showed stable growth. The Δslr0906-s showed decreased growth curve.

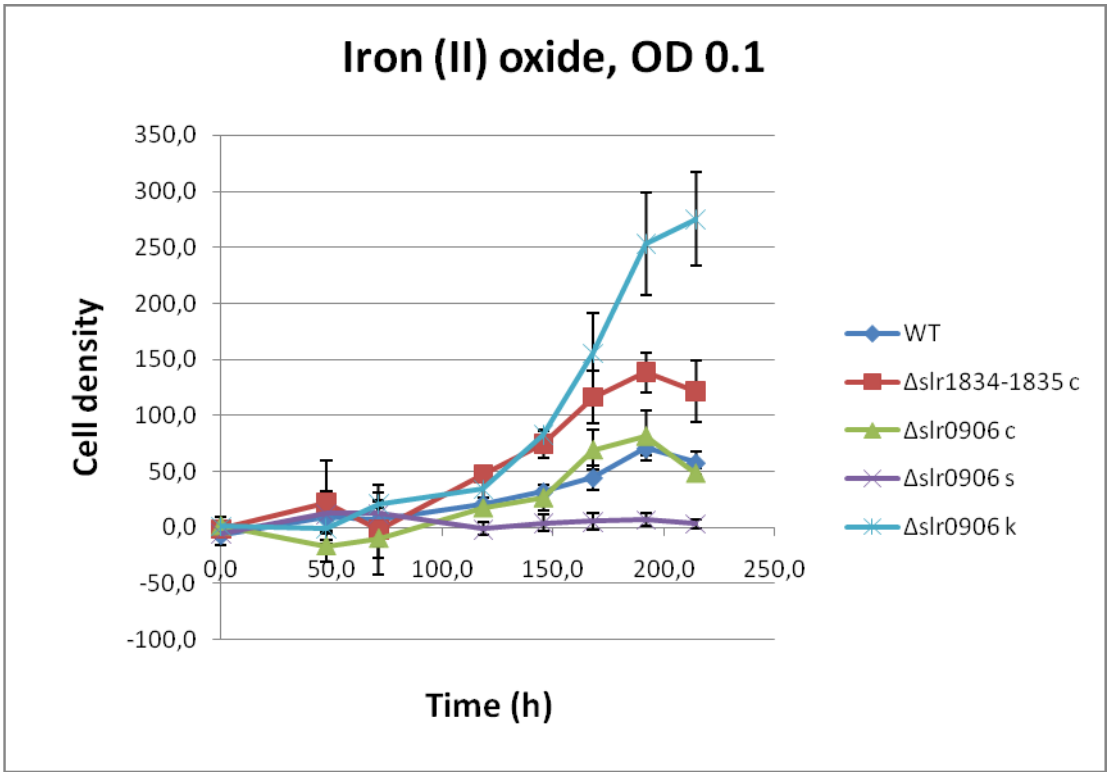

Figure 40 Growth curves of strains grown on iron (II) oxide source in dark condition at 30°C. The optical density spotted strains is 0.1. In the chart are shown error bars, marked as black lines. The error bars represent the lowest and highest values of cell density in each of the time points.

Goethite

The strains growth curves were observed on the plates with the solid medium supplemented with goethite. The samples were diluted to an OD 1, the growth curves are showed in Figure 41. The Δslr0906-k strain showed increased growth. The Δslr0906-c and Δslr1834-1835-c showed stable growth, between 158.2 hours to 214.6 hours of incubation. The wild-type, Δslr0906-s showed minimal growth curves along the time axis.

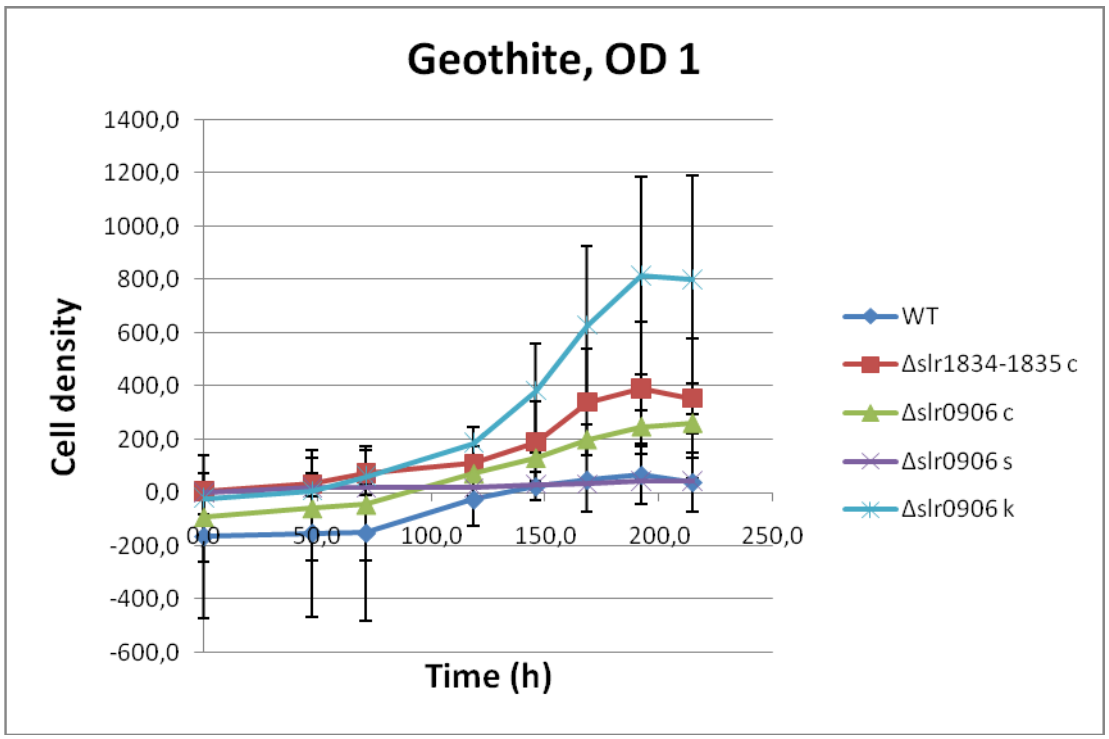

Figure 41 Growth curves of strains grown on goethite source in dark condition at 30°C. The optical density spotted strains is one. In the chart are shown error bars, marked as black lines. The error bars represent the lowest and highest values of cell density in each of the time points.

The strains growth curves were observed on the plates with the solid medium supplemented with goethite. The samples were diluted to an OD 0.1, the growth curves are showed in Figure 42. The wild-type and strains showed slow growth during the incubation, wherein the Δslr0906-c,-k and Δslr1834-1835-c showed increased growth after 192.1 hours of incubation.

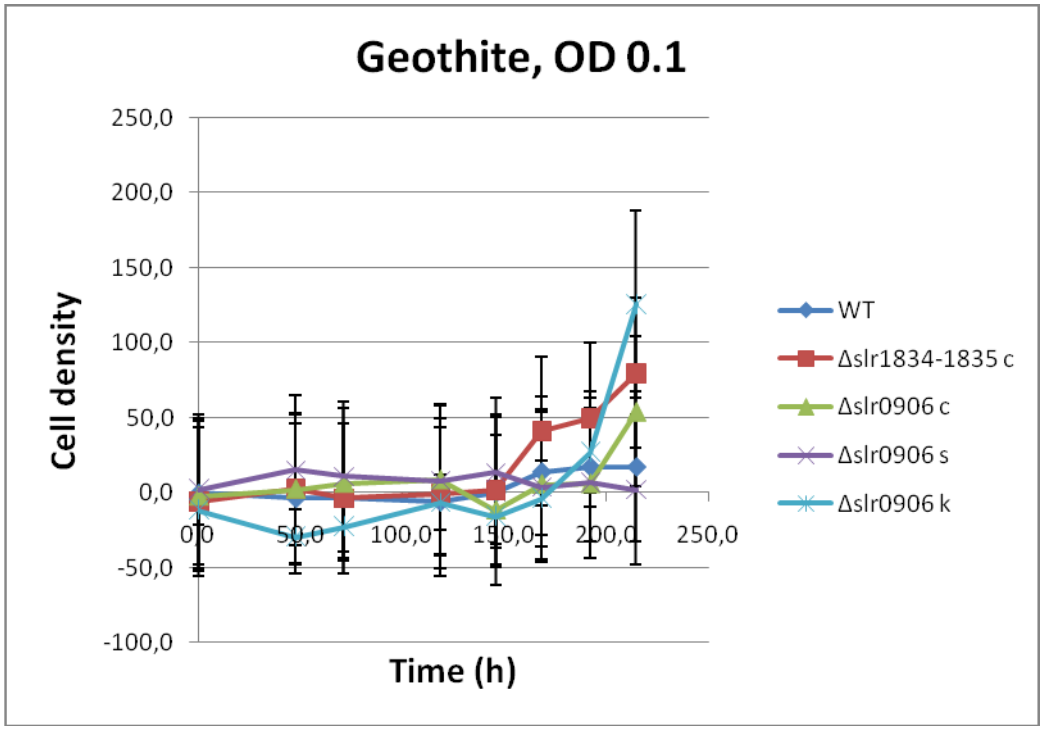

Figure 42 Growth curves of strains grown on goethite source in dark condition at 30°C. The optical density spotted strains is 0.1. In the chart are shown error bars, marked as black lines. The error bars represent the lowest and highest values of cell density in each of the time points.

Ammonium iron (III) citrate

The strains growth curves were observed on the plates with the solid medium supplemented with ammonium iron (III) citrate**.** The samples were diluted to an OD 1, the growth curves are showed in Figure 43. The Δslr0906-k showed high growth around 800 of cell density. The Δslr0906-c and Δslr1834-1835-c showed optimal growth in range 400-600 of cell density. The wild-type and Δslr0906-s showed a minimal increase in cells density.

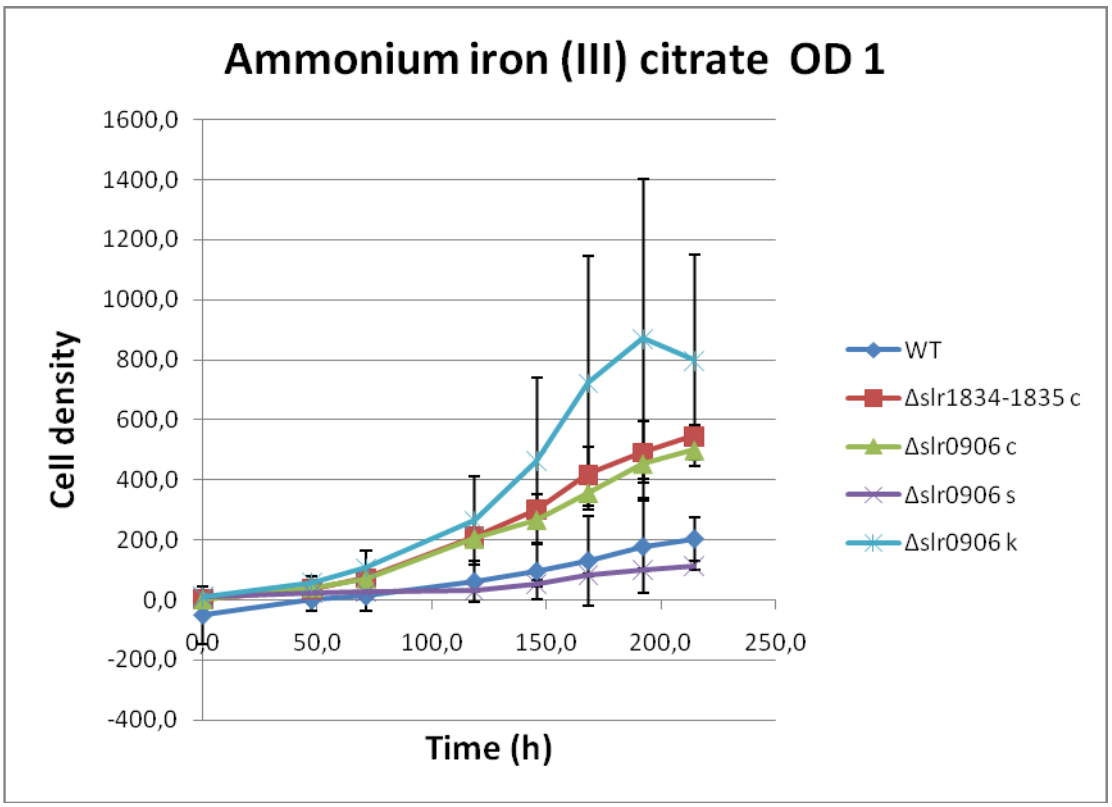

Figure 43 Growth curves of strains grown on ammonium iron (III) citrate source in dark condition at 30°C. The optical density spotted strains is one. In the chart are shown error bars, marked as black lines. The error bars represent the lowest and highest values of cell density in each of the time points.

The strains growth curves were observed on the plates with the solid medium supplemented with ammonium iron (III) citrate**.** The samples were diluted to an OD 0.1, the growth curves are showed in Figure 44. The wild-type and the other strains showed a slower rate of growth curve of cells density in the first days of incubation, wherein in the last days of incubation Δslr0906-k showed high increased growth. The Δslr0906-c and Δslr1834-1835-c showed increased growth in the 192.1 hours of incubation.

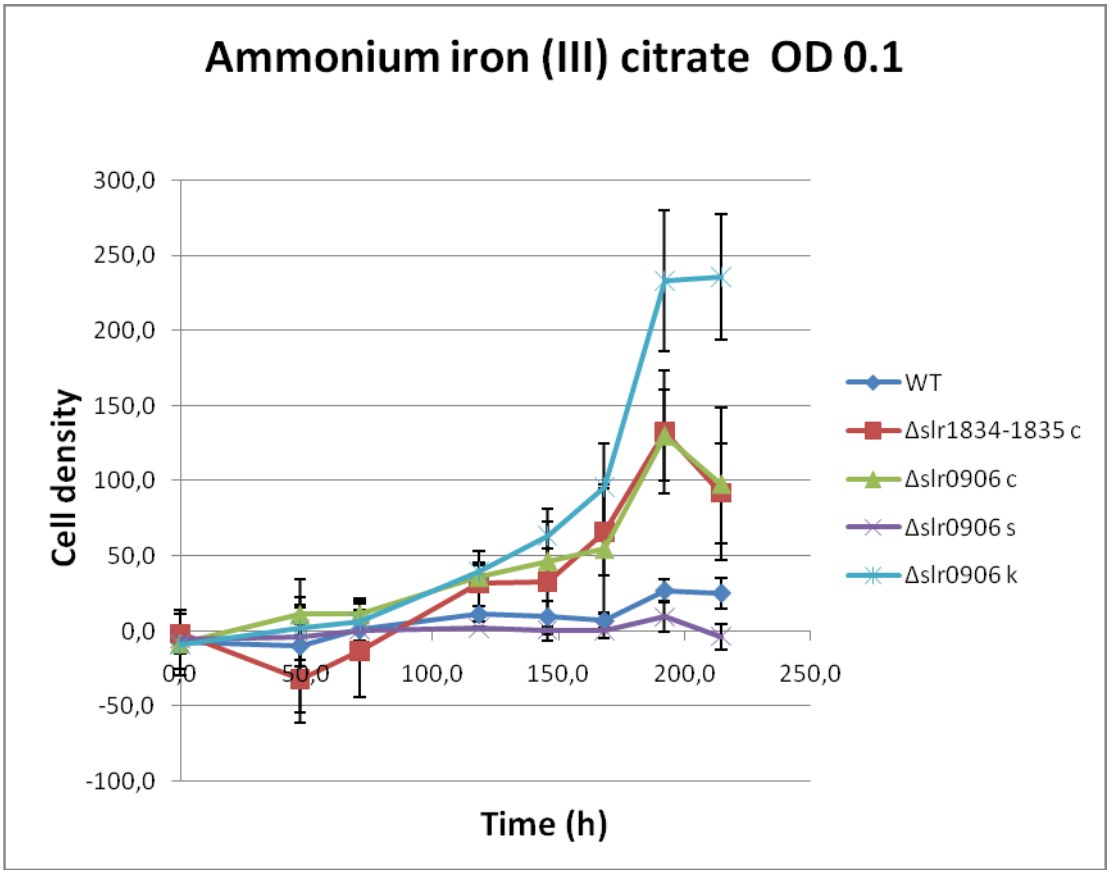

Figure 44 Growth curves of strains grown on Ammonium iron (III) citrate source in dark condition at 30°C. The optical density spotted strains is 0.1. In the chart are shown error bars, marked as black lines. The error bars represent the lowest and highest values of cell density in each of the time points.

The results showed that Δslr1834-1835-c strain growth rate is very high on media contained manganese as a source under the dark condition. However, the media that contained iron as a source showed increased growth of the strain, although cell densities oscillate around ~400 of cell density. The highest growth of strain Δslr0906-k in dark condition was observed on the plate containing the media with iron (II) oxide, were the strain reached 1296 of cell density along with time axis. The second media that Δslr0906-k showed high growth rate on iron (II, III) oxide were the cell density oscillates around ~1000.

Light condition

The *Synechocystis* sp. PCC6803 wild-type, and the mutants Δslr1834-1835-c and Δslr0906-c, *-s, -k* showed the growth (Figure 45). The plates was uncovered and exposed to full light 30 $\mu E.m^{-2}.s^{-1}$ in the incubator. The growth experiment exposed to light condition was conducted over a period of ten days. Analysis of wild-type and mutants showed in graphs with cells density along with the time (h) axis. The mix conditions of the 2 iron and 2 manganese sources are: ammonium iron (III) citrate + $MnCl_2$, ammonium iron (III) citrate + Mn (IV) oxide, iron (II) oxide + $MnCl_2$ and iron (II) oxide + Mn (IV) oxide.

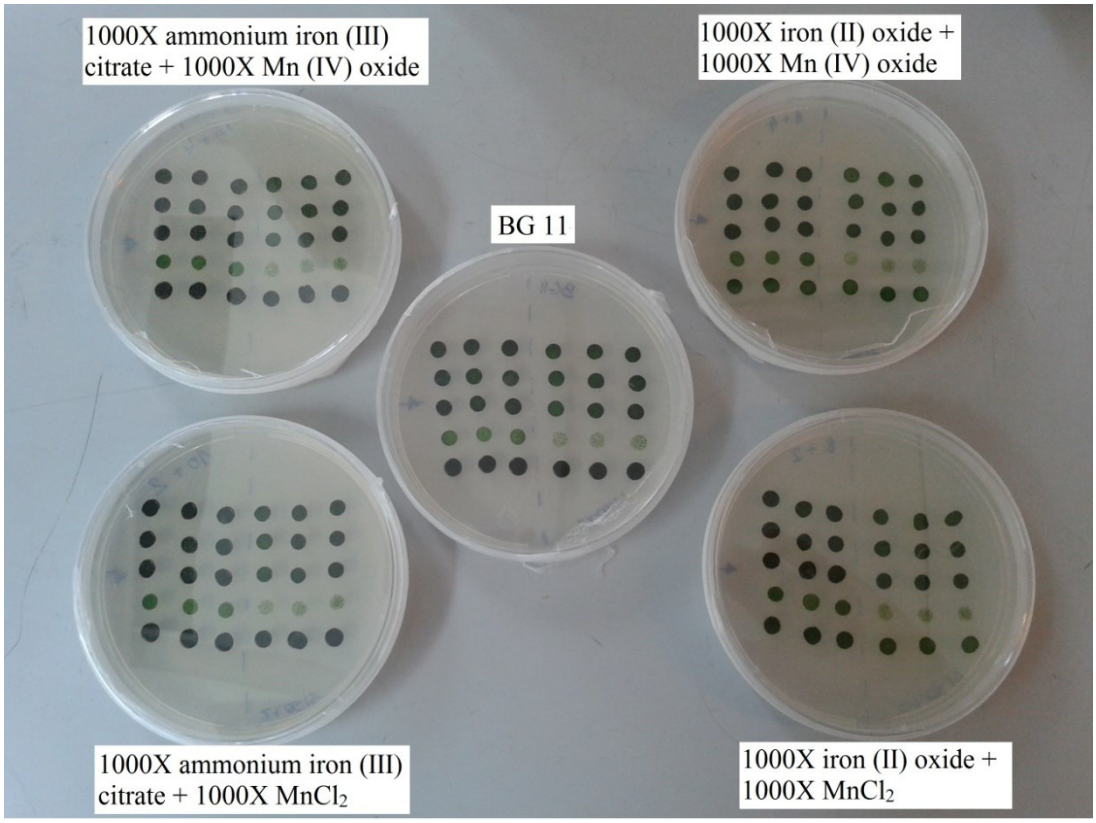

Figure 45 Growth experiment carried out under the light condition. Order of spotted strains is shown in Figure 10.

Iron (II) oxide + $MnCl_2$

The plates with the media were supplemented with iron (II) oxide + $MnCl_2$ sources, the strains were spotted and diluted to an OD 1, and the growth was observed in Figure 46. The wild-type and Δslr0906-c,-s, k showed increased growth curve at 89.5 hours of incubation. The Δslr1834-1835-c showed increased growth curve at 138.1 hours of incubation.

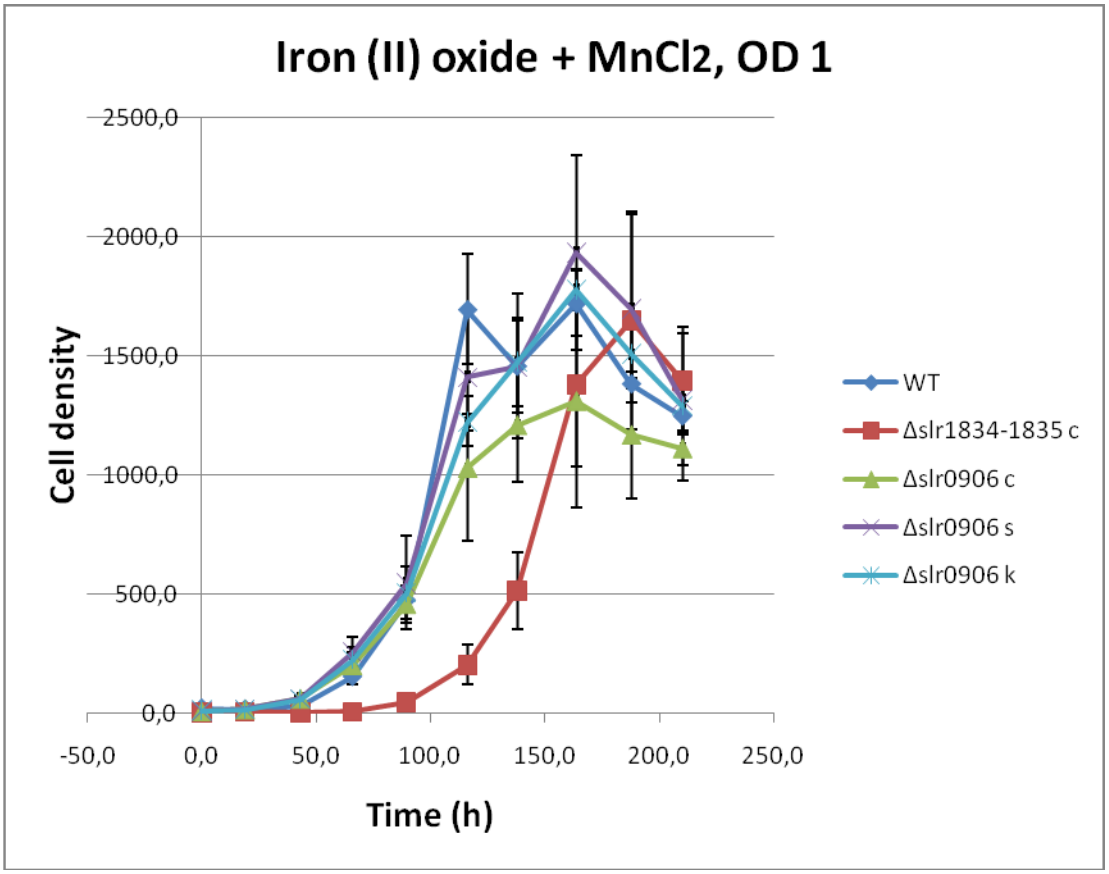

Figure 46 Growth curves of strains grown on iron (II) oxide + MnCl2 source in light condition at 30°C. The optical density spotted strains is one. In the chart are shown error bars, marked as black lines. The error bars represent the lowest and highest values of cell density in each of the time points.

The plates with the media were supplemented with iron (II) oxide + $MnCl_2$ sources, the strains were spotted and diluted to an OD 0.1, and the growth was observed in Figure 47. The wild-type and the Δslr0906-c,-s,-k showed increased growth curve after 138.1 hours of incubation. The Δslr1834-1835-c showed slower increased growth curve at 188.1 hours of incubation.

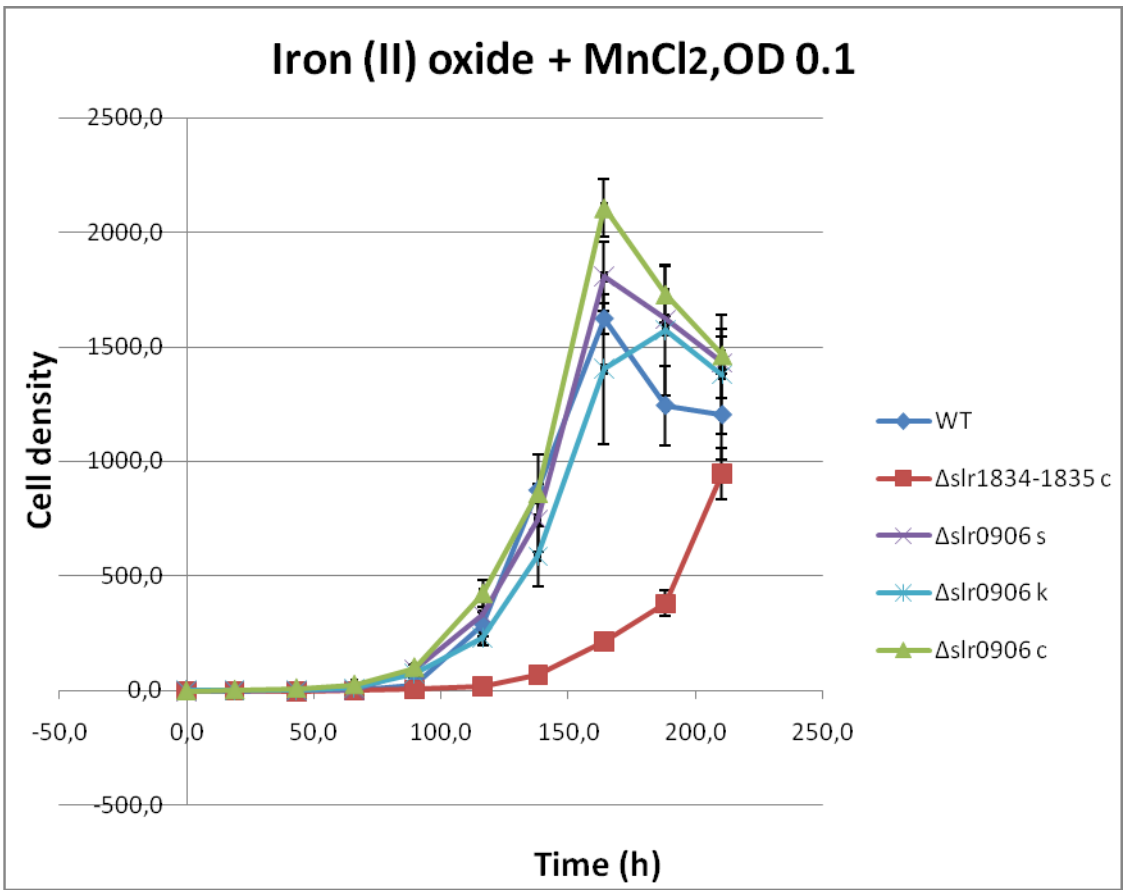

Figure 47 Growth curves of strains grown on iron (II) oxide + $MnCl_2$ source in light condition at 30°C. The optical density spotted strains is 0.1. In the chart are shown error bars, marked as black lines. The error bars represent the lowest and highest values of cell density in each of the time points.

Iron (II) oxide + Mn (IV) oxide

The plates with the media were supplemented with iron (II) oxide + Mn (IV) oxide sources, the strains were spotted and diluted to an OD 1, and the growth was observed in Figure 48. The wild-type and the Δslr0906-c,-s,-k showed increased growth curve from 89.5 hours of incubation. The Δslr1834-1835-c showed slower increased growth curve at 138.1 hours of incubation.

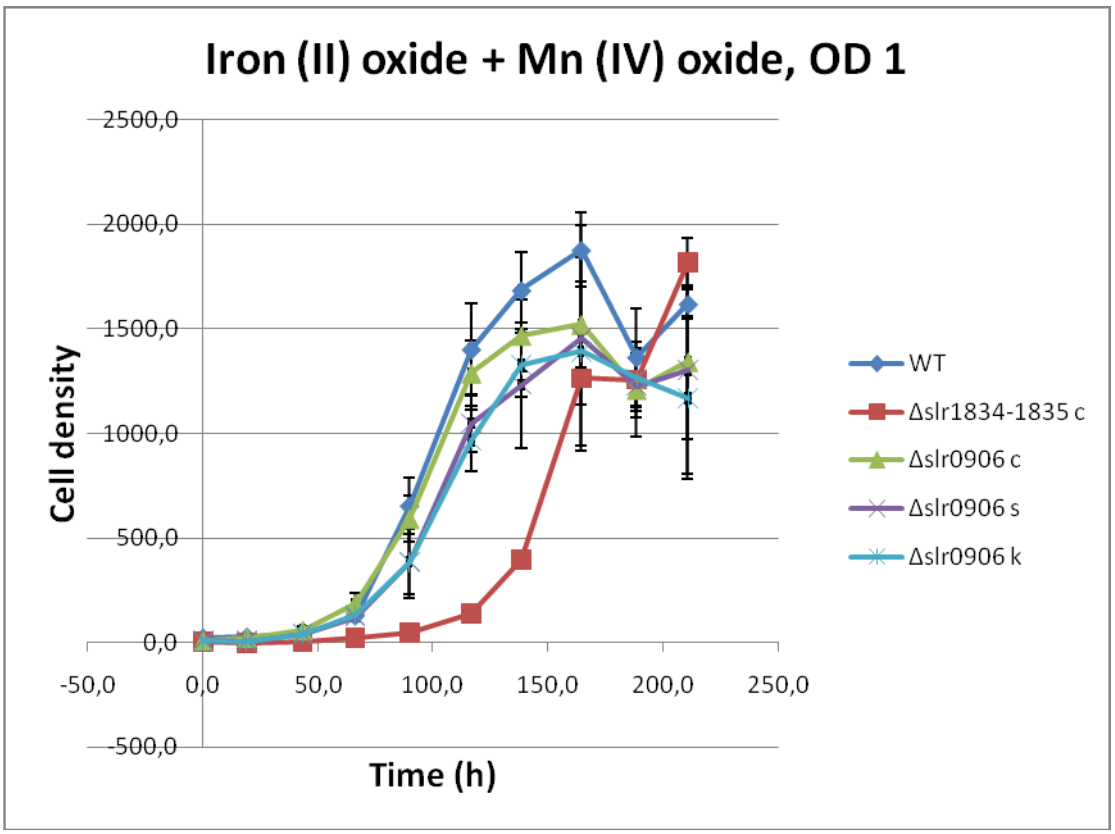

Figure 48 Growth curves of strains grown on iron (II) oxide + Mn (IV) source in light condition at 30°C. The optical density spotted strains is one. In the chart are shown error bars, marked as black lines. The error bars represent the lowest and highest values of cell density in each of the time points.

The plates with the media were supplemented with iron (II) oxide + Mn (IV) oxide sources, the strains were spotted and diluted to an OD 0.1, and the growth was observed in Figure 49. The wild-type and the Δslr0906-c,-s,-k showed increased growth curve from 116.4 hours of incubation. The Δslr1834-1835-c showed smooth increased growth curve.

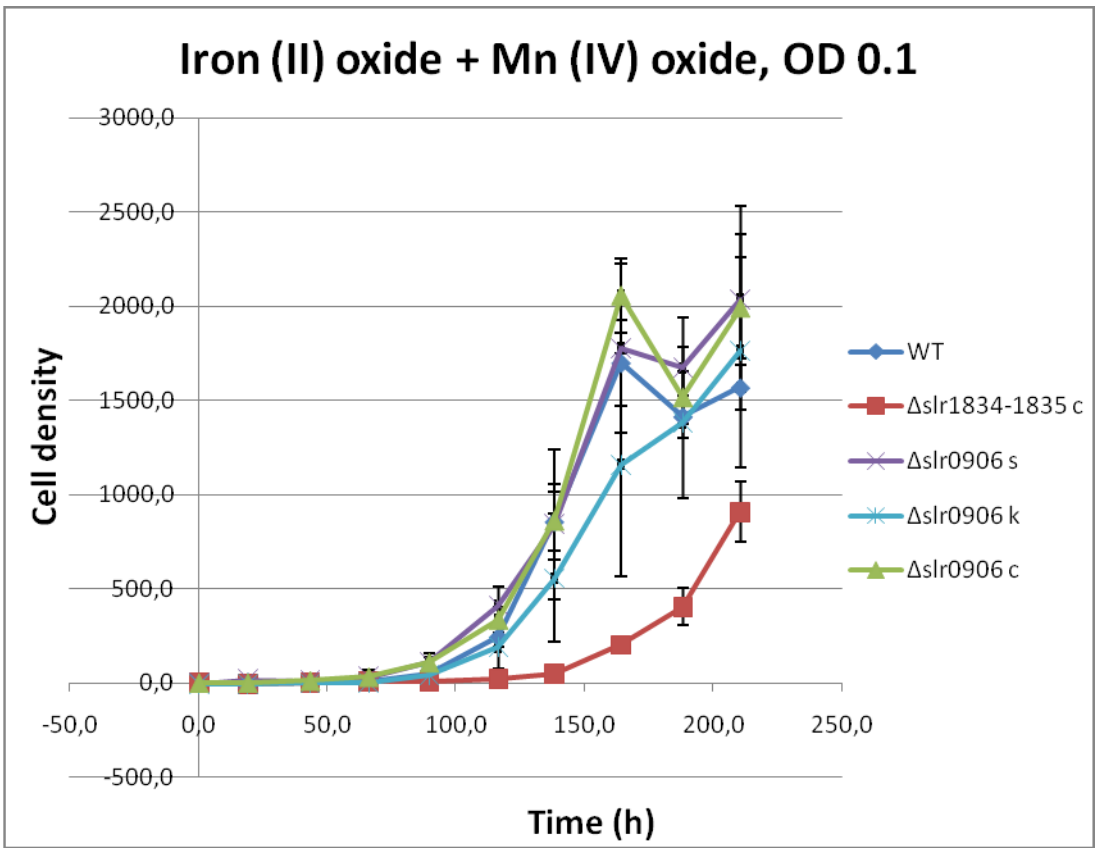

Figure 49 Growth curves of strains grown on iron (II) oxide + Mn (IV) source in light condition at 30°C. The optical density spotted strains is 0.1. In the chart are shown error bars, marked as black lines. The error bars represent the lowest and highest values of cell density in each of the time points.

Ammonium iron (III) citrate + $MnCl_2$

The plates with the media were supplemented with ammonium iron (III) citrate + $MnCl_2$ sources, the strains were spotted and diluted to an OD 1, and the growth was observed in Figure 50. The wild-type showed increased growth curve at 116.4 hours of incubation, however after this time the growth decreasing rapidly. The Δslr0906-c,-s,-k showed stable increased growth curve. The Δslr1834-1835-c showed slower increased growth curve at 89.5 hours of incubation.

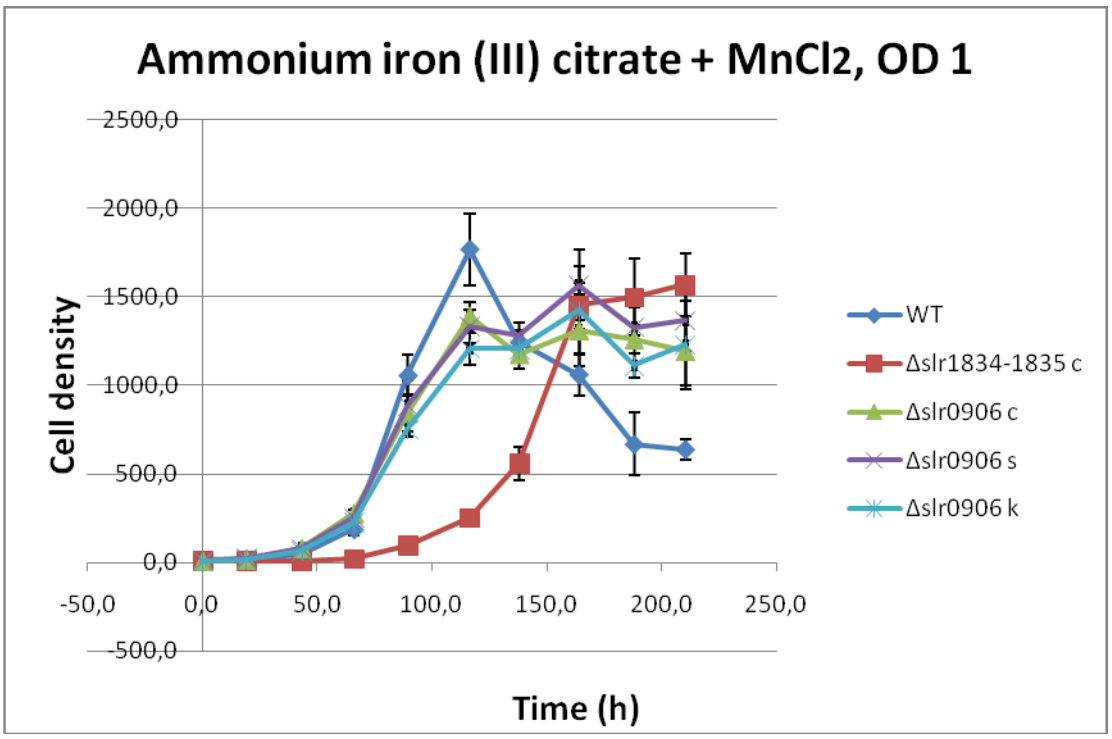

Figure 50 Growth curves of strains grown on ammonium iron (III) citrate + $MnCl_2$ source in light condition at 30°C. The optical density spotted strains is one. In the chart are shown error bars, marked as black lines. The error bars represent the lowest and highest values of cell density in each of the time points.

The plates with the media were supplemented with ammonium iron (III) citrate + $MnCl_2$ sources, the strains were spotted and diluted to an OD 0.1, and the growth was observed in Figure 51. The wild-type and the Δslr0906-c,-s,-k showed increased growth curve from 89.5 hours of incubation. The Δslr1834-1835-c showed slower increased growth curve at 138.1 hours of incubation.

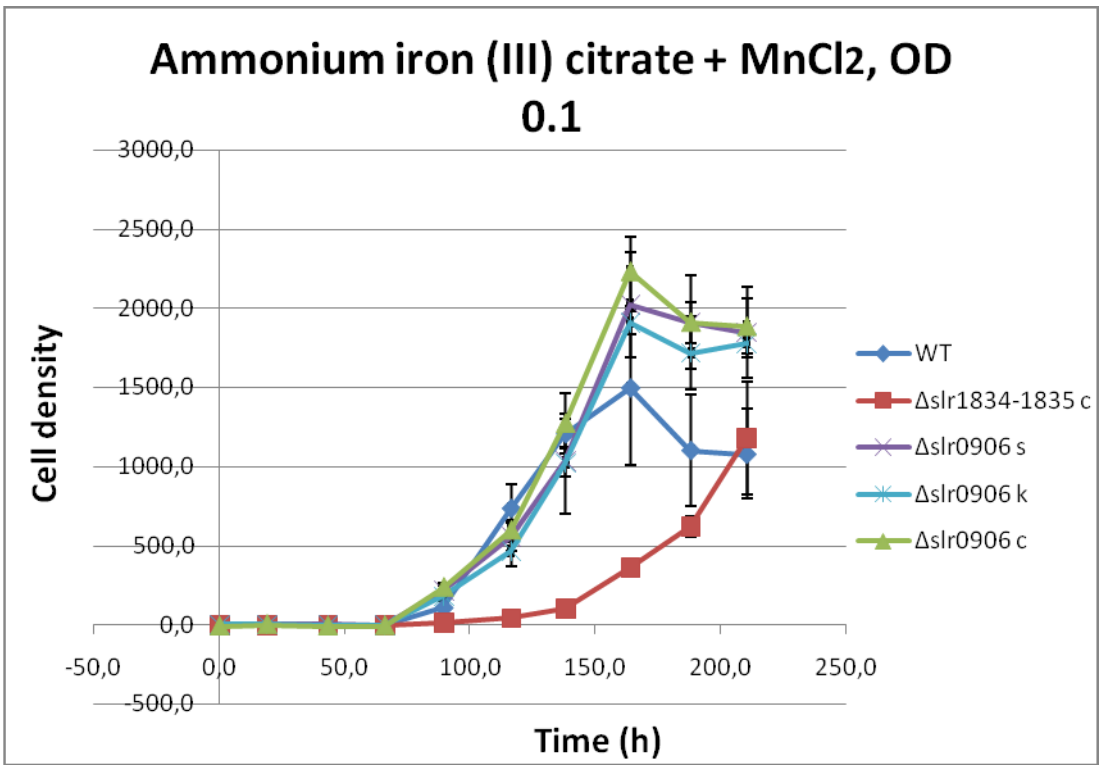

Figure 51 Growth curves of strains grown on ammonium iron (III) citrate + $MnCl_2$ source in light condition at 30°C. The optical density spotted strains is 0.1. In the chart are shown error bars, marked as black lines. The error bars represent the lowest and highest values of cell density in each of the time points.

Ammonium iron (III) citrate + Mn (IV) oxide

The plates with the media were supplemented with ammonium iron (III) citrate + Mn (IV) oxide sources, the strains were spotted and diluted to an OD 1, and the growth was observed in Figure 52. The wild-type and the Δslr0906-c,-s,-k showed increased growth curve from 66 hours of incubation, wherein the wild-type from 116.4 hours drops down drastically. The Δslr1834-1835-c showed slower increased growth curve from 89.5 hours of incubation.

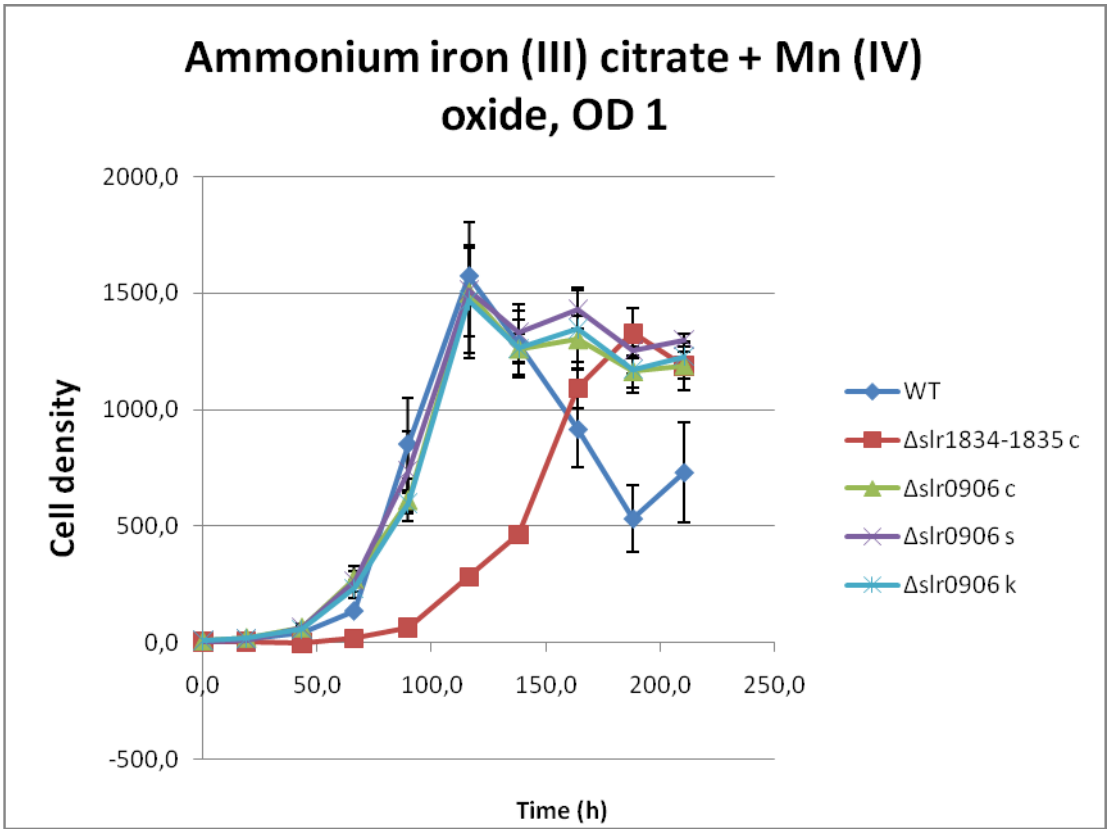

Figure 52 Growth curves of strains grown on ammonium iron (III) citrate + Mn (IV) oxide source in light condition at 30°C. The optical density spotted strains is one. In the chart are shown error bars, marked as black lines. The error bars represent the lowest and highest values of cell density in each of the time points.

The plates with the media were supplemented with ammonium iron (III) citrate + Mn (IV) oxide sources, the strains were spotted and diluted to an OD 0.1, and the growth was observed in Figure 53. The wild-type and the Δslr0906-c,-s,-k showed increased growth curve from 89.5 hours of incubation. The Δslr1834-1835-c showed slower increased growth curve from 138.1 hours of incubation.

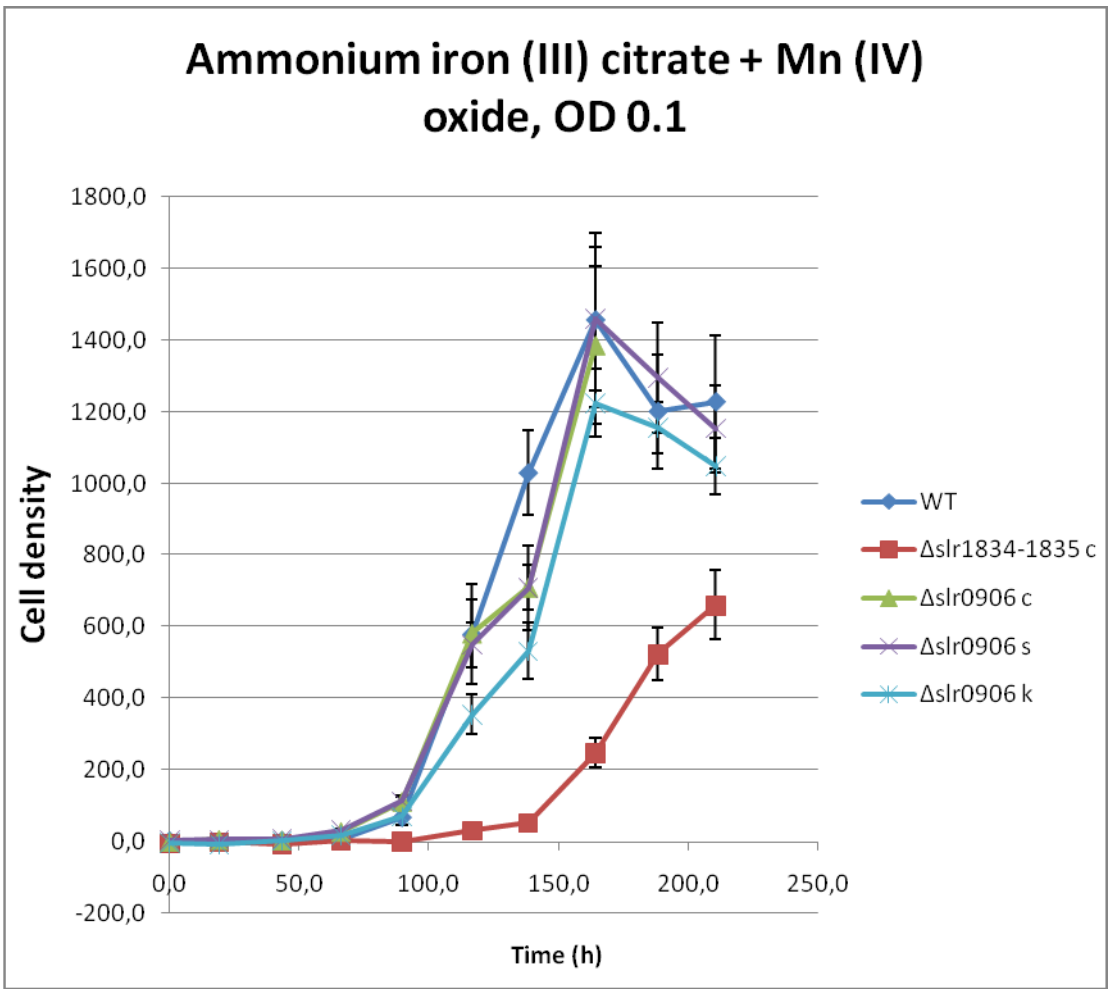

Figure 53 Growth curves of strains grown on ammonium iron (III) citrate + Mn (IV) oxide source in light condition at 30°C. The optical density spotted strains is 0.1. In the chart are shown error bars, marked as black lines. The error bars represent the lowest and highest values of cell density in each of the time points.

The Δslr1834-1835-c on the media contained mix with the two metals iron and manganese as a source showed delayed growth, although in a later period of incubation showed increased growth that aligns to the value of cell density of other strains. The Δslr0906-s,-c,-k grown on light condition with the medium mixed with two metals: iron and manganese as a source, strains showed equal growth curve in four different variations. The plates with media contained mix with the two metals iron and manganese as a source showed that all the strains grown to high cell density minimum 15000 of cell density. The Δslr0906-k strain under dark condition showed the biggest growth compared to Δslr1834-1835-c, but when exposed to intense light indicates even more significant growth.

4 Discussion

Discussion

The wild-type *Synechocystis* sp. PCC6803 and the mutant's Δslr0906 and Δslr1834-1835 showed growth on all of the variants of the media and as well under the light and dark conditions. The growth experiments were performed in dark (covered with aluminum foil) and light condition at 30°C. The Δslr0906-s showed decreased growth curve on all the media supplemented with different iron and manganese sources under the dark condition. The Δslr0906-s strain does not exceed the value of 309.7 of cell density on media with manganese sources, likewise on media containing iron sources where the strain showed very low growth curve not exceeding the volume of 114.3 of cell density. The Δslr0906-k strain showed more effectively growth on media with iron sources rather than on media with manganese as a source. The Δslr1834-1835-c grown on media with manganese source in dark condition shows approximately more effectively growths curve then grown on media with iron sources. However, all the mutants that grown on light condition showed increased growth rate in the range of 1500 of cell density.

The *Synechocystis* sp. PCC6803 strains wild-type and mutants were cultured on solid media containing iron and manganese sources. The agar plates were imaged every day using the digital camera which was placed in the plate imaging apparatus. The digital camera was not permanently mounted on a pedestal therefore, could be easy removed [Figure 15]. Therefore, during performing images of the plates it is easy to create image distortion; this further can influence obtained results which commercial program analyze. The image distortion could also affect the negative value of growth or standard deviation (error bars). The negative value of growth rate was found in many of the strains on different media under the dark condition; despite the fact that on the plates with spotted strains the growth was visible around third day. In some of the variant with different iron or manganese sources decreased growth with the negative value was observed, this may be caused by interference due to the background; in this case the media or plate stage [Figure 26, 28,34, 36, 38]. Noticeable negative values are largely visible in the samples diluted to an OD 0.1. The standard deviation are used to describe error bars, which allow the researcher to complete analysis of results. It allows you to show how the data is spread, includes the highest and lowest volume of cell density of the

samples (Cumming, Fidler, & Vaux, 2007). The standard deviation shown in the graphs reveal error bars for the triple repetition, every day of each strain. The big error bars are shown in the chart with iron (III) chloride hexahydrate where the samples were diluted to an OD 0.1 (Figure 34). The large value of error bars are found in the strains which showed incred growth rate in triple repeated sample (no visible differences in growth). Wherein, the samples diluted to an OD 1, the standard deviations are not observed; this may be due to the fact that triple repeated sample showed diferent growth rate in particule time of incubation.

The Δslr0906 that lack the *slr0906* gene have inactive complex of photosystem II and thus the photosystem I will be activate (Figure 23). The photosystem I has ability to facilitate iron acquisition (Briat et al., 1995). The result showed major growth of Δslr0906 on media supplemented with iron sourceses under the dark condition. This is due to the fact that PSI that has ability to assimilate iron works with high efficiency only under exposure to the light. Under the dark condition the iron assimilation is decreased (Briat et al., 1995). The Lis research on iron uptake in cyanobacteria showed that whether the strains were iron limited or non-limited conditions it exhibit linear iron uptake (Lis, Kranzler, Keren, & Shaked, 2015b). The results presented in experiment carried out under dark condition present that the mutants with deletion of core light harvesting protein showed increased growth on media supplemented with iron as well as manganese as a source [Figure 24]. This may be due to the fact that the removal of core light harvesting protein inhibits light harvesting in PSII, although do not inhibit process of water oxidation where the manganese works as a essential cofactor (Yachandra, Sauer, & Klein, 1996). The exemption is Δslr0906-k mutant that showed increased growth curve on both media supplemented with iron and manganese sources, under the dark condition [Figures 24, 33-44]. Interestingly, the Δslr0906 strains that have different antibiotic resistance cassette inserted (describes as: Δslr0906-s,-c,-k) exhibit distinct growth curve from the plates with different iron and manganese sources exposed to dark condition.

The Δslr1834-1835 mutant that lack the *slr1834-1835* have inactive complex of photosystem I, thus the photosystem II will be active (Figure 22). The photosystem II has incorporate Mn atoms in the centrum of complex which is involved in process of water oxidation (Blankenship, 2002; Shcolnick & Keren, 2006). The Salomon and Keren research showed that Mn accumulation does not take place in conditions of darkness (Salomon & Keren, 2011). However, obtained results with mutant *slr1834-1835* gene deletion cultured during dark condition showed growth on media supplemented with manganese as a sources

[Figure 25-32]**.** This may prove that in condition of limited availability to light the process of photosynthesis is not inhibited, however, growth rate is slow with stationary phase extended. The PSI complex plays key role in producing carbon as a sources, therefore the cyanobacteria are self-sufficient organisms (Blankenship, 2002). The result presented in experiment carried out under light condition showed that the Δslr1834-1835 growth slower than others strains [Figure 46-53]. This may be due to the fact that deletion of P700 apoprotein subunit Ia and Ib results in inhibition of electron transfer, thereby causing inhibition of carbon assimilation.

5 Conclusion

Conclusion

The Δslr1834-1835 mutant with deletion of *slr1834-1835* gene showed increased high growth on the manganese sources in condition of darkness. The Δslr1834-1835 growths slow growth on media contained with two-mixed iron and manganese as a source, exposed to light condition. The Δslr0906 mutant with deletion of *slr0906* gene showed increased high growth on iron sources in condition of darkness. The Δslr0906-k showed increased growth on the media contained iron sources rather than on manganese. Implemented different antibiotic resistance cassettes into the Δslr0906 strain showed diverse growth on the media. The Δslr0906-c,-s,-k showed increased growth on condition with two-mixed iron and manganese as a source. All the strains conducted under the light condition increased growth into large number cell density. The water oxidation and iron acquisition require light condition, therefore Δslr1834-1835 and Δslr0906 showed increased growth on light. The strains that were grown under the light condition showed the most increased growth rate compared to the dark condition.

References

Bartsevich, V. V., & Pakrasi, H. B. (1996). Manganese Transport in the Cyanobacterium Synechocystis sp. PCC 6803. *Journal of Biological Chemistry*, *271*(42), 26057–26061. http://doi.org/10.1074/jbc.271.42.26057

Blankenship, R. (2002). *Molecular mechanisms of photosynthesis*. Oxford ;;Malden MA: Blackwell Science.

Briat, J.-F., Fobis-Loisy, I., Grignon, N., Lobréaux, S., Pascal, N., Savino, G., … Van Wuytswinkel, O. (1995). Cellular and molecular aspects of iron metabolism in plants. *Biology of the Cell*, *84*(1–2), 69–81. http://doi.org/10.1016/0248-4900(96)81320-7

Chauvat, & Cassier-Chauvat. (2013). *Genomics of Cyanobacteria, 1st Edition*. Academic Press.

Cumming, G., Fidler, F., & Vaux, D. L. (2007). Error bars in experimental biology. *The Journal of Cell Biology*, *177*(1), 7–11. http://doi.org/10.1083/jcb.200611141

Freer, A., Prince, S., Sauer, K., Papiz, M., Lawless, A. H., McDermott, G., … Isaacs, N. W. (1996). Pigment–pigment interactions and energy transfer in the antenna complex of the photosynthetic bacterium Rhodopseudomonas acidophila. *Structure*, *4*(4), 449–462. http://doi.org/10.1016/S0969-2126(96)00050-0

Lis, H., Kranzler, C., Keren, N., & Shaked, Y. (2015a). A Comparative Study of Iron Uptake Rates and Mechanisms amongst Marine and Fresh Water Cyanobacteria: Prevalence of Reductive Iron Uptake. *Life*, *5*(1), 841–860. http://doi.org/10.3390/life5010841

Lis, H., Kranzler, C., Keren, N., & Shaked, Y. (2015b). A Comparative Study of Iron Uptake Rates and Mechanisms amongst Marine and Fresh Water Cyanobacteria: Prevalence of Reductive Iron Uptake. *Life*, *5*(1), 841. http://doi.org/10.3390/life5010841

Ogawa, T. (2002). A Two-component Signal Transduction Pathway Regulates Manganese Homeostasis in Synechocystis 6803, a Photosynthetic Organism. *Journal of Biological Chemistry*, *277*(32), 28981–28986. http://doi.org/10.1074/jbc.M204175200

Salomon, E., & Keren, N. (2011). Manganese Limitation Induces Changes in the Activity and in the Organization of Photosynthetic Complexes in the Cyanobacterium Synechocystis sp. Strain PCC 6803. *Plant Physiology*, *155*(1), 571–579. http://doi.org/10.1104/pp.110.164269

Shcolnick, S., & Keren, N. (2006). Metal Homeostasis in Cyanobacteria and Chloroplasts. Balancing Benefits and Risks to the Photosynthetic Apparatus. *Plant Physiology*, *141*(3), 805–810. http://doi.org/10.1104/pp.106.079251

Srivastava, A., Rai, A., & Neilan, B. (2013). *Stress Biology of Cyanobacteria: Molecular Mechanisms to Cellular Responses*. CRC Press. Retrieved from http://www.crcnetbase.com/doi/book/10.1201/b13853

van Thor, J. J., Gruters, O. W. M., Matthijs, H. C. P., & Hellingwerf, K. J. (1999). Localization and function of ferredoxin:NADP+ reductase bound to the phycobilisomes of Synechocystis. *The EMBO Journal*, *18*(15), 4128–4136. http://doi.org/10.1093/emboj/18.15.4128

Wei Xing, Wen-min Huang, Dun-hai Li, & Yong-ding Liu. (2006). Effects of Iron on Growth, Pigment Content, Photosystem II Efficiency, and Siderophores Production of Microcystis aeruginosa and Microcystis wesenbergii.

Wim FJ Vermaas. (2001). Photosynthesis and Respiration in Cyanobacteria. http://doi.org/DOI: 10.1038/npg.els.0001670

Xu, W., Wang, Y., Taylor, E., Laujac, A., Gao, L., Savikhin, S., & Chitnis, P. R. (2011). Mutational Analysis of Photosystem I of Synechocystis sp. PCC 6803: The Role of

Four Conserved Aromatic Residues in the j-helix of PsaB. *PLoS ONE*, *6*(9), e24625. http://doi.org/10.1371/journal.pone.0024625

Yachandra, V. K., Sauer, K., & Klein, M. P. (1996). Manganese Cluster in Photosynthesis: Where Plants Oxidize Water to Dioxygen. *Chemical Reviews*, *96*(7), 2927–2950. http://doi.org/10.1021/cr950052k

Z-Scheme Figure Legend. (n.d.). Retrieved July 1, 2015, from http://www.life.illinois.edu/govindjee/Z-Scheme.html

Appendix

Dark condition

Manganese(II, III) oxide

Table Appendix 1 Cell density of strains grown on manganese(II, III) oxide source in dark condition at 30°C. The spotted strains were repeated three times and optical density is one.

	OD 1														
Time (h)	WT			PSI			slr 0906 c			slr 0906 s			slr 0906 k		
0,0	12	5	-311	0	26	4	14	18	-151	-8	0	7	25	13	-20
47,6	35	35	-313	52	66	44	49	28	-171	26	3	-14	41	61	43
71,1	32	54	-361	134	156	107	111	74	-141	18	14	6	122	111	86
118,5	214	287	71	499	606	465	475	432	251	60	53	20	386	428	416
145,7	332	446	230	479	630	676	483	563	297	129	114	70	318	420	572
168,2	459	580	347	521	696	835	605	715	318	191	178	122	414	509	783
192,1	543	642	401	572	744	844	700	819	368	259	250	167	434	535	761
214,5	545	682	408	535	529	788	501	455	266	402	321	206	265	319	716

Table Appendix 2 Cell density of strains grown on manganese(II, III) oxide source in dark condition at 30°C. The spotted strains were repeated three times and optical density is 0.1.

	OD 1														
Time (h)	WT			PSI			slr 0906 c			slr 0906 s			slr 0906 k		
0,0	10	-5	-442	5	-6	-5	4	-31	-19	-13	5	3	-25	4	-38
47,6	-1	-216	-430	9	-5	-2	-11	3	1	2	3	3	-14	-9	-36
71,1	1	-187	-438	15	22	3	14	-2	29	-3	14	1	-12	-9	-15
118,5	3	-61	-224	89	125	103	47	37	79	9	-1	-3	27	58	-5
145,7	5	-50	-191	180	266	224	83	85	148	18	17	22	42	82	1
168,2	15	-69	-221	271	410	295	83	175	203	23	9	49	119	146	-35
192,1	13	-48	-191	375	519	371	151	237	264	34	25	61	239	291	6
214,5	18	-35	-159	413	572	407	134	273	346	55	42	73	233	180	6

Manganese(II) chloride

Table Appendix 3 Cell density of strains grown on manganese(II) chloride source in dark condition at 30°C. The spotted strains were repeated three times and optical density is one.

	OD 1														
Time (h)	WT			PSI			slr 0906 c			slr 0906 s			slr 0906 k		
0,0	22	6	17	17	15	6	14	22	22	-1	5	1	-7	8	-9
47,6	63	36	40	98	88	55	64	70	49	11	7	-6	26	33	57
71,3	44	124	129	194	166	119	128	128	131	4	11	-11	95	80	90
118,5	327	173	215	446	488	398	429	401	388	41	40	32	531	392	437
145,7	612	287	281	639	683	473	639	587	593	73	81	72	720	567	623
168,2	579	417	393	797	842	600	809	735	778	120	125	105	867	760	804
192,1	679	434	356	905	871	649	779	734	659	149	157	166	735	499	655
214,5	667	513	477	796	833	592	836	758	789	165	183	165	815	754	809

Table Appendix 4 Cell density of strains grown on manganese(II) chloride source in dark condition at 30°C. The spotted strains were repeated three times and optical density is 0.1.

	OD 0.1														
Time (h)	WT			PSI			slr 0906 c			slr 0906 s			slr 0906 k		
0,0	17	-2	1	-11	0	1	-19	-1	-8	-8	-12	20	-23	15	-708
47,6	31	15	8	6	13	0	-8	2	-7	-3	-15	9	-7	23	-541
71,3	-43	-6	-15	5	12	-2	-14	2	-17	7	-19	29	1	6	-706
118,5	36	15	23	90	83	99	17	73	82	5	0	-1	12	59	-107
145,7	53	48	41	129	130	152	47	100	119	12	23	8	-8	53	-191
168,2	56	53	59	218	207	258	97	166	196	20	21	15	60	138	-113
192,1	76	58	66	238	230	226	77	119	101	26	14	25	-21	62	-44
214,5	101	91	86	327	301	356	153	246	281	35	18	35	165	369	244

Manngeses(III) oxide

Table Appendix 5 Cell density of strains grown on manganese (III) oxide source in dark condition at 30°C. The spotted strains were repeated three times and optical density is one.

	OD 1														
Time (h)	WT			PSI			slr 0906 c			slr 0906 s			slr 0906 k		
0,0	3	6	3	8	4	-3	-4	3	12	-1	8	-18	8	14	5
47,6	43	49	27	95	67	35	37	26	28	1	25	-8	57	41	28
71,2	81	90	91	191	161	99	85	62	78	28	14	-24	114	85	61
118,5	233	236	243	394	383	354	270	277	277	36	38	23	315	222	188
145,7	274	357	362	507	510	450	355	425	428	55	70	47	478	362	382
168,2	299	359	405	547	581	631	402	505	540	81	90	46	550	376	462
192,1	362	430	490	666	698	808	572	652	700	113	106	71	854	689	827
214,5	404	446	383	709	660	681	592	583	641	123	117	88	697	487	666

Table Appendix 6 Cell density of strains grown on manganese(III) oxide source in dark condition at 30°C. The spotted strains were repeated three times and optical density is 0.1.

						OD 0.1								
WT			PSI			slr 0906 c			slr 0906 s			slr 0906 k		
-19	12	-20	-4	2	-5	-8	-16	1	-20	-9	-17	-4	-11	0
-17	4	-3	-11	10	-10	-10	-4	1	-11	6	-15	13	-6	-5
-19	12	-13	1	9	-8	-7	-11	23	1	15	-36	5	-16	-35
3	-1	-56	54	36	43	36	24	17	-1	-3	6	41	-4	-8
30	41	16	106	93	98	64	60	63	6	5	18	78	52	53
39	13	12	128	144	132	86	63	78	4	17	7	116	31	9
58	50	33	215	225	230	164	130	155	17	12	20	275	214	226
39	32	17	172	241	173	137	95	110	11	22	17	301	162	145

Manganese(IV) oxide

Table Appendix 7 Cell density of strains grown on manganese(IV) oxide source in dark condition at 30°C. The spotted strains were repeated three times and optical density is one

	OD 1														
Time (h)	WT			PSI			slr 0906 c			slr 0906 s			slr 0906 k		
0,0	44	51	45	23	30	37	47	24	18	44	31	-8	26	31	47
23,7	91	85	68	65	93	88	68	57	61	33	13	-5	18	89	80
70,9	283	307	298	259	448	413	260	347	454	61	42	46	226	311	293
98,1	402	439	402	315	518	492	298	430	562	144	67	121	290	354	380
120,6	452	502	418	319	464	599	328	431	608	198	119	184	376	426	460
144,5	580	611	591	418	691	622	419	640	780	250	137	234	297	359	423
167,0	483	508	468	275	427	531	246	437	544	242	114	248	193	238	305
191,2	550	573	491	284	413	510	299	441	579	336	174	346	163	210	295

Table Appendix 8 Cell density of strains grown on manganese(IV) oxide source in dark condition at 30°C. The spotted strains were repeated three times and optical density is 0.1.

	OD 0.1														
Time (h)	WT			PSI			slr 0906 c			slr 0906 s			slr 0906 k		
0,0	0	29	9	-7	-5	-8	-35	-9	25	-13	-1	13	-6	26	0
23,7	1	13	1	-2	8	22	-36	-3	48	1	16	1	0	6	16
70,9	18	21	45	56	78	117	-11	75	90	10	4	14	52	99	79
98,1	13	5	54	68	113	175	-10	98	151	8	2	15	92	153	120
120,6	-3	16	9	58	152	231	49	34	99	7	13	29	115	143	179
144,5	47	31	105	215	279	367	44	224	290	16	33	36	337	466	393
167,0	40	54	97	129	223	330	60	214	308	30	40	38	388	489	446
191,2	-8	-17	34	123	235	357	64	134	209	47	51	66	374	472	422

Iron (III) chloride hexahydrate

Table Appendix 9 Cell density of strains grown on iron (III) chloride hexahydrate source in dark condition at 30°C. The spotted strains were repeated three times and optical density is one

	OD 1														
Time (h)	WT			PSI			slr 0906 c			slr 0906 s			slr 0906 k		
0,0	-13	-1	-3	-5	-15	-17	13	7	-16	-16	-15	-6	16	12	13
47,6	14	43	13	51	-10	21	31	27	16	-8	-13	-15	57	38	25
71,2	47	66	-3	132	-16	50	79	52	33	7	0	-27	150	100	69
118,5	166	200	56	316	17	241	177	98	209	3	9	8	265	199	136
145,7	232	320	127	421	75	471	330	212	321	4	7	28	499	395	294
168,2	258	342	85	513	72	532	392	230	475	-1	30	37	646	517	406
192,1	298	381	119	525	106	665	455	281	503	2	34	63	743	607	487
214,6	345	427	174	517	151	665	437	302	461	17	40	63	678	483	369

Table Appendix 10 Cell density of strains grown on iron (III) chloride hexahydrate source in dark condition at 30°C. The spotted strains were repeated three times and optical density is 0.1

	OD 0.1														
Time (h)	WT			PSI			slr 0906 c			slr 0906 s			slr 0906 k		
0,0	-14	5	-10	-13	11	-7	6	-9	19	-7	20	-16	-6	-13	-57
47,6	-9	14	0	-2	1	2	0	-19	-1	7	-2	5	-39	-12	-40
71,2	0	11	-2	-49	50	28	-8	-48	39	-13	13	-5	-23	-14	-122
118,5	10	-2	8	11	29	55	3	1	49	-4	8	0	3	19	28
145,7	9	-1	8	18	45	101	-1	-14	59	6	5	-4	13	5	12
168,2	4	-11	-18	11	23	120	-20	-31	31	-4	11	7	17	3	40
192,1	23	-7	-7	17	56	147	-4	-30	29	9	15	4	76	67	84
214,6	12	-13	1	24	77	161	-4	-35	28	-7	-8	5	126	116	157

Potassium hexacyanoferrate (III)

Table Appendix 11 Cell density of strains grown on potassium hexacyanoferrate (III) source in dark condition at 30°C. The spotted strains were repeated three times and optical density is one

	OD 1														
Time (h)	WT			PSI			slr 0906 c			slr 0906 s			slr 0906 k		
0,0	18	14	-5	10	27	0	17	23	6	-2	6	8	11	26	2
47,6	47	49	-24	68	74	48	56	75	25	7	-1	3	77	62	33
71,2	124	101	25	194	188	150	195	144	82	4	1	18	217	174	65
118,5	212	179	136	437	326	329	348	280	162	30	26	19	411	362	261
145,7	322	206	203	553	355	333	405	408	186	40	37	31	916	494	380
168,2	408	292	263	688	430	482	532	551	242	73	62	45	1162	676	591
192,1	487	304	314	689	470	430	508	540	253	86	70	57	1287	637	615
214,6	513	414	358	789	626	679	669	633	405	109	75	68	1118	836	763

Table Appendix 12 Cell density of strains grown on potassium hexacyanoferrate (III) source in dark condition at 30°C. The spotted strains were repeated three times and optical density is 0.1.

	OD 0.1														
Time (h)	WT			PSI			slr 0906 c			slr 0906 s			slr 0906 k		
0,0	8	20	-16	-2	-1	-5	-3	3	4	4	-7	11	4	4	-131
47,6	17	19	-20	15	4	-1	-3	33	7	8	-12	7	-19	11	-151
71,2	44	-33	-1	29	15	-10	19	39	19	-4	19	-3	13	-5	-169
118,5	6	9	7	62	66	45	36	52	37	-1	0	9	33	53	1
145,7	25	14	15	76	81	50	40	68	55	2	0	9	7	66	12
168,2	29	31	30	116	109	101	78	107	95	6	12	12	58	126	47
192,1	30	19	36	134	153	107	89	124	119	7	10	19	55	174	130
214,6	42	44	56	216	223	209	169	198	190	8	18	24	293	362	236

Iron (II, III) oxide

Table Appendix 13 Cell density of strains grown on iron (II, III) oxide source in dark condition at 30°C. The spotted strains were repeated three times and optical density is one

	OD 1														
Time (h)	WT			PSI			slr 0906 c			slr 0906 s			slr 0906 k		
0,0	18	27	14	37	-6	-126	16	11	-258	22	5	-259	20	-2	-69
47,6	36	55	6	91	50	4	51	47	-176	9	14	-114	80	41	31
71,1	46	76	55	139	87	-158	113	78	-224	22	22	-465	188	57	-33
118,5	58	124	35	301	163	193	233	131	107	17	24	-109	426	136	200
145,7	110	154	62	459	231	259	315	259	-41	59	42	-35	681	296	521
168,2	123	209	102	585	274	330	378	307	14	79	49	-6	935	461	776
192,1	144	221	93	523	286	366	422	294	70	73	59	-173	1160	561	744
214,6	152	251	91	501	305	353	444	284	231	70	79	-156	1375	740	892

Table Appendix 14 Cell density of strains grown on iron (II, III) oxide source in dark condition at 30°C. The spotted strains were repeated three times and optical density strains is 0.1

	OD 0.1														
Time (h)	WT			PSI			slr 0906 c			slr 0906 s			slr 0906 k		
0,0	8	0	-218	0	0	-7	11	27	5	-20	-7	28	5	-18	-5
47,6	8	13	-117	11	44	-2	7	24	-1	0	-18	32	17	18	-24
71,1	13	15	-344	7	33	17	20	38	17	-3	-23	17	10	28	-23
118,5	-22	-4	-301	28	57	27	21	46	23	2	-1	4	21	31	21
145,7	5	9	19	31	39	53	28	53	34	11	-11	1	48	77	34
168,2	14	15	34	36	49	63	32	63	47	4	-10	7	71	106	36
192,1	2	4	-9	51	66	86	39	88	65	-1	9	8	114	170	112
214,6	3	3	0	79	78	102	37	100	66	7	12	3	166	261	165

Iron (II) oxide

Table Appendix 15 Cell density of strains grown on iron (II, III) oxide source in dark condition at 30°C. The spotted strains were repeated three times and optical density is one

	OD 1														
Time (h)	WT			PSI			slr 0906 c			slr 0906 s			slr 0906 k		
0,0	15	33	36	24	3	-3	30	11	6	4	7	-13	-5	20	1
47,6	96	92	64	84	109	8	75	7	16	47	25	2	33	41	98
71,3	111	116	86	138	171	57	140	59	98	22	11	-30	56	103	163
118,5	253	254	163	322	294	199	208	124	184	24	26	5	131	393	439
145,7	293	357	251	376	414	294	321	250	294	33	34	27	243	498	670
168,2	463	485	275	569	506	346	368	261	360	43	60	37	377	907	894
192,1	444	497	298	606	579	396	404	231	317	79	78	54	598	1239	1516
214,6	577	573	289	701	611	369	407	233	329	91	92	64	782	1417	1690

Table Appendix 16 Cell density of strains grown on iron (II, III) oxide source in dark condition at 30°C. The spotted strains were repeated three times and optical density is 0.1

	OD 0.1														
Time (h)	WT			PSI			slr 0906 c			slr 0906 s			slr 0906 k		
0,0	-15	2	-8	1	-1	-5	-2	-4	10	-8	-8	0	-4	3	4
47,6	27	17	-18	34	-20	52	-32	-6	-12	31	8	-3	-9	-5	11
71,3	30	8	-17	44	-21	-30	-30	-2	2	10	3	24	18	20	25
118,5	27	17	18	56	42	44	17	23	12	-1	-7	4	20	44	39
145,7	35	29	31	67	68	88	20	40	19	-2	2	12	85	78	85
168,2	40	36	57	96	110	142	53	88	67	10	9	-3	115	178	174
192,1	77	70	65	146	118	151	74	64	107	1	10	10	209	250	301
214,6	64	46	63	113	99	152	52	43	50	4	-1	7	228	294	304

Goethite

Table Appendix 17 Cell density of strains grown on goethite source in dark condition at 30°C. The spotted strains were repeated three times and optical density is one

	OD 1														
Time (h)	WT			PSI			slr 0906 c			slr 0906 s			slr 0906 k		
0,0	5	19	-520	-1	8	3	2	4	-283	20	-4	-19	13	11	-89
47,6	19	34	-513	11	18	68	43	60	-282	56	3	-4	45	45	-71
71,2	26	45	-530	58	46	112	66	81	-286	45	16	-5	84	78	25
118,5	30	31	-139	78	64	183	62	96	55	49	-8	12	159	147	254
145,7	49	59	-37	112	90	368	146	106	136	48	20	26	336	235	576
168,2	126	111	-92	252	198	571	265	153	178	34	30	33	598	347	940
192,1	137	122	-59	284	219	677	303	181	258	44	37	46	759	477	1210
214,6	115	92	-88	233	221	615	240	239	302	53	38	43	615	538	1249

Table Appendix 18 Cell density of strains grown on goethite source in dark condition at 30°C. The spotted strains were repeated three times and optical density is 0.1

	OD 0.1														
Time (h)	WT			PSI			slr 0906 c			slr 0906 s			slr 0906 k		
0,0	-11	13	-3	-1	1	-18	-1	-1	-5	6	-9	10	-7	-5	-23
47,6	-5	13	-19	33	-37	12	2	10	-5	33	3	9	-43	-37	-9
71,2	-3	6	-14	4	-32	17	16	14	-11	11	3	19	-4	-16	-48
118,5	8	-1	-25	17	-22	3	6	10	10	15	-16	25	-25	12	-7
145,7	5	3	-8	10	-14	10	-20	-7	-8	20	2	17	-25	5	-28
168,2	18	8	16	42	35	46	-24	14	27	7	4	1	-19	25	-17
192,1	15	1	36	45	46	58	-29	13	34	9	4	7	8	69	4
214,6	17	14	21	83	67	89	10	73	79	3	-2	5	82	197	98

Ammonium iron (III) citrate

Table Appendix 19 Cell density of strains grown on ammonium iron (III) citrate source in dark condition at 30°C. The spotted strains were repeated three times and optical density is one

	OD 1														
	WT			PSI			slr 0906 c			slr 0906 s			slr 0906 k		
0,0	5	2	-161	1	11	-8	11	-3	-7	11	17	6	4	29	1
47,6	16	26	-44	24	38	45	53	31	36	6	12	57	40	70	70
71,2	33	45	-44	57	64	96	67	49	94	16	9	55	59	172	93
118,5	106	92	-18	221	184	231	204	192	215	32	33	28	113	408	277
145,7	164	130	-10	276	267	361	253	279	268	46	51	68	225	765	402
168,2	234	197	-42	358	373	522	312	356	401	79	86	83	353	1186	632
192,1	283	245	3	406	468	606	394	481	488	96	104	101	516	1483	615
214,6	252	238	118	543	515	583	470	495	534	109	103	131	563	1201	629

Table Appendix 20 Cell density of strains grown on Ammonium iron (III) citrate source in dark condition at 30°C. The spotted strains were repeated three times and optical density is 0.1

	OD 0.1														
	WT			PSI			slr 0906 c			slr 0906 s			slr 0906 k		
0,0	2	-12	-11	-2	-2	-1	-4	-12	-9	-14	-19	17	-18	14	-24
47,6	13	19	-61	-54	1	-43	18	5	10	-13	-17	19	5	21	-21
71,2	11	13	-21	-49	5	5	6	23	4	1	-13	14	6	18	-7
118,5	16	12	6	8	40	48	45	33	30	3	2	1	42	44	32
145,7	18	13	-2	-8	71	36	37	53	50	3	-2	1	43	68	79
168,2	10	1	10	34	91	72	104	37	23	1	-5	5	96	125	67
192,1	19	33	29	85	156	156	149	95	147	13	17	-2	181	271	248
214,6	17	37	22	56	122	97	155	59	80	-4	5	-12	246	272	190

Light condition

Iron (II) oxide + MnCl2

Table Appendix 21 Cell density of strains grown on iron (II) oxide + MnCl2 source in light condition at 30°C. The spotted strains were repeated three times and optical density is one

Time (h)	OD 1														
	WT			PSI			slr 0906 c			slr 0906 s			slr 0906 k		
0,0	24	24	20	9	9	5	14	8	4	12	13	9	11	17	9
19,0	14	14	28	13	8	7	24	7	20	15	19	30	13	19	19
43,2	38	30	33	9	2	6	79	49	59	49	68	75	57	60	61
66,0	161	149	158	7	6	14	285	130	192	193	269	320	205	211	264
89,5	522	452	455	58	30	65	544	445	389	324	643	682	472	416	630
	179	185	143				138		83	109	167	147	124	118	123
116,4	7	8	1	248	109	263	1	877	0	7	1	0	9	5	1
	163	148	125				145	117	99	111	170	154	155	126	160
138,1	6	6	2	629	333	591	8	7	1	8	5	8	0	4	9
	187	168	160	164		150	181	111	99	146	213	220	170	175	187
164,0	2	6	5	0	990	6	9	7	4	7	6	6	7	3	4
	136	140	139	179	113	201	147	107	96	124	199	185	141	146	164
188,1	0	2	1	8	5	4	0	5	0	8	4	9	8	0	4
	131	123	119	147	114	157	123	112	96	100	153	141	123	122	141
210,4	5	7	6	1	2	4	6	9	9	6	5	2	2	3	5

Table Appendix 22 Cell density of strains grown on iron (II) oxide + MnCl2 source in light condition at 30°C. The spotted strains were repeated three times and optical density is 0.1

Time (h)	OD 0.1														
	WT			PSI			slr 0906 c			slr 0906 s			slr 0906 k		
0,0	1	-7	1	0	1	-2	0	-2	-9	-10	-16	4	-10	5	4
19,0	-6	0	-3	4	-2	-2	3	-2	1	-4	-2	-5	-1	6	-2
43,2	2	5	-3	-2	-3	-7	12	9	2	-3	-14	9	-9	-5	11
66,0	4	0	4	-5	6	-4	28	21	20	9	-17	5	-7	27	8
89,5	37	47	-4	8	12	-3	87	116	95	69	86	116	82	73	59
116,4	251	346	267	22	14	19	365	423	478	263	364	358	266	213	210
		104													
138,1	744	7	826	76	64	73	812	883	884	582	823	825	662	659	433
	166	165	154		17	24	196	213	221	163	186	191	177	125	117
164,0	7	6	2	224	9	2	9	3	7	4	5	7	8	5	2
	130	104	137		32	42	161	171	185	160	163	161	188	133	149
188,1	7	7	3	393	0	7	3	9	4	9	3	2	7	2	7
	113	142	104	105	82	95	137	148	153	126	145	156	152	153	107
210,4	9	0	7	4	9	6	3	0	5	5	3	6	6	2	8

Iron (II) oxide + Mn (IV) oxide

Table Appendix 23 Cell density of strains grown on iron (II) oxide + Mn (IV) source in light condition at 30°C. The spotted strains were repeated three times and optical density is one

Time (h)	OD 1														
	WT			PSI			slr 0906 c			slr 0906 s			slr 0906 k		
0,0	28	19	12	6	9	3	10	9	10	9	13	12	12	5	10
19,0	29	33	9	-18	20	-8	12	41	14	-4	31	-9	7	13	-8
43,2	48	39	34	7	9	-6	42	81	53	44	39	42	54	34	34
66,0	155	122	103	18	28	20	143	245	167	112	124	131	170	99	133
89,5	806	602	549	42	45	55	482	588	706	374	219	562	531	221	406
	157	115	146				119	119	146	108		116	110		
116,4	8	7	8	110	149	162	6	8	9	7	893	3	6	810	981
	175	182	147				140	133	166	115		156	147	117	133
138,1	1	4	7	370	381	434	7	5	1	3	978	3	8	0	6
	201	194	167	114	124	139	128	160	166	121	108	207	183		141
164,0	4	1	5	9	3	6	6	8	8	6	3	5	4	932	1
	146	109	152	108	132	135		126	140	121	107	138	139	111	128
188,1	1	9	9	7	9	1	959	8	2	9	8	6	3	6	9
	167	154	163	169	182	193		153	156	107		187	155		118
210,4	5	0	9	7	1	1	918	9	9	8	959	0	0	772	4

Table Appendix 24 Cell density of strains grown on iron (II) oxide + Mn (IV) source in light condition at 30°C. The spotted strains were repeated three times and optical density is 0.1

Time (h)	OD 0.1														
	WT			PSI			slr 0906 c			slr 0906 s			slr 0906 k		
0,0	-9	3	-2	5	9	-11	-3	-3	-1	-2	-6	-2	-8	-6	-2
19,0	7	11	-17	-1	-6	-12	-13	-37	43	22	24	11	-11	4	0
43,2	2	7	-17	1	4	2	10	0	18	29	6	-4	1	-14	15
66,0	18	17	-22	17	7	-1	44	-17	59	74	21	4	13	-7	6
89,5	45	38	47	-6	21	8	141	80	95	61	151	123	28	12	96
116,4	246	188	287	26	23	16	405	278	318	312	508	410	140	111	322
	107						103				125				
138,1	4	688	797	50	54	47	4	735	810	451	0	823	310	413	943
	196	155	157	19		17	228	192	196	130	220	182			183
164,0	4	7	3	5	236	7	0	4	0	7	3	1	712	933	2
	146	128	148	37		32	167	146	140	150	198	153	111	118	184
188,1	9	1	8	5	515	1	3	6	4	2	1	5	2	6	4
	170	147	152	86	108	77	229	186	180	168	259	182	127	155	245
210,4	2	8	1	4	8	7	8	7	4	2	9	8	3	8	7

Ammonium iron (III) citrate + MnCl2

Table Appendix 25 Cell density of strains grown on ammonium iron (III) citrate + $MnCl_2$ source in light condition at 30°C. The spotted strains were repeated three times and optical density is one

Time (h)	OD 1														
	WT			PSI			slr 0906 c			slr 0906 s			slr 0906 k		
0,0	20	14	13	12	8	5	3	8	6	16	4	-3	0	9	6
19,0	16	20	27	9	8	7	19	14	16	22	22	15	11	16	10
43,2	41	47	55	9	4	1	76	78	83	84	63	80	50	73	57
66,0	168	163	229	28	13	14	257	280	295	302	207	242	193	275	204
	110		114							102					
89,5	2	923	3	82	104	97	962	790	778	2	733	893	710	783	757
	160	171	199				148	134	135	130	143	125	128	110	122
116,4	0	4	2	218	254	278	0	4	6	0	9	5	4	7	7
	120	115	137				126	115	111	126	131	125	121	123	116
138,1	9	5	1	448	627	595	8	0	1	7	8	9	6	9	0
		110	115	136	159	138	152	130	111	179	143	146	133	170	123
164,0	925	7	4	7	8	3	1	1	4	4	5	7	4	3	2
				125	157	166	117	131	129	120	143	133	110	118	104
188,1	866	518	620	2	5	8	0	4	6	9	6	7	1	4	9
				151	176	142	139	118	100	154	120	135	114	151	103
210,4	648	577	692	2	6	8	5	5	6	4	3	1	1	1	1

Table Appendix 26 Cell density of strains grown on ammonium iron (III) citrate + $MnCl_2$ source in light condition at 30°C. The spotted strains were repeated three times and optical density is 0.1

Time (h)	OD 0.1														
	WT			PSI			slr 0906 c			slr 0906 s			slr 0906 k		
0,0	0	0	-6	-7	-1	1	-16	-10	-4	-1	-6	6	0	2	-4
19,0	0	-2	-6	2	2	-3	8	-3	0	1	-2	3	-4	2	0
43,2	0	-4	-8	-7	5	-7	-14	-9	-2	-7	6	5	2	-10	-12
66,0	0	0	-3	4	0	-8	-13	1	-6	-7	-12	6	-2	-3	-12
89,5	201	30	94	11	9	19	203	242	263	184	254	203	150	185	195
116,4	631	673	906	78	31	22	546	670	574	454	594	616	403	417	572
	126	109	125				105	143	132		113	100			138
138,1	8	9	3	165	62	86	9	0	7	955	5	2	808	868	2
	204	109	135		32		197	233	238	188	239	177	183	192	197
164,0	4	2	4	369	2	393	8	5	3	8	6	4	2	5	4
	143	114			55		180	224	168	181	185	206	180	145	189
188,1	2	0	734	608	9	685	7	4	2	8	0	0	4	2	5
	136		107	106	89	157	168	201	195	169	217	166	182	183	167
210,4	4	796	3	8	0	6	5	2	8	5	7	1	5	9	6

Ammonium iron (III) citrate + Mn (IV) oxide

Table Appendix 27 Cell density of strains grown on ammonium iron (III) citrate + MnCl2 source in light condition at 30°C. The spotted strains were repeated three times and optical density is one

Time (h)	OD 1														
	WT			PSI			slr 0906 c			slr 0906 s			slr 0906 k		
0,0	13	14	7	5	9	-3	13	4	10	12	5	5	10	8	7
19,0	24	11	20	6	5	4	18	30	17	22	11	10	3	30	17
43,2	54	41	41	13	1	-21	80	69	51	77	56	62	43	67	58
66,0	138	142	138	26	18	11	331	271	224	277	215	298	200	275	222
89,5	106 9	683	810	66	74	53	706	607	525	931	612	672	547	622	623
116,4	165 6	164 2	142 5	274	309	266	166 2	155 6	129 3	159 7	118 7	175 0	132 2	172 8	135 4
138,1	142 3	128 6	114 7	468	492	438	138 4	126 9	113 4	147 1	124 4	126 9	125 9	132 6	120 0
164,0	896	108 8	766	104 4	119 2	104 6	136 8	135 0	119 0	139 0	137 2	152 4	119 7	154 1	130 0
188,1	425	694	482	138 1	140 1	120 5	118 8	122 1	108 8	116 1	123 9	135 7	110 0	128 3	113 4
210,4	511	942	742	120 6	128 4	107 6	121 1	123 8	112 5	127 0	130 7	132 0	124 0	128 0	116 1

Table 28 Cell density of strains grown on ammonium iron (III) citrate + MnCl2 source on light condition at 30°C. The spotted strains were repeated three times and optical density is 0.1

Time (h)	OD 0.1														
	WT			PSI			slr 0906 c			slr 0906 s			slr 0906 k		
0,0	7	3	-2	-1	-1	-10	-1	1	0	0	2	6	1	2	-7
19,0	-13	-4	17	-2	6	-6	4	7	7	-1	10	7	-2	-4	-14
43,2	-8	4	15	-9	-9	-4	10	-1	4	3	11	6	-1	19	-8
66,0	7	7	11	6	3	-2	29	33	23	33	36	28	23	22	11
89,5	47	89	70	-7	-1	11	121	93	123	107	127	102	69	94	49
116,4	716	583	438	28	42	25	658	476	612	578	592	476	330	418	318
138,1	107 5	111 8	895	61	52	46	755	638	737	810	737	578	562	592	445
164,0	152 6	165 6	118 7	24 1	29 2	21 1	160 4	116 3	139 2	147 5	165 0	125 1	120 4	132 9	114 2
188,1	133 2	124 7	102 4	55 0	58 1	44 2	143 7	107 1	124 6	134 7	141 5	112 0	113 4	123 7	109 7
210,4	124 4	140 5	103 5	68 8	74 0	55 4	120 8	976	110 8	120 6	123 9	101 3	103 9	113 3	975